

12-11-2009

Osteogenic Regulatory Mechanisms Activated By Pressure In Aortic Heart Valve

Carol Andrea Pregonero Gamez

Follow this and additional works at: <https://scholarsjunction.msstate.edu/td>

Recommended Citation

Gamez, Carol Andrea Pregonero, "Osteogenic Regulatory Mechanisms Activated By Pressure In Aortic Heart Valve" (2009). *Theses and Dissertations*. 3420.
<https://scholarsjunction.msstate.edu/td/3420>

This Dissertation - Open Access is brought to you for free and open access by the Theses and Dissertations at Scholars Junction. It has been accepted for inclusion in Theses and Dissertations by an authorized administrator of Scholars Junction. For more information, please contact scholcomm@msstate.libanswers.com.

OSTEOGENIC REGULATORY MECHANISMS ACTIVATED BY PRESSURE IN
AORTIC HEART VALVE

By

Carol Andrea Pregonero Gamez

A Dissertation
Submitted to the Faculty of
Mississippi State University
in Partial Fulfillment of the Requirements
for the Degree of Doctor of Philosophy
in Biomedical Engineering
in the Department of Agricultural and Biological Engineering

Mississippi State, Mississippi

December 2009

OSTEOGENIC REGULATORY MECHANISMS ACTIVATED BY PRESSURE IN
AORTIC HEART VALVE

By

Carol Andrea Pregonero Gamez

Approved:

James N. Warnock
Assistant Professor of Agricultural
and Biological Engineering
(Director of Dissertation)

Steven Elder
Associate Professor of Agricultural
and Biological Engineering
Graduate Coordinator
(Committee Member)

Shane C. Burgess
Director Life Sciences and
Biotechnology Institute
(Committee Member)

Fiona McCarthy
Assistant Research Professor
Department of Basic Sciences
College of Veterinary Medicine
(Committee Member)

Jun Liao
Assistant Professor of Agricultural
And Biological Engineering
(Committee Member)

Sara A. Rajala
Dean of the College of Engineering

Name: Carol Andrea Pregonero Gamez

Date of Degree: December 11, 2009

Institution: Mississippi State University

Major Field: Biomedical Engineering

Major Professor: Dr. James N. Warnock

Title of Study: OSTEOGENIC REGULATORY MECHANISMS ACTIVATED BY
PRESSURE IN AORTIC HEART VALVE

Pages in Study: 117

Candidate for Degree of Doctor of Philosophy

Calcific aortic valve disease (CAVD) is the most common cause of aortic valve failure and replacement in the elderly population, affecting 25% of the population over 65 years of age. Current pharmacological approaches for preventing the onset and progression of calcific aortic valve disease have not shown consistent benefits in clinical studies. Differentiation of valvular interstitial cells (VICs) into osteoblast-like cells is an integral step in the calcification process. Although clinical evidence suggests hypertension as a potential candidate contributing to the development of CAVD, the underlying molecular mechanisms that cause de-differentiation remain unclear. The present study investigates the role of elevated cyclic pressure in modulating osteoblast differentiation pathways in VICs *in vitro*.

We used a combination of systems biology modeling and pathway-based analyses to identify novel genes and molecular mechanisms that are activated in valve tissue during exposure to elevated pressure conditions. Our results show that elevated pressure induces a gene expression pattern in valve tissue that is considerably similar to that seen

in CAVD, underlining the key role of hypertension as an initiating factor in the onset of pathogenesis. In addition, our analysis revealed a set of genes that was not previously known to be regulated in valve tissue in a pressure dependent manner. Currently, the molecular mechanisms involved in CAVD and their associations with changes in local mechanical environment are poorly understood, and thus a better understanding of the cell based process mediating CAVD progression will improve our ability to develop potential medical therapies for this disease.

DEDICATION

Vivian y María

Quienes siempre están presentes en mi mente y en mi corazón

ACKNOWLEDGEMENTS

. I would like to give my complete appreciation to my family for their continual love, support, and interest in my professional goals. Primary among them is my brother Camilo, who is the source of strength and the inspiration in everything I do. From the bottom of my heart, I am eternally grateful and forever indebted to my mother Isabel for her unparalleled love, strength, for supporting and encouraging me to pursue my academic goals, hopefully in the next coming years I can repay some of that support. I would also like to thank my aunt Rocio, thanks for your love, spiritual guidance, endless laughs and ultimately for being my best friend.

I wish to express my endless and sincere gratitude to my advisor, Dr. James N. Warnock, for his dedicated instruction, patience, guidance, and full support during my Ph.D. studies. Thanks for your vote of confidence to reach my goals at MSU and for giving me the time to visit my family in those good and bad days as a Ph.D. student. I would also like to thank my committee members, Dr. Shane Burgess, Dr. Fiona McCarthy, Dr. Jun Liao and Dr. Steven Elder for their suggestions and supports. I would like to thank all the members of our research group, past and present. Their support, training, mentoring, and tolerance were indispensable. I especially thank Pooja Kothari, Steven Waller and Scott Meztler for their enthusiasm and constant willingness to help me out in the lab.

I would like to give special thanks to Dr. Mark Horstemeyer, Dr. Flip To, Dr. Bindu Nanduri, Dr. Sam Borazjani, Ms. Juliet Tang and staff members of Life Science and Biotechnology Institute for their help and collaboration. I also appreciate the funds provided by Life and Science Biotechnology Institute and Agricultural and Biological Engineering department.

I would like to express my appreciation to all of my friends in Starkville and long distance friends for their spiritual support all these years. Especially, my dear friend Laura thanks for your hospitality, amazing friendship, advice, support and so many other things. You, Matthew and the kids were my family here; I will always be in debt with you. Naty, thanks for your friendship, faith, encouragement, your cheerful support in good and bad times is priceless; Dani, thanks for your friendship, loyalty, help, for your cheerful company and always-ready smile (thanks also to your wonderful parents Sandra and Edgar); my Puerto Rican friends (Edda, Kesito, Will, Rafa' Jaime,), thanks for the incalculable and excellent times we shared. Nicolas thanks for your invaluable help, infinite patience, your support and encouragement during the last months made this a reality.

TABLE OF CONTENTS

	Page
DEDICATION	ii
ACKNOWLEDGEMENTS	iii
LIST OF TABLES	viii
LIST OF FIGURES	ix
LIST OF ABBREVIATIONS.....	xiii
 CHAPTER	
1. INTRODUCTION AND REVIEW OF LITERATURE	1
1.1 Aortic Heart Valve Structure and Function.....	1
1.2 Aortic Heart Valve Cell Phenotypes	6
1.2.1 Valve endothelial cells (VECs).....	6
1.2.2 Valve interstitial cells (VICs)	8
1.3 Aortic Heart Valve Biomechanics.....	10
1.4 Aortic Heart Valve Calcification.....	16
1.4.1 Clinical Risk Factors.....	18
1.4.2 Pathological Characteristics.....	19
1.4.2.1 Lipid Deposition.....	19
1.4.2.2 Inflammation	20
1.4.2.3 ECM Remodeling.....	20
1.4.2.4 Angiogenesis	21
1.4.2.5 Osteoblast Differentiation	21
1.4.3 Genetic Factors	22
1.4.4 Pharmacological Treatment	23
1.4.5 Signaling Pathways of Calcification.....	24
1.4.5.1 Renin–Angiotensin System.....	24
1.4.5.2 Wnt Signaling.....	26
1.4.5.3 TGF- β Signaling.....	28
1.4.5.4 RANK-OPG Signaling.....	30
1.5 Hypertension.....	32
1.6 Statement of Hypothesis.....	36
1.6.1 Hypothesis.....	36

1.6.2	Specific aims	36
1.7	References	37
2.	GENERAL METHODOLOGY	45
2.1	Tissue Extraction and Culture	45
2.2	RNA Isolation.....	47
2.3	Real Time Quantitative –PCR.....	47
2.4	<i>In vitro</i> Pressure Bioreactor.....	48
3.	REGULATION OF PORCINE AORTIC VALVE INTERSTITIAL CELL PHENOTYPE BY MECHANICAL AND BIOCHEMICAL STIMULI.....	51
3.1	Introduction	51
3.2	Materials and Methods	53
3.2.1	Tissue and RNA Harvest	53
3.2.2	Real Time Quantitative–PCR	54
3.2.3	Immunohistochemistry	55
3.2.4	Western Blot	55
3.2.5	Statistical Analysis	56
3.3	Results.....	57
3.3.1	Elevated Pressure Induces Osteogenic differentiation of VICs	57
3.3.2	Exposure to Ang II Decreases Osteogenic Gene Expression of VICs.....	57
3.3.3	Exposure to Pressure Increases Osteogenic markers in Valve Leaflets.	60
3.3.4	Expression of Ang II Receptors in VICs	62
3.4	Discussion.....	64
3.4.1	A Major Role of Elevated Pressure in VICs Osteogenic Differentiation.....	65
3.4.2	Regulatory Role of Ang II in VICs Osteogenic Differentiation.....	68
3.5	References	73
4.	FUNCTIONAL MODELING OF PRESSURE INDUCED GENE EXPRESSION REVEALS MECHANOSENSITIVE SIGNALING PATHWAYS IN THE AORTIC VALVE	77
4.1	Introduction	77
4.2	Materials and Methods	79
4.2.1	Tissue Culture and RNA Harvest	79
4.2.2	cDNA Microarrays.....	79
4.2.3	Microarray Data Analysis	80
4.2.4	Gene Ontology Analysis and Data Modeling.....	80

LIST OF TABLES

Table		Page
3.1	Primers used for RT- PCR analysis	54
3.2	Antibodies used for Immunohistochemistry and Western Blot.....	56
4.1	Selected GO Biological Processes with differentially expressed genes associated with aortic valve disease.....	81
4.2	Primers used for RT- PCR validation	82

LIST OF FIGURES

Figure		Page
1.1	Aortic valve location in the heart ³	2
1.2	Anatomical characteristics of aortic valve leaflets. A. Localization of leaflets in the aortic valve. B. Schematic representation of a valve leaflet showing the location of the commissures, free edge and connection to the aortic wall.	3
1.3	Aortic valve leaflet structure. Photomicrograph showing immunohistochemical staining of an aortic valve leaflet emphasizing localization of three major layers (ventricularis, spongiosa, and fibrosa), and cellular types (endothelial and interstitial cells). Adapted from Schoen et al ¹	4
1.4	Schematic representation of the aortic valve leaflet. A. Cross sectional view of the leaflet showing localization of each layer relative to the aorta. B. Leaflet trilaminar configuration illustrating the elastin sheets within the ventricularis, GAG-rich matrix comprising the spongiosa, and the collagen fibers contained within the fibrosa. A. B modified from Vesely et al ¹⁵	5
1.5	Aortic valve dynamics in the cardiac cycle. A. Mechanical behavior of elastin and collagen fibers during valve motion. B. Schematic representation of architecture and configuration of collagen and elastin in systole and diastole. Modified from Schoen et al ¹	13
1.6	Typical plot of leaflet length vs. pressure gradient across the leaflet <i>in vivo</i> in a single dog. The circles represent measured leaflet length and measured pressure gradient in diastole. The bars represent measured leaflet length and assumed pressure gradient of 0 to 10mmHg in systole. The lengths ℓ_0 , ℓ , ℓ_1 , and ℓ_2 correspond to the gradients of 0, 10, 60, and 200mmHg, respectively. Diastolic strain is represented by ϵ_D , whereas systolic strain is represented by ϵ_S ¹⁴	15

1.7	Progression in Calcific Aortic valve disease. Morphological changes observed in aortic-valve anatomy as result of calcification are viewed from the aortic side with the valve open in systole. Adapted from Otto et al ⁶⁶	17
1.8	Pathological characteristics of aortic valve calcification.....	22
1.9	Renin- Angiotensin Signaling Pathway.....	26
1.10	Wnt Signaling Pathway.....	28
1.11	TGF- β Signaling Pathway.	30
1.12	RANK-OPG Signaling Pathway.....	32
1.13	Renin-Angiotensin vasoconstrictor mechanism for arterial pressure control.	35
2.1	Schematic representation of the <i>in vitro</i> pressure system. Valve leaflets were placed in 6-well tissue cultures plates within a stainless steel pressure chamber and placed inside an incubator (5% CO ₂ , 37°C) for 24 hours.....	50
3.1	mRNA expression levels of osteogenic markers, relative to 18s, in VICs exposed to normotensive (0-80 mmHg) and hypertensive conditions (0-120 mm Hg) for 24 hours. A. RUNX2, B. SSP1 C. ALP. Bars represent mean values + 95% confidence interval: * = p \leq 0.05.....	59
3.2	mRNA expression levels of osteogenic markers, relative to 18s, in VICs exposed to normotensive (0-80 mmHg) and hypertensive conditions (0-120 mm Hg) for 24 hours. A. SMAD1. B. BMP-7. Bars represent mean values + 95% confidence interval: * = p < 0.05.	60
3.3	Evidence of osteogenic proteins in porcine aortic valve exposed to: normotensive conditions (A - C); hypertensive conditions (D-F), normotensive conditions and Ang II (G-I); hypertensive conditions and Ang II (J-L). Representative immunohistochemical staining (brown, shown by arrows) of RUNX2 (A,D,G,J);SSP1 (B,E,H,K), and ALP (C,F,I,L) .Cell nuclei counterstained blue. All frames 40X magnification.	62

3.4	Protein expression of Angiotensin type 1 and Angiotensin type 2 receptors from valve leaflets exposed to cyclic pressure and Ang II treatment. Lane 1. normotensive cyclic pressure (0-80 mmHg), Lane 2. hypertensive cyclic pressure (0-120 mmHg); Lane 3. normotensive cyclic pressure Ang II (+), Lane 4. Hypertensive cyclic pressure Ang II (+).....	63
3.5	Schematic representation of and molecular interactions and cellular location among significantly expressed genes involved in BMP osteogenic signaling pathway. Nodes are displayed using various shapes that represent the functional class of the gene product: Y shaped figures represent transmembrane receptors; down-pointing triangles represent cytokines, horizontal ovals represent transcription regulators. Continuous lines show direct interactions between nodes and dashed lines show indirect interactions. Lines beginning and ending on the same node show self regulation. Arrowheads show directionality of the relationship. SPP1 is the alternative name of SSP1.....	68
4.1	The image shows a total mRNA gel like-image produced by the Bioanalyzer. (Six samples used in the microarray experiment are shown). Lane L: Size markers. Lanes 1-3: total mRNA from valve leaflets exposed to normotensive cyclic pressure (0-80 mmHg), Lanes 4-6: total mRNA from valve leaflets exposed to hypertensive cyclic pressure (0-120 mmHg). The 28S and 18S distinctive ribosomal RNA bands are observed for all samples.....	83
4.2	Real-time PCR validation of microarray data. Gene expression patterns from microarray analysis (dark bars) and semi-quantification through RT-PCR (clear bars). Values represent fold change in gene expression of samples in hypertensive conditions relative to normotensive conditions.	85
4.3	Cellular localization of differentially expressed transcripts from hypertensive tissue. GO Cellular Component annotations were summarized to broad level terms using the GOA whole proteome GO Slim set. The net regulatory effect was determined by subtracting the number of decreased proteins from the number of increased proteins in each GOSlim category.....	87

4.4	Molecular Functions of differentially expressed transcripts from hypertensive tissue. GO Molecular function annotation were summarized to broad level terms using the GOA whole proteome GO Slim set. The net regulatory effect was determined by subtracting the number of decreased proteins from the number of increased proteins in each GOSlim category.....	88
4.5	Biological Process of differentially expressed transcripts from hypertensive tissue. GO Biological Process were summarized to broad level terms using the GOA whole proteome GO Slim set. The net regulatory effect was determined by subtracting the number of decreased proteins from the number of increased proteins in each GOSlim category.	89
4.6	Potential biological processes involved in valve remodeling. Comparison of gene expression levels of four potential valve remodeling mechanisms suggested by hypothesis-driven GO modeling.	90
4.7	TP53 network. The network shows molecular interactions among significantly expressed genes involved in cell inflammatory response, ECM remodeling, oxidative stress and the transcription factor TP53 under elevated pressure conditions. Green color represents a decrease and red represents an increase in gene expression. Nodes displayed represent the functional class of the gene product: down-pointing triangles represent kinases; diamonds represents enzymes, horizontal ovals represent transcription regulators; and circles represent other types of molecules. Continuous lines show direct interactions between nodes and dashed lines show indirect interactions. Lines beginning and ending on the same node show self regulation. Arrowheads show directionality of the relationship.....	92
4.8	Cell Death network. The network shows the molecular interactions among significantly expressed genes involved in pro apoptotic mechanisms in which gene expression was altered by elevated pressure. Symbols are as described in the legend for figure 4.7.....	93

LIST OF ABBREVIATIONS

ALP	Alkaline phosphatase
Ang II	Angiotensin II
AT1	Angiotensin receptor type 1
AT2	Angiotensin receptor type 2
BMP-7	Bone Morphogenic protein 7
ECM	Extracellular matrix
GTX7	Glutathione peroxidase 7
MMPs	Matrix metalloproteases
SSP1	Osteopontin
RUNX2	Runt-related transcription factor 2
SMAD1	Mad-related protein 1
SOD2	superoxide dismutase 2
TIMPs	Tissue inhibitor of matrix metalloproteasesg
VECs	Valvular interstitial cells
VICs	Valvular interstitial cells

CHAPTER 1

INTRODUCTION AND REVIEW OF LITERATURE

1.1 Aortic Heart Valve Structure and Function

The heart is a three-dimensional hollow, cone-shaped muscle that is responsible to drive blood from the low-pressure venous system to the high – pressure arterial side of the circulation. The heart is anatomically divided in four chambers: the right atrium (RA), right ventricle (RV), left atrium (LA), and left ventricle (LV)^{1,2}. Efficient blood pumping occurs because the organized sequence contraction of the chambers and the presence of heart valves that ensure unidirectional blood flow through the circulatory system³. Cardiac valves are structures that are designed to work like one-way doors. When each chamber contracts, the valve at its exit opens, and when the contraction is finished, the valve closes so that blood does not flow backwards⁴. Normally, there are four valves within the heart: the tricuspid valve located between the right atrium and the right ventricle, the pulmonary valve between the right ventricle and the pulmonary artery, the mitral valve between the left atrium and the left ventricle and the aortic valve between the left ventricle and the aorta⁵.

The aortic valve (AV), located on the left-hand side of the heart, ensures unidirectional blood flow from the left ventricle to the ascending aorta without obstruction or regurgitation during ventricular contraction (systole) and prevents backflow during ventricular relaxation (diastole) and filling^{1, 6, 7} (Figure 1). Of the four

valves, the AV is the most frequently associated with disease and surgery ⁸. The aortic valve is functionally and mechanically very different from other cardiovascular structures (e.g. blood vessels, myocardium), and its unique structural conformation is designed to provide a high degree of flexibility during systole, but also a high degree of strength to resist the diastolic pressure load ⁹.

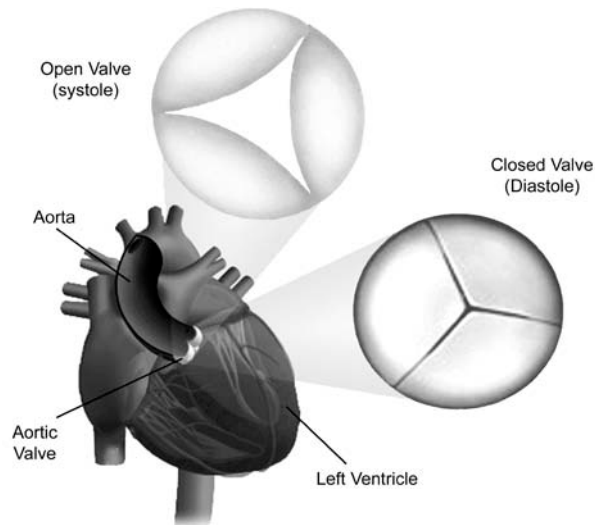


Figure 1.1 Aortic valve location in the heart ³.

The normal aortic valve is composed by three semilunar-shaped leaflets. The curved edge of the leaflet is attached to the aortic wall while the straight edge is free ². The aortic wall bounded by the attachments of the curved edge forms a saccular dilation called the sinus of Valsalva ^{2, 4, 7, 10}. Each leaflet and corresponding sinus of Valsalva are named according to their anatomical position to the coronary arteries, thus, they are known as left coronary (LC) and right coronary (RC) leaflets ^{7, 10}. The remaining leaflet is not associated with any coronary artery and is subsequently recalled noncoronary (NC) leaflet (Figure1.2 A) ^{7, 10}. The right coronary leaflet has generally a larger size in

comparison to the left one and the non-coronary leaflets. In addition, the three leaflets are completely separated at the free edges by commissures (Figure 1.2 B). The commissures are named relative to the leaflet on either side, thus, the intercoronary commissure is located between the left and right coronary leaflets; the left-noncoronary commissure is located between the left and the noncoronary; and the right-noncoronary commissure is located between the right and the noncoronary leaflets ².

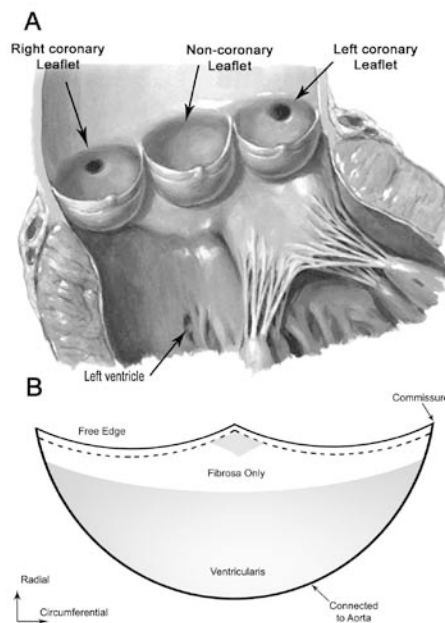


Figure 1.2 Anatomical characteristics of aortic valve leaflets. A. Localization of leaflets in the aortic valve. B. Schematic representation of a valve leaflet showing the location of the commissures, free edge and connection to the aortic wall.

Structural integrity of the leaflets is vital for proper valve function as they carry most of the mechanical stress during the cardiac cycle ^{5, 11}. Each leaflet is a trilaminar structure with an approximate thickness of 0.605 ± 0.196 mm ¹. Each layer has a specific arrangement of cells (fibroblasts, mesenchymal cells, endothelial cells) and a

polysaccharide-rich extracellular matrix (collagen, elastin, GAGs) (Figure 1.3)¹². It has been demonstrated that these layers work in concert to provide tensile strength and pliability to the aortic valve, as there are approximately 40 million openings and closures of the valve per year (equivalent to approximately 3.7 billion cycles in a single lifetime)⁹.

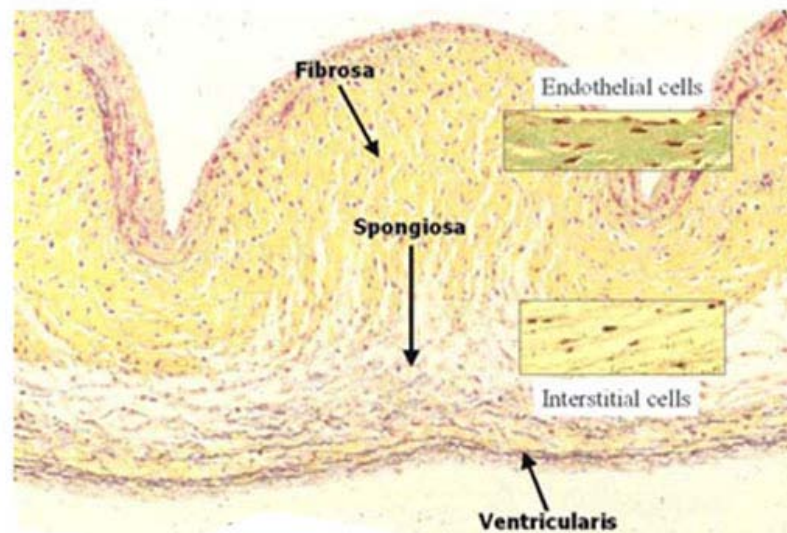


Figure 1.3 Aortic valve leaflet structure. Photomicrograph showing immunohistochemical staining of an aortic valve leaflet emphasizing localization of three major layers (ventricularis, spongiosa, and fibrosa), and cellular types (endothelial and interstitial cells). Adapted from Schoen et al¹.

In addition, the composition and structural organization of each layer are major determinants of valvular mechanical function¹². Facing the left ventricle is the ventricularis layer; it constitutes about 29% of the overall leaflet thickness and forms the inflow surface of the valve. It is composed of elastin fibers that are aligned in a radial direction, perpendicular to the leaflet free margin (Figure 1.4 A)^{5, 12, 13}. Located immediately below the aorta is the fibrosa layer; it constitutes 41% of the overall leaflet

thickness and forms the outflow surface of the valve. It is primarily composed of interstitial cells and a dense network of collagen fibers 13, 14. These circumferentially-oriented packed collagen fibers run parallel to the free edge of the leaflets and they form the macroscopical folds seen in the aortic surface of each leaflet 11, 12. Both the ventricularis and the fibrosa are covered by a thin layer of endothelial cells. Finally, the spongiosa, between the fibrosa and ventricularis, constitutes the larger portion of the overall leaflet thickness and it is composed of fibroblasts, mesenchymal cells, a disperse proteoglycans and glycosaminoglycans (GAGs)- rich matrix and water (Figure 1.4 B) 15, 16.

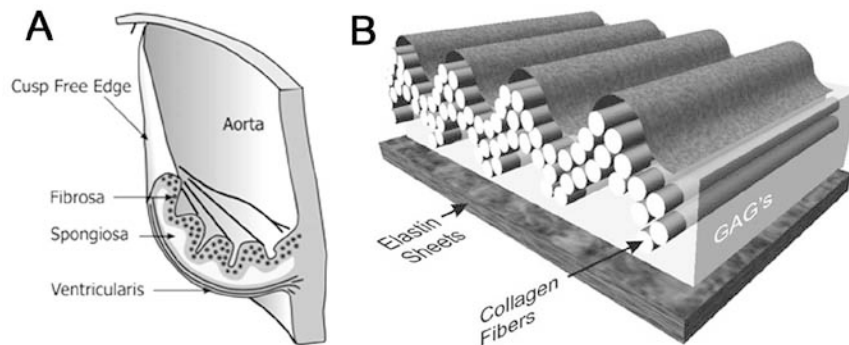


Figure 1.4 Schematic representation of the aortic valve leaflet. A. Cross sectional view of the leaflet showing localization of each layer relative to the aorta. B. Leaflet trilaminar configuration illustrating the elastin sheets within the ventricularis, GAG-rich matrix comprising the spongiosa, and the collagen fibers contained within the fibrosa. A. B modified from Vesely et al ¹⁵

The functional consequence of this organization is that each layer displays differential mechanical properties that contribute to dynamic movement of the valve during the cardiac cycle ^{12, 13}. Hence, the fibrosa, rich in collagen fibers, provides

resistance to the tensile forces experienced by the leaflets during valve closing (diastole); the ventricularis, rich in elastin fibers, allows stretching of the leaflet during valve opening (systole) and the spongiosa provides a cushioning, shear absorption function, and enables local movement and shearing between the fibrosa and ventricularis layers during dynamic load ^{11, 12}

1.2 Aortic Heart Valve Cell Phenotypes

The normal aortic valve leaflet is populated with two main cellular phenotypes: (1) valve endothelial cells (VECs) and (2) valve interstitial cells (VICs) ⁹. Both cell types reside within the valve extracellular matrix (ECM) composed by collagen, elastin, and GAGs ¹⁷. VICs are embedded within the extracellular matrix (ECM) of the leaflet while VECs line the surfaces of each leaflet. Importantly, there is a three way communication system between VECs/VICs and EMC, in which ECM structure depends on biosynthetic activity of VECs/VICs, and valve cell phenotype is influenced by the mechanical properties of the ECM ^{18, 19}. The interactions between valve cells and ECM are major determinants of normal aortic valve structure. Thus, abnormal mechanical and biochemical stimuli on valve leaflets precipitate a series of biological changes in the cells and in the ECM around cells, which in turn results in alterations in the mechanical behavior of the valve ^{1, 5, 20}. In addition, it has been proved that communication between VICs and VECs plays an important role in valve ECM homeostasis ²¹.

1.2.1 Valve endothelial cells (VECs)

Valvular endothelial cells line the outer layers of the leaflet. They provide a smooth and non thrombogenic blood interface on the ventricular and aortic side of each

of the valve leaflets^{17, 22}. Additionally, VECs regulate immune and inflammatory reactions in the valve; and regulate valve interstitial cell phenotype⁹. It has been shown that VECs are phenotypically different from endothelial cells located in other sites of the in the vascular system, they have unique characteristics that include: (1) specific pattern of aligning, as VECs align perpendicular to the direction of blood flow^{19, 23}, (2) proliferative activity, VECs under shear are more proliferative than their aortic counterparts²¹, (3) specific genetic profiles, VECs located on aortic side of the valve over express genes that promote valve calcification (i.e. BMP4), this is coupled with under expression of genes that act as inhibitors of calcification (i.e OPG)²⁴. Additionally, VECs from the aortic side appear to express low levels of pro inflammatory genes and antioxidative enzymes, underlining the protective role of valve endothelium in against ROS- and inflammatory mechanisms^{21, 25}.

VECs are directly exposed to shear stress, and thus, they are highly responsive to the local shear changes. Alterations in stretch or shear stress correlate with pathological activation of VECs and valvular endothelial dysfunction that triggers a series of clinical events, including inflammatory reactions, release of vasoactive agonists, calcification, and blood clots²¹. In addition, activated VECs play a key role in proinflammatory mechanisms; by increasing the expression of pro inflammatory proteins such as ICAM-1, VCAM-, and E-selectin VECs facilitate inflammatory cell recruitment and accumulation within the valve^{9, 25}. Extensive infiltration of inflammatory cells is associated with altered ECM synthesis and calcification in valve tissue; hence alterations in the biosynthetic activity of VECs may lead to structural alteration and dysfunction of the valve. Another critical role of VECs in valve homeostasis is the regulation of valvular

interstitial cell phenotype. *In vitro* studies have shown that VECs influences the valvular interstitial cell phenotype by modulating the expression of α smooth muscle actin (SMA)¹⁹. In addition, it has been show that VICs proliferation is also influence by communication with VECs.

1.2.2 Valve interstitial cells (VICs)

Valvular interstitial cells (VICs) are the major cellular components of the aortic valve²⁶. They are distributed through all layers of the leaflet and play a key role in regulating valve tissue homeostasis in normal and pathological conditions. Several studies have demonstrated the multiple and diverse roles that VICs have in maintaining normal valve functions¹⁸. One of the main roles of VICs is regulation of ECM remodeling. VICs maintain optimal valve function through continual synthesis and repair of structural components of the ECM (collagen, elastin, GAGs)²⁷⁻²⁹. Furthermore, VICs are able to regulate and remodel the ECM through expression of matrix metalloproteinases MMPs and their inhibitors TIMPs³⁰. These proteins are involved in synthesis and degradation of collagen and elastin³¹. Experimental evidence shows that alterations in the native environment of VICs results in increased ECM degradation and remodeling that leads dysregulation of normal valve architecture³².

A major feature of VICs is their extraordinary capacity to modulate their biosynthetic activity and phenotype in response to the local biomechanical environment experienced by the valve^{9, 33, 34}. *In vitro* studies show that VICs in the normal valve are quiescent but in response to mechanical and biochemical stimuli they activate and differentiate into diverse phenotypes associated with remodeling and repair mechanisms. Therefore, five different phenotypes have been described:

(1) Embryonic progenitor mesenchymal cells (eVICs): this cell subset is mainly present during valve development. They are involved in the process that initiates valve formation in the embryo. Cellular migration and proliferation of eVICs give rise to quiescent VICs (q VICs) ³².

(2) Quiescent VICs (qVICs): this cell subset is mainly present in the normal adult valve. They are thought to maintain physiological valve structure and function through synthesis and release of ECM remodeling proteins. qVICs display a fibroblast-like phenotype, characterized by the presence of vimentin (intermediate filaments), and very low levels of α -SMA, MMP-13 (proteolytic enzymes), and SMemb (non-muscle myosin heavy chain) ^{29, 35}. However, transition of qVICs to an activated phenotype results in response mechanical and biochemical signals. This phenotypic transition is often associated with valve injury response and/ or abnormal mechanical conditions ³⁶.

(3) Activated VICs (aVICs): this cell subset is regularly associated with pathological conditions in aortic valve. aVICs express high levels of α - smooth muscle actin, and other contractile proteins ¹⁸. They are believe to activate cellular repair processes including proliferation, migration, and abnormal extracellular matrix remodeling through increased expression of a variety of catabolic enzymes, membrane proteins and growth factors, and cytokines ^{37, 38}. aVICs have a unique proliferative and differentiation potential, and it is believed in response to specific biochemical signals (i.e. TGF- β , BMP2) they trans differentiate into osteoblast-like cells ^{39, 40}.

(4) Osteoblastic VICs (obVICs); this cell subset is frequently found in calcified valves ^{41, 42}. They regulate osteogenic and calcification mechanisms in heart valve. obVICs characterize by the expression of multiple bone-related molecules

including alkaline phosphatase (ALP), Runx2, type I collagen (Col I) and osteocalcin (OC) and the formation of mineralized bone-like structures^{43, 44}. During osteoblast differentiation these molecules are expressed at different phases and reflect different aspects of osteoblast function and bone formation⁴⁵.

(5) Progenitor VICs (pVICs): also referred as valvular stem cells is the valvular cell type least well defined in the aortic valve. They consist of a heterogeneous population of progenitor cells that derive from bone marrow cells, circulating cells, and resident valvular progenitors cells⁴⁶. They characterize by the expression of stem cell markers such as CD34, CD133. In addition, they have a high proliferative potential and the ability to form blood vessels³². At present there is very limited knowledge of the role of this cell type in aortic valve homeostasis, but it is believed that they may be important in valve repair mechanisms.

VICs are strongly attached to the surrounding ECM via diverse of cell-surface, cytoskeletal and a muscle protein, this fact enables them to sense and response to the biochemical and mechanical signals experienced by the valve²⁷. Therefore, any substantial change in the native environment of the valve can result in abnormal cellular phenotypes, secretion of diverse growth factors, cytokines, chemokines and matrix remodeling enzymes (MMPs, TIMPs), which can compromise the durability and stability of the valve^{31, 47, 48}.

1.3 Aortic Heart Valve Biomechanics

The dynamic movement the aortic valve is driven by the highly dynamic and complex mechanical forces generated by the higher transvalvular pressure gradients present on the left side of the heart⁴⁹. This includes radial pressure, shear stress that

accompanies blood flow, and hoop stress associated with the cardiac cycle ^{1, 2}. It is estimated that the normal aortic valve opens and closes more than 3 billion times during average lifetime ⁵. Opening and closing of the valve involves changes in the shape, dimensions, and stress in the structural components of the leaflets (i.e. collagen realignment and crimping, elastin stretching and shortening) ^{12, 13, 50}.

During systole, the pressure gradient across the valve is basically zero, as the left ventricle contracts and pumps the blood, the aortic valve opens widely and blood flows freely from the left ventricle to the aorta ^{1, 5}. During this time, as the valve opens, each leaflet bends towards the aortic wall. To allow efficient valve opening elastin fibers in the ventricularis layer recoil decreasing the surface area of each leaflet ¹⁶. In addition, during systole, two different patterns of flow are generated in each side of the leaflet, thus, the ventricularis layer is exposed to laminar shear stress, and the fibrosa layer is exposed to a disturbed, oscillatory shear stress ¹³.

During diastole, the normal pressure gradient across the valve is approximately 80mmHg. As the valve closes, and as a result of the increasing pressure, valve leaflets experience compressive strain and biaxial planar stretch ¹³. Thus, in order to withstand the increasing pressure, the collagen fibers in the fibrosa layer unfold, taut and align with each other. At the end of diastole the leaflets are perfectly aligned preventing blood from flowing backward to the left ventricle from the aorta. Aortic valve is constructed with a special strong, yet pliable, fibrous tissue that can withstand the regimens experienced in every cardiac cycle. Hence, in order to respond to the mechanical demands during systole (flexion) and diastole (tension) the aortic and ventricular sides of valve leaflets exhibit drastically different mechanical properties, underlining the anisotropic behavior of valve

tissue^{12, 13}. Indeed, it has been demonstrated that each layer makes a mechanical contribution during each phase of the cardiac cycle. During systole, the leaflet response to mechanical flexure is mainly transmitted by radially-oriented elastin fiber network in the ventricularis^{15, 51}, whereas in diastole the leaflet response to mechanical tension is mainly transmitted by the circumferentially oriented collagen fibers in the fibrosa layer (Figure 1.5)^{12, 52, 53}.

Cyclic pressure is one of the most important mechanical forces to which the aortic valve is exposed during the cardiac cycle. Normally, the pressure gradient across the aortic valve is approximately 80mmHg; however, the pressure gradient can increase and become quite high during hypertension (>100 mmHg). Any major increase in the diastolic pressure gradient across the valve leads to changes in valve leaflet perimeter, thus imposing larger stresses within the leaflets⁹.

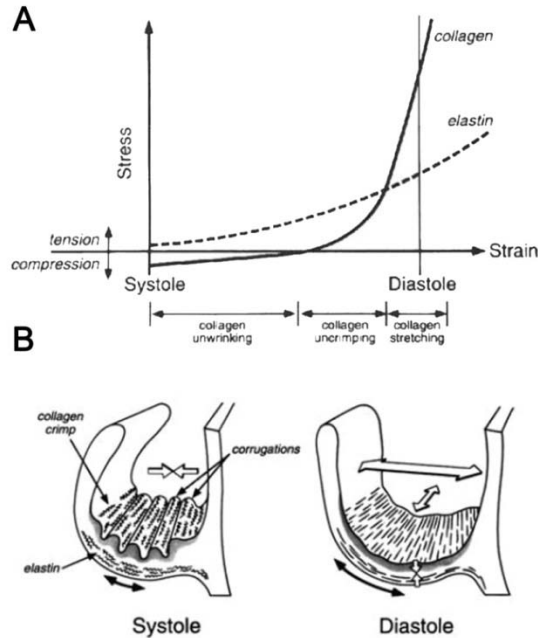


Figure 1.5 Aortic valve dynamics in the cardiac cycle. A. Mechanical behavior of elastin and collagen fibers during valve motion. B. Schematic representation of architecture and configuration of collagen and elastin in systole and diastole. Modified from Schoen et al ¹.

In an important study by Thubrikar et al ¹⁴, the effects of transvalvular pressure on aortic valve length were measured (Figure 1.6). In addition, they developed a model of the *in vivo* leaflet stresses as a function of the transvalvular pressure and considering bending and stretching as independent components, thus:

$$Stress = \frac{PR}{T} \pm \frac{E(T)}{2R} \quad (1-1)$$

P is the transvalvular pressure, R is the radius of the leaflet, T is the thickness, E is the tissue modulus of elasticity, and the bending stresses are either tensile (+) or compressive (-) depending on the side of the leaflet ¹⁴.

Furthermore, several studies have evaluated the effects of elevated pressure by measuring three types of mechanical loads known to be involved in cardiac cycle namely stretch, shear and pressure. First, non physiological mechanical stretch has been known to stimulate cell proliferation, apoptosis and capthesin expression ⁵⁴. In addition, non physiological stretch induces increase in collagen content and alteration in valve mechanical properties. Secondly, cyclic pressure is involved in altered DNA and collagen synthesis, increased cellular stiffness and altered collagen arrangement in valve tissue ^{50, 55, 56}. Some studies have suggested that altered shear stress regimens result in endothelial injury and activation of pro inflammatory mechanisms in the valve.

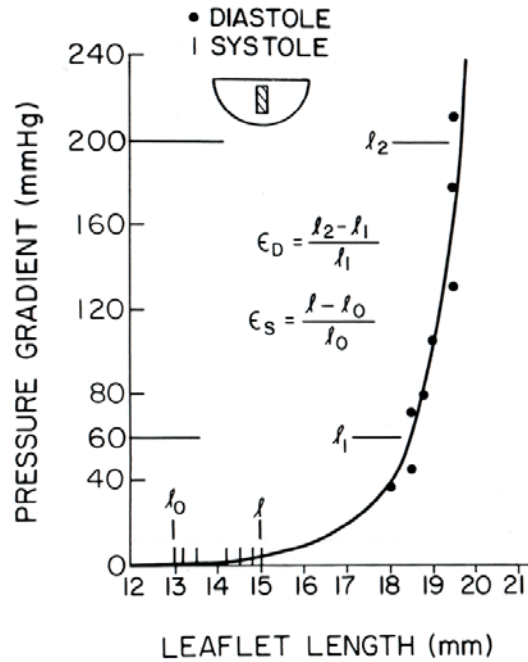


Figure 1.6 Typical plot of leaflet length vs. pressure gradient across the leaflet *in vivo* in a single dog. The circles represent measured leaflet length and measured pressure gradient in diastole. The bars represent measured leaflet length and assumed pressure gradient of 0 to 10mmHg in systole. The lengths l_0 , l , l_1 , and l_2 correspond to the gradients of 0, 10, 60, and 200mmHg, respectively. Diastolic strain is represented by ϵ_D , whereas systolic strain is represented by ϵ_S ¹⁴.

Several experimental models have revealed the drastic changes that occur in valve structure during each cardiac cycle^{5, 7}. Moreover, it has been shown that the long-term consequences of extreme and continual loading conditions may include alterations in valve cell phenotype, abnormal ECM architecture, valve degeneration and failure⁵⁷. These studies underline the significant role of mechanical loads in regulating the mechanical and biological behavior of the aortic valve.

1.4 Aortic Heart Valve Calcification

Calcific aortic valve disease (CAVD) is the most common disease of the aortic valve. Epidemiological studies of different populations have shown that CAVD is present in 28% of adults with a mean age of 50 years⁵⁸. Similar results have been found in previous population-based studies, where the prevalence of the disease is between 21%-26% in adults aged 55–71 years^{59,60}. It is estimated that CAVD is the most prevalent valvular disease in western population and the main cause of heart valve replacement in the elderly, with about 40,000 valve operations in Europe and 95,000 in the United States done per year⁸.

Increased leaflet stiffness and thickness, reduction in the orifice area, and incomplete opening of the valve are the main characteristics of calcified human valves⁶¹⁻⁶³. When calcification and thickening are severe, the increased stiffness of the valve leaflets results in an obstruction at the valvular level. Presumably, valvular narrowing associated with obstruction due to restricted opening of valve leaflets generates turbulent flow in the region of the sinus of Valsalva⁹. Increased Reynolds stress causes lysis and fragmentation of red blood cells leading to the release of prothrombotic agents.

Functionally, calcific aortic valve disease can be divided into two stages. The first is calcific aortic sclerosis, in which valve leaflet thickening and calcification are present; blood flow and leaflet mobility are not compromised¹. In contrast, calcific aortic stenosis, the end stage of the disease, the leaflet mobility is sufficiently restricted to impede left ventricular outflow (Figure 1.7)^{2,3}. Calcific aortic sclerosis is present in more than 30% of patients over 65 years of age, with 2% showing signs of calcific aortic stenosis. The prevalence of aortic sclerosis increases to 48% in people above 84 years.

Severe symptomatic calcific aortic stenosis is associated with a life expectancy of less than 5 years.

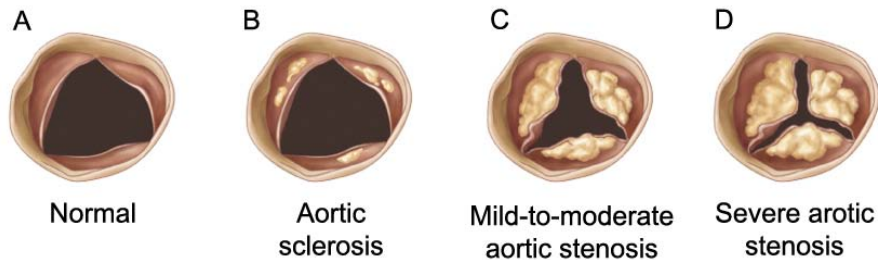


Figure 1.7 Progression in Calcific Aortic valve disease. Morphological changes observed in aortic-valve anatomy as result of calcification are viewed from the aortic side with the valve open in systole. Adapted from Otto et al ⁶⁶

Although the prevalence of the disease increases with age, clinical evidence suggests that calcific aortic valve disease does not develop due to age-related degeneration process but is an activated cell process with identifiable clinical risk factors, pathological characteristics, genetic factors, and molecular pathways that mediate disease progression ⁴. Furthermore, several lines of evidence underline mechanical stress as a key factor initiating the development of CAVD, as calcific lesions occur preferentially in the fibrosa layer and correlate with areas of functional stress⁵. The susceptibility to lesion formation on the aortic rather than ventricular surface of the aortic valve may result from the higher absolute pressure and transvalvular pressure gradients present on the left side of the heart ⁶. Pressure is one of the hemodynamic forces to which the aortic valve is exposed during the cardiac cycle, and thus, hypertension is an obvious candidate for the development of calcific aortic valve disease.

Potential explanations for the association of hypertension with aortic valve disease include the possibility that hypertension results in abnormally high tensile stress on the aortic leaflets^{7,8}. Furthermore, blood pressure is an important determinant of the mechanical environment of the aortic valve⁹. The assessment of patients with CAVD includes the measurement of transvalvular pressure gradient and aortic valve area, as well as assessment of left ventricular geometry and function¹⁰. Alternatively, effects of hypertension may be flow dependent. Hypertension changes the flow patterns across the valve. Acute changes in blood pressure can significantly result in turbulent flow regimes across the valve, as a consequence of changes in transvalvular pressure gradient, resulting in low shear stress and endothelial injury¹¹⁻¹³. Despite the incidence of hypertension and CAVD, it remains unknown how hypertension might influence the progression and severity of the disease.

1.4.1 Clinical Risk Factors

Conventional risk factors that are characteristic of atherosclerosis such as age, active smoking, male gender, renal failure, high low-density lipoprotein (LDL), hypercholesterolemia, hypertension, diabetes, and metabolic syndrome are also associated with development of CAVD¹⁴⁻¹⁶. Clinical studies have shown high levels of LDL in human calcified valves¹⁷. In addition, it has been revealed that patients with family history of hypercholesterolemia also develop aortic valve lesions that calcify with age^{18, 19}. In other studies, hypertension was correlated with CAVD, as one third of patients with calcific aortic stenosis also have concomitant systemic hypertension^{20, 21}. Although CAVD shares some histological similarities with atherosclerosis, including the presence of oxidized lipoproteins, inflammatory cells, calcification and the production of

proteins by activated macrophages, there are substantial differences as well. In atherosclerosis the clinical effects of the disease are related to the instability of the plaques and associated formation of thrombus that can lead to other cardiovascular episodes (i.e. stroke), in CAVD tissue calcification is more severe, the clinical effects are associated with leaflet stiffness and narrowing at the opening of the aortic valve, ventricular outflow obstruction, angina, ventricular overload ²². In addition, it has been observed that even minor calcification of the valve increases the risk of other cardiovascular disorders (stroke, myocardial infarction) by 50% ²³. Further studies to determine whether control of risk factors prevents CAVD appear to be necessary, as lipid-lowering therapies and control of blood pressure have shown limited effects in the control and progression of CAVD²⁴.

1.4.2 Pathological Characteristics

The most critical morphological features of calcified valves include: ECM remodeling, increased expression of pro-inflammatory cytokines, calcification, angiogenesis, lipid deposition, and changes in valve cell phenotype ²⁵⁻²⁷ (Figure 1.8).

1.4.2.1 Lipid Deposition

One of the main histological features associated with calcific aortic valve disease is the presence and accumulation of lipids in calcified lesions. Further evidence showing the involvement of lipid levels have been shown in animal models that develop calcification secondary to a high cholesterol/high lipid diet. In addition, clinical evidence shows that valve lesions express high levels of oxidized lipids, apolipoproteins A, E, and B in areas of severe calcification ²⁸⁻³⁰.

1.4.2.2 Inflammation

Both *in vitro* and *in vivo* evidence have shown that valvular calcification is an active process controlled by inflammatory mediators. Several histological studies demonstrate the presence of monocytes, macrophage infiltration, T Lymphocytes, and mast cells in early calcified lesions³¹⁻³³. These cells are normally not expressed in aortic valve and their presence indicates the initiation of an injury response mechanism. Additionally, it has been proven the presence of potent cytokines, chemokines and members of the complement system in calcified valves including: IL2, IL1 β , MCP-1, ICAM-1, HLA-DR³⁴. In addition, it has been shown the expression of tenascin C, a protein involved in inflammatory responses³⁵. These evidences along with findings that pro-inflammatory cytokines promote calcification *in vitro* further indicate that inflammation is a crucial factor that contributes to valve calcification.

1.4.2.3 ECM Remodeling

Immunohistochemical evidence shows that calcified aortic valves present an altered pattern of ECM remodeling. This is evidenced by the increased expression of Matrix Metalloproteases (MMPs) and capthesins (K, V, S)³⁶⁻³⁸. MMPs are a family of proteinases that regulate collagen turnover and ECM synthesis in the valve. Up regulation of MMP3/2/9 has been found in calcified valves; furthermore it has been shown that inflammatory cytokines (i.e IL1 β , TNF- α) enhance the expression and activities of MMPs³⁹. Valve ECM synthesis is dependent on the balance between MMPs and their inhibitors TIMPs. The MMP and TIMP proteases regulate ECM remodeling through the degradation of diverse ECM components including collagen, elastin and proteoglycans⁴⁰. In addition, calcified valves show increased expression of capthesins, a group of

proteases that mediate ECM remodeling through the degradation of elastin fibers. Dysregulation of ECM remodeling leads to valve calcification and stiffening⁴¹.

1.4.2.4 Angiogenesis

It has been reported that in contrast to normal heart valves, calcific aortic valve show signs of neo vascularization in areas of bone lesion. Formation of new capillary enhances the calcification process by facilitating the entry of inflammatory cells and lipids to the lesion site. In addition, it has been shown that VEGF1, VEGF-A, and VEGF1/2 receptors are present in high levels in calcified human valves⁴². The importance of these pro-angiogenic factors resides in their capacity to promote endothelial cells migration and proliferation required to neovascularization⁴³. Additionally, anti angiogenic factors such as chondromodulin I, SPARC and endostatin have been found to be reduced in calcified valves, reduced levels of these factors may lead to rapid outgrowth of capillaries that facilitates bone formation in the calcified valve^{44, 45}.

1.4.2.5 Osteoblast Differentiation

Histological studies suggest that CAVD may result from a process similar to that of active bone formation. Calcified valves characterized by the presence of calcific deposits and osteoblast like cells that express high levels of bone markers, extracellular matrix proteins such as alkaline phosphatase, osteopontin, osteoprotegrin, bone morphogenetic proteins, and the osteoblast-specific transcription factor CBFA-1⁴⁶⁻⁴⁹.

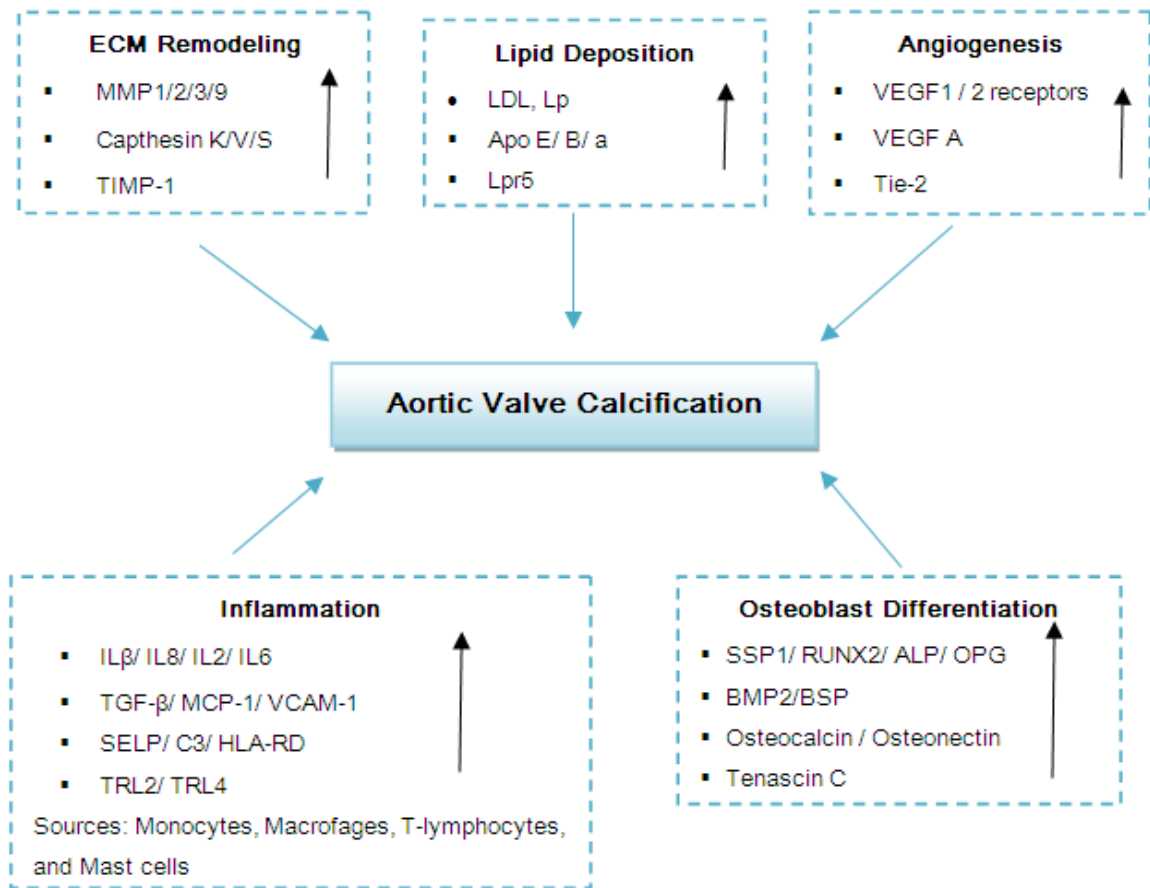


Figure 1.8 Pathological characteristics of aortic valve calcification.

1.4.3 Genetic Factors

Growing evidence suggests that genetic factors may not only predispose to developmental defects such as bicuspid aortic valve but also modulate the risk of calcific valve disease. Congenitally bicuspid aortic valve, which is present in about 0.5 to 0.8% of the population, is the underlying anatomy dysfunction in the majority of valve replacements for aortic stenosis⁵⁰⁻⁵². Clinical evidence supports this fact, with evidence that ≈49% valve replacement correspond to patients with congenital bicuspid valve⁵³⁻⁵⁵. Although it has been demonstrated the genetic nature of congenital bicuspid valve and its association with calcific valve disease, the exact mode of inheritance has not been

elucidated ^{56, 57}. In addition, some epidemiological studies have shown that genetic mutations in NOTCH1 gene, polymorphisms in the vitamin D receptor, estrogen receptor, interleukin-10, and apolipoprotein E4 allele increase the risk of developing CAVD , underlining the genetic contribution in the development of CAVD ⁵⁴.

1.4.4 Pharmacological Treatment

The presence of high levels of lipids and cholesterol in calcified valve lesions have led to the novel proposal that pharmacological strategies effective in atherosclerosis, such as hepatic hydroxymethylglutaryl coenzyme A reductase-inhibitor (statin) therapy, might slow the progression of CAVD ⁵⁸. However, recent clinical studies have shown the limited effects of lipid-lowering statins treatment on slowing or reversing CAVD. Another class of therapy with potential benefits in the treatment of CAVD is the use of Angiotensin-converting enzyme inhibitors and Angiotensin 1 receptor blockers (ARBs). Previous studies have shown high levels of members of the RAS system in human calcified valves raising the possibility that the calcification process might be attenuated by inhibiting the activity of ACE and blocking AT-1R. The results of these studies are contradictory, while some clinical studies have shown reduction in the levels of progression of CAVD; others suggest that may be used to slow the rate of progression of the disease but not for its prevention ⁵⁹. Other interesting studies show the association of low levels of Fetuin-A and progression of aortic valve calcification. Fetuin-A is a serum-based inhibitor of calcification, and low levels of this protein in the plasma are associated with an accelerated progression of AVC. Thus, stabilization of fetuin-A serum levels may appear as possible approach. However, these results are based on a relatively small patient population and a therapeutic approach has not yet been investigated ⁶⁰. Although

several clinical evidence show that CAVD is an actively cell regulated process, and thus it could be potentially treatable, currently there are no known pharmaceutical therapies to prevent calcific aortic valve disease progression.

1.4.5 Signaling Pathways of Calcification

Although the mechanisms regulating aortic valve calcification are not completely understood⁶¹, experimental evidence shows that there are several signaling mechanisms that are associated with the initiation and progression of aortic valve disease which include: Renin-Angiotensin System, Wnt Signaling, TGF β signaling, and RANKL-OPG signaling.

1.4.5.1 Renin–Angiotensin System

Recent studies suggest a role for the renin-angiotensin system (RAS) in calcific valve stenosis progression⁶²⁻⁶⁴. The RAS signaling begins with the production of angiotensinogen in the liver. Sympathetic stimulation, hypotension, and sodium alteration in the plasma stimulate the release of renin by the kidney. Renin hydrolyzes angiotensinogen to produce the inactive precursor angiotensin I. Angiotensin I is cleaved by angiotensin converting enzyme (ACE) to yield active angiotensin II (ATII). Angiotensin II stimulation of AT1 receptors stimulates systemic vasoconstriction and expression of plasminogen activator inhibitor (PAI), while Angiotensin II stimulation of AT2 receptors may cause vasodilation and apoptosis⁶⁵. Histological evidence shows that angiotensin-converting enzyme (ACE), Angiotensin II, and the angiotensin II type 1 receptor are up-regulated in human calcific aortic valves⁶⁶. Importantly, Angiotensin II (Ang II) has been shown to cause oxidative stress, inflammation, increased ECM

remodeling, cell proliferation, and migration of vascular and valvular cells *in vitro* ⁶⁷. In addition, cathepsin G and chymase ⁶⁸, two enzymatic mediators of Ang II, are also frequently found in calcified valves. Another interesting link between valve calcification and RAS signaling is the presence of bradykinin (BK), a potent antifibrotic agent that is degraded by ACE, cathepsin G, neural endopeptidase (NEP). Degradation of bradykinin results in adverse ECM remodeling and fibrosis, implying that bradykinin is essential for the functional and structural integrity of the valve ⁶⁹. Recent studies reveal that NEP is also up regulated in calcified valves, giving more evidence of the role of RAS in valve calcification (Figure 1.9).

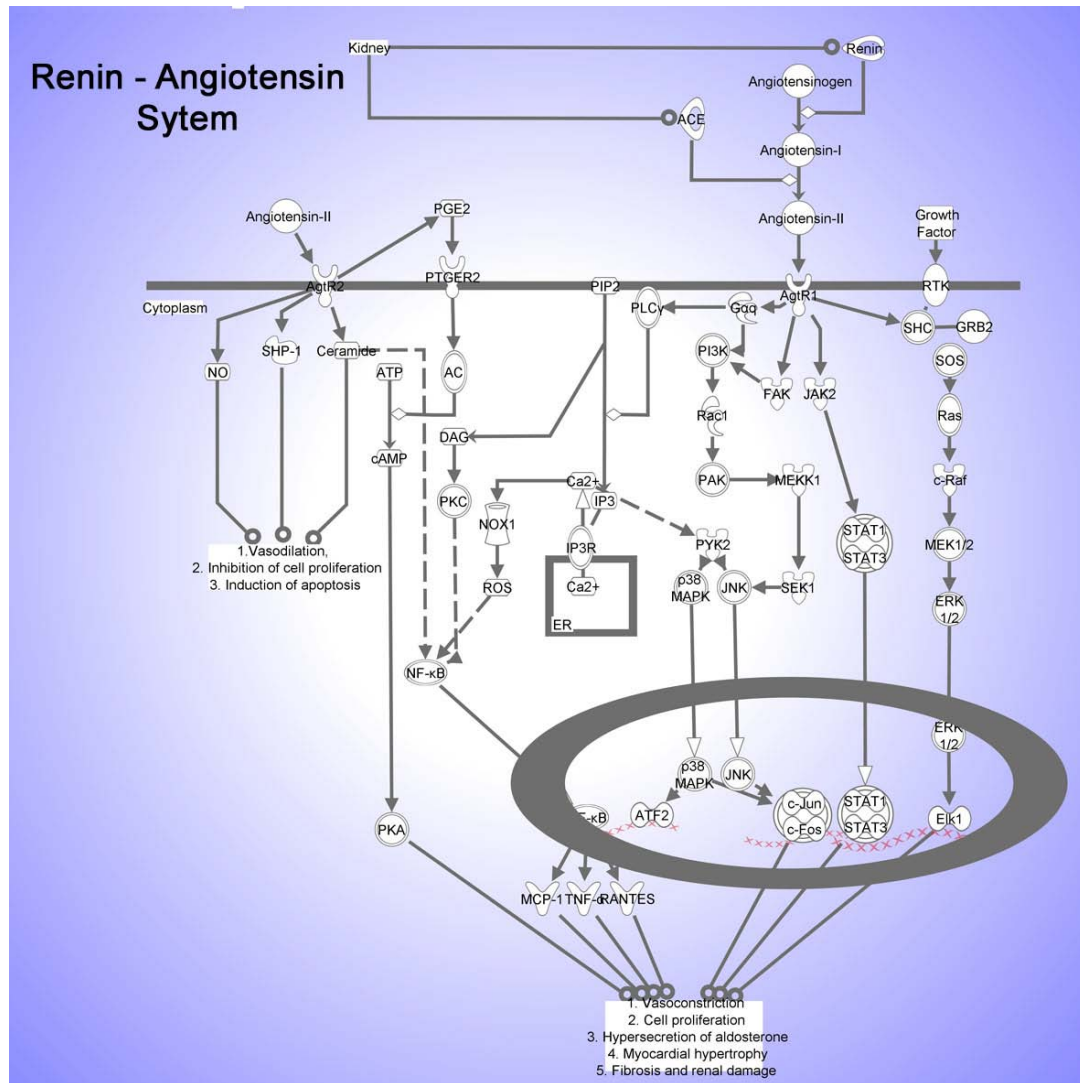


Figure 1.9 Renin- Angiotensin Signaling Pathway.

1.4.5.2 Wnt Signaling

Wnt signaling has a major role in bone mass homeostasis and development ⁷⁰. Wnt molecules exert their functions by activating several distinct intracellular pathways, including that mediated by β -catenin. The association between Wnt proteins, the Frizzled family of receptors, and the low-density lipoprotein receptor-related proteins (Lrp5, Lrp6) results in activation of β -catenin. Once activated, β -catenin is translated to the nucleus

where it interacts with transcription regulators essential for osteoblast development ⁷¹. Recently, Wnt/Lrp5 pathway was found to be activated by oxidized LDL in patients with calcified aortic valves ⁷². In addition, *in vitro* studies show that valvular interstitial cells express Wnt receptors, and that treatment with cholesterol leads to increased levels of Lrp5 and β -catenin ⁷³. Further evidence of the involvement of Wnt signaling in calcification has been proved in mice expressing Msx2, which is a potent transcription factor that regulates chondrocyte and osteoblast differentiation ⁷⁴. Mice over expressing Msx2, express high levels of ALP and develop vascular calcification via Wnt- dependent mechanism. (Figure1.10).

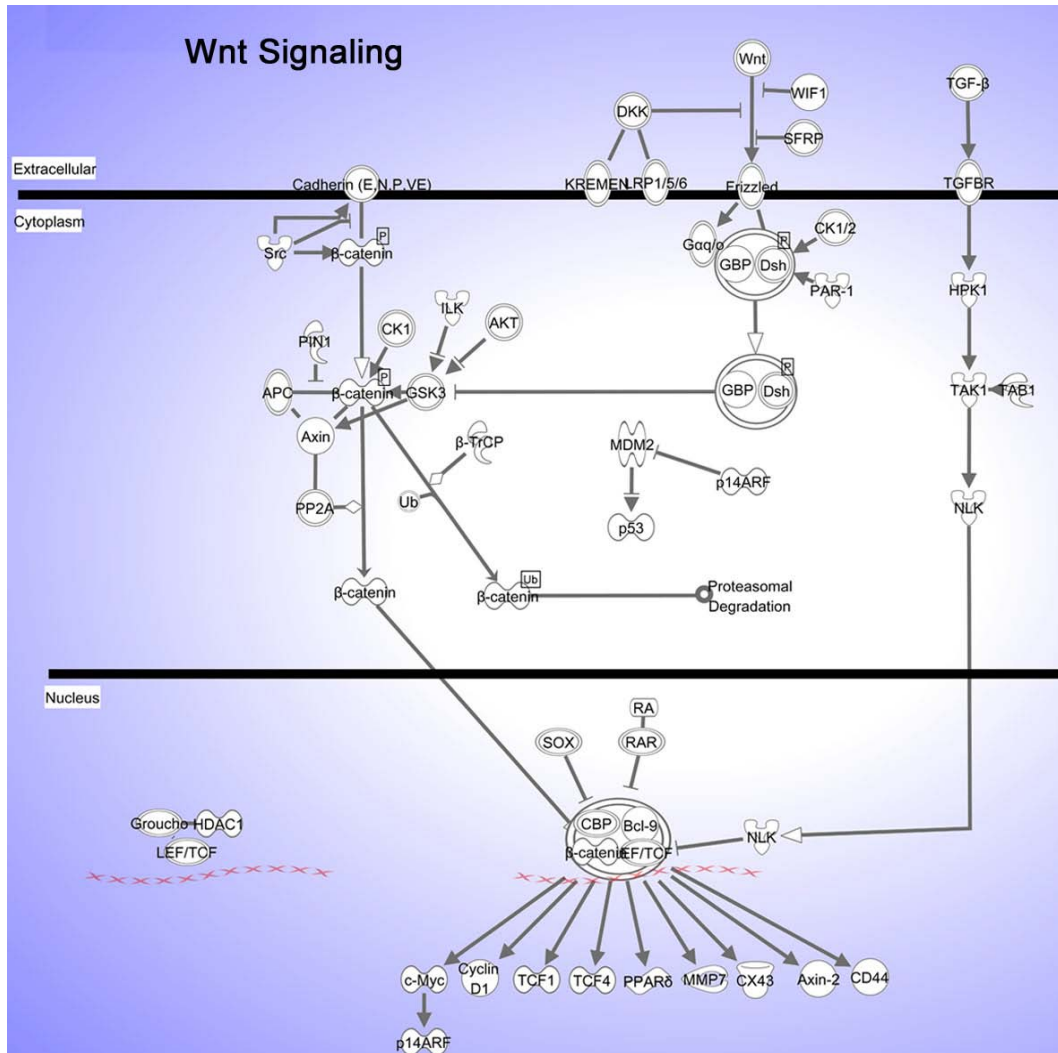


Figure 1.10 Wnt Signaling Pathway.

1.4.5.3 TGF- β Signaling

The transforming growth factor β (TGF- β) family of proteins is an important mediator of diverse signaling mechanisms in the cell ⁷⁵. TGF- β family members act by modifying the expression of specific sets of target genes. The bone morphogenetic proteins (BMPs) form the largest group within the TGF- β family and including BMP2, BMP4 and BMP7 ⁷⁶. BMP signaling is one of the most important pathways for bone

development, and differential osteoinductive activities of BMPs are elicited through different receptors. The basic signaling cascade consists of two receptors serine/threonine protein kinases (receptor types I and II) and a family of receptors substrates (the Smad proteins) that move into the nucleus. The ligand assembles a receptor complex that activates Smads, and the Smads assemble multisubunit complexes that regulate transcription ⁷⁷. The Smad family of proteins are essential components of the TGF- β signaling system, they play a key role in transmitting the signals of BMPs from the activated receptors at the cell surface to the nucleus to regulate gene expression.

Receptor-mediated phosphorylation of Smads by BMPs leads to their activation and nuclear accumulation whereby they regulate transcription of transcription factors that promote osteoblast differentiation. Immunohistochemical studies show high levels of TGF- β , BMP2 and BMP4 in calcified valves. In addition, it has been shown that valvular interstitial cells stimulated with BMP2/BMP4/ BMP7 and TGF- β 1 differentiate into osteoblast like cells and form calcific nodules , underlining the potential role of TGF β signaling in valve calcification (Figure 1.11) ^{78, 79}.

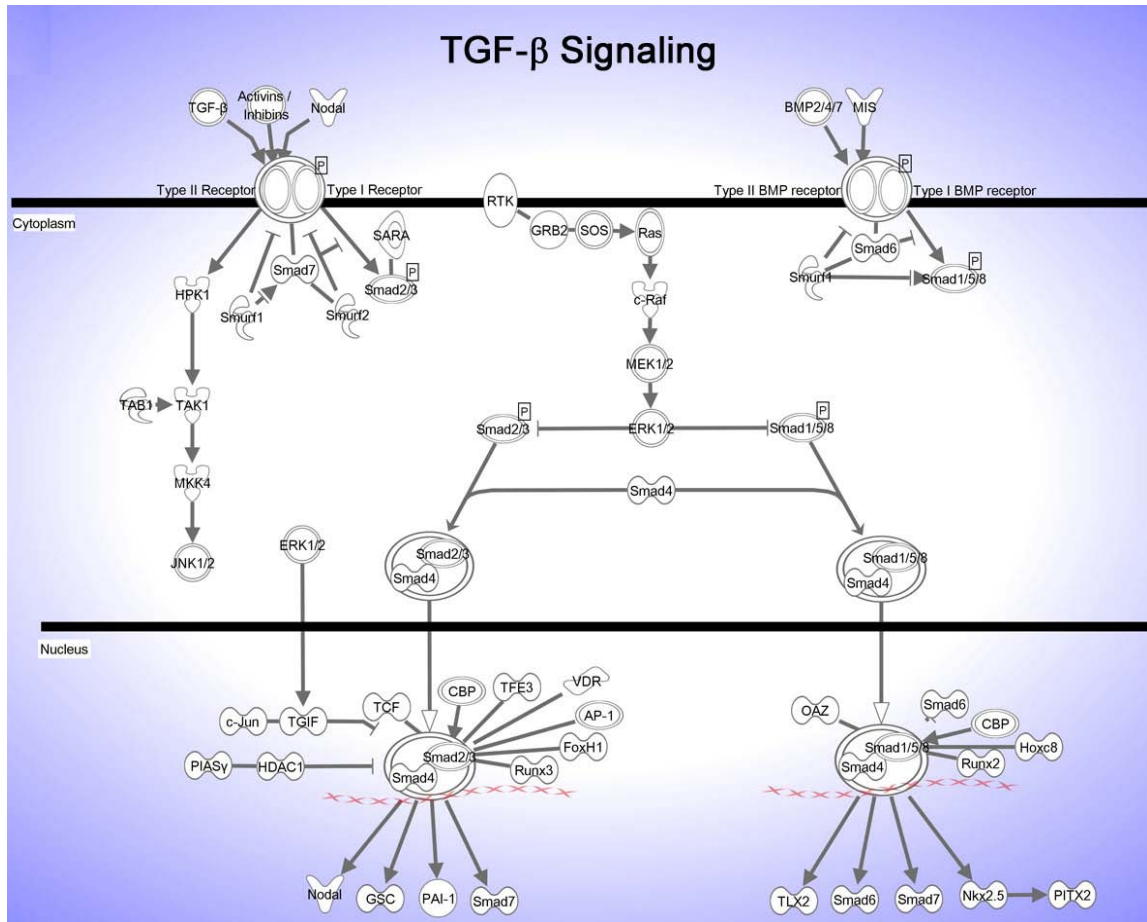


Figure 1.11 TGF- β Signaling Pathway.

1.4.5.4 RANK-OPG Signaling

The receptor activator of NF- κ B (RANK), its ligand RANKL and the decoy receptor for RANKL, osteoprotegerin (OPG) are members of the cytokine system that plays a central role in regulating bone turnover⁸⁰. Binding of RANKL to its receptor RANK provides the crucial signal to drive osteoclast development from haematopoietic progenitor cells as well as to activate mature osteoclasts. OPG negatively regulates RANKL binding to RANK and therefore inhibits bone turnover by osteoclasts. Many factors stimulate RANKL expression including prostaglandin E2, interleukin-1 (IL-1) and

tumor necrosis factor α (TNF α). By contrast, estrogen or transforming growth factor β (TGF β) attenuates RANKL expression⁸¹. Some experimental data suggests that deregulation of OPG RANKL and RANK could also affect the cardiovascular system. For example, OPG-deficient mice show medial calcification of the aorta and renal arteries. In addition, activation of RANK-OPG pathway in valve calcification has been proved, as calcified valves have differential expression of RANKL and osteoprotegerin. Further evidence of the role of RANKL/RANK signaling in valve calcification is that stimulation with RANKL and TNF- α resulted in ECM calcification, increased expression of alkaline phosphatase, RUNX2, and osteocalcin in valvular interstitial cells *in vitro* (Figure 1.12)⁸².

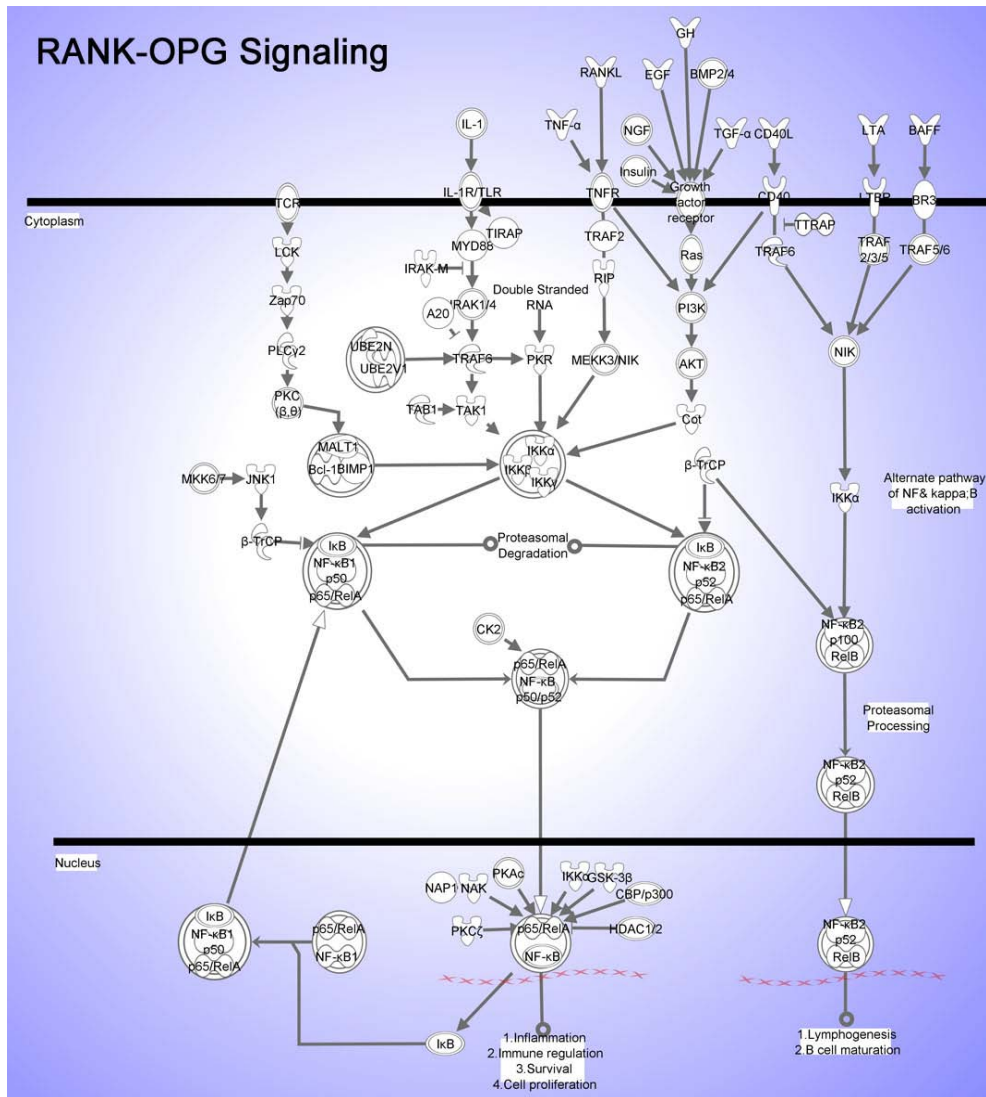


Figure 1.12 RANK-OPG Signaling Pathway.

1.5 Hypertension

High blood pressure (HBP) or hypertension is a condition in which the blood pressure in the arteries is chronically elevated¹². Hypertension affects one in three adults in the United States and causes more than 7 million deaths worldwide each year. It is also estimated to affect about two million American teens and children. In 2004, high blood pressure total mention mortality was around 300,000 which is a 56.1% increase in deaths

since 1994^{83, 84}. Although the exact causes of hypertension are usually unknown, there are several factors that have been highly associated with the condition which includes renal diseases, smoking, obesity, diabetes, high levels of salt intake, aging, genetic predisposition and chronic kidney disease. In addition, hypertension can be caused by over expression of Angiotensin II, an important member of the renin-angiotensin system (RAS)⁸⁵.

In addition, hypertension is the leading cause of coronary heart disease, heart failure, stroke, kidney failure and a major risk factor for calcific aortic valve disease (CAVD). Epidemiological studies have highlighted that a large proportion (51%) of elderly patients with CAVD also have concomitant arterial hypertension (>65years)⁸⁶. These studies suggest that hypertension may contribute with the development of calcific aortic valve disease^{87, 88}.

Under physiological conditions *in vivo*, the normal mean arterial blood pressure is approximately 80mmHg. A mean arterial pressure above 90 mmHg is considered to be stage I hypertension. In stage II hypertension, the mean arterial pressure can rise above 150 mmHg⁸⁹. Even moderate elevation of arterial pressure leads to shortened life expectancy¹². One of the principal effects of hypertension is an increase in the transvalvular pressure gradient across the aortic valve. Pressure is one of the main forces experienced by the aortic valve during the cardiac cycle, it has been shown to play an important role in valve tissue homeostasis and any substantial change in the pressure gradient can alter the mechanical environment of the aortic valve (i.e increases in compressive and tensile forces)^{90, 91}. However, the mechanical effects of hypertension on the aortic valve have not been fully defined at the cellular level.

The Renin-Angiotensin system (RAS) is a powerful mechanism for controlling blood pressure. This system helps to regulate arterial pressure through the release of Renin, an enzyme that is stored in kidney cells and that is released into the renal blood when blood pressure values are too low . Renin itself does not control blood pressure, instead it acts as an enzymatic mediator for the conversion of angiotensinogen to angiotensin I. Angiotensin I is a mild vasoconstrictor that in turn is the precursor of Angiotensin II (Ang II). The conversion of Angiotensin I to Angiotensin II occurs in the almost entirely in the lungs and it is mediated by Angiotensin Converting Enzyme (ACE)⁹².

Angiotensin II is a potent vasoconstrictor hormone that plays a central role in hypertension; it has two principal effects that can raise the blood pressure: (1) causes vasoconstrictor in large and small arteries, and (2) decreases the excretion of salt and water by the kidneys, with subsequent increases in extracellular fluid blood volume and arterial blood pressure. Elevated levels of Ang II in the blood can increase the pressure as much as 55% above normal levels (Figure 1.13)⁹³.

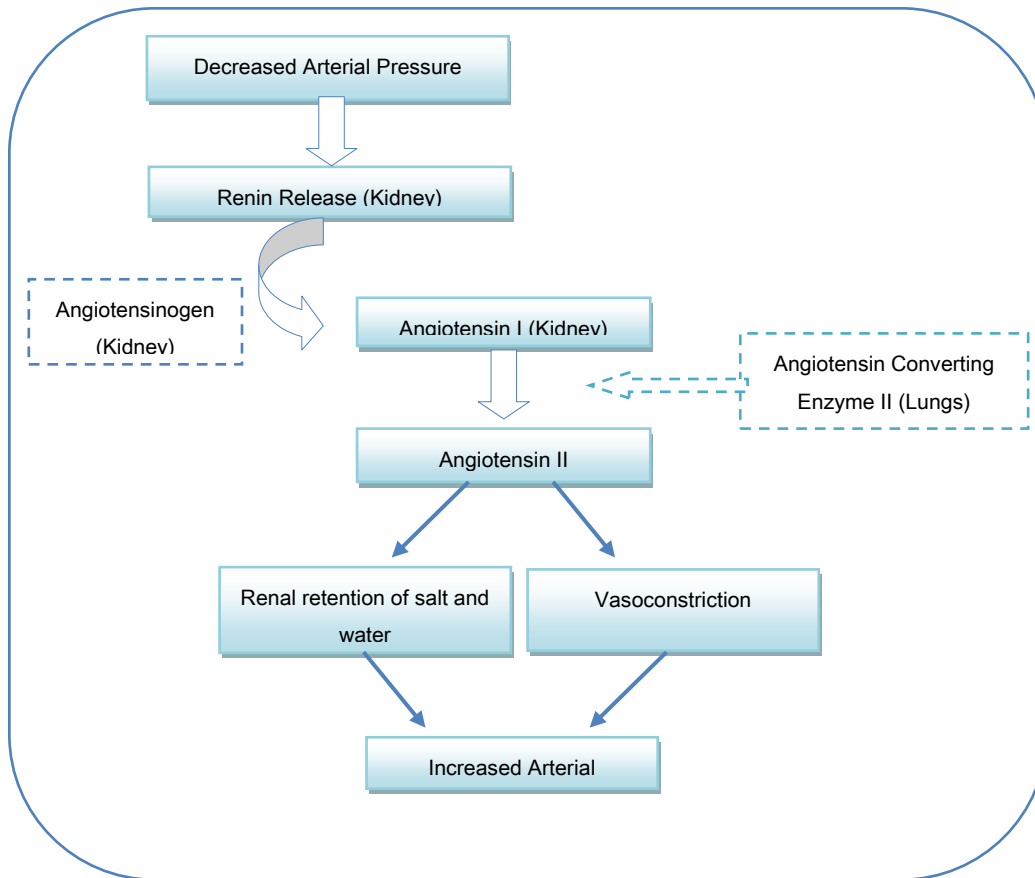


Figure 1.13 Renin-Angiotensin vasoconstrictor mechanism for arterial pressure control.

Some recent studies focused on the significance of the pressure-independent mechanism of Ang II action. However, the tissue-specific function of local Ang II is not well understood. Evidence suggests that effects of Ang II are mediated by the differential expression of Ang II receptors type 1 (AT1) and type 2 (AT2). Ang II stimulation of AT1 receptors results in proliferation of cells and stimulation of AT2 receptors results in apoptosis. Specifically, Ang II stimulation of ATR1 receptors causes hypertension, while stimulation of AT2 and angiotensin converting enzyme 2 (ACE2) appear to play a protective role in atherogenesis⁹⁴. The regulation of RAS system with

Angiotensin converting enzyme (ACE) activity by ACE inhibitors and the resulting limitation of Angiotensin II has been recognized as an essential method for maintaining normal blood pressure as well as inhibiting cardiovascular remodeling^{95,96}.

1.6 Statement of Hypothesis

The main purpose of this dissertation was to evaluate if elevated pressure can induce osteogenic differentiation of valve interstitial cells *in vitro*, and if so, identify of the potential molecular mechanisms mediating the differentiation process.

1.6.1 Hypothesis

Elevated cyclic pressure activates osteoblastic differentiation mechanisms in aortic heart valve leading to changes in valve interstitial cells (VICs) phenotype and activity, which can result in valve calcification and disease.

1.6.2 Specific aims

1. Characterize phenotypic changes of valve interstitial cells from porcine aortic heart valves exposed to simulated normotensive and hypertensive pressure for 24 hours.
2. Identify global gene expression patterns of aortic heart valves exposed to normotensive and hypertensive mechanical pressure using microarray technology.
3. Identify the functional signaling pathways activated by hypertensive pressure in aortic heart valve.

1.7 References

- (1) Levitt LC, Thubrikar MJ, Nolan SP. Patterns and pathogenesis of calcification in pathologic human aortic valves. *Curr Surg* 1984 January;41(1):17-9.
- (2) Akat K, Borggrefe M, Kaden JJ. Aortic valve calcification: basic science to clinical practice. *Heart* 2009 April;95(8):616-23.
- (3) Lippert JA, White CS, Mason AC, Plotnick GD. Calcification of aortic valve detected incidentally on CT scans: prevalence and clinical significance. *AJR Am J Roentgenol* 1995 January;164(1):73-7.
- (4) Stewart MD, Siscovick MD, Lind MS et al. Clinical Factors Associated With Calcific Aortic Valve Disease. *Journal of the American College of Cardiology* 1997 March 1;29(3):630-4.
- (5) Akat K, Borggrefe M, Kaden JJ. Aortic valve calcification: basic science to clinical practice. *Heart* 2009 April;95(8):616-23.
- (6) Merryman WD, Youn I, Lukoff HD et al. Correlation between heart valve interstitial cell stiffness and transvalvular pressure: implications for collagen biosynthesis. *Am J Physiol Heart Circ Physiol* 2006 January 1;290(1):H224-H231.
- (7) Balachandran K, Sucusky P, Jo H, Yoganathan AP. ELEVATED CYCLIC STRETCH ALTERS MATRIX REMODELING IN AORTIC VALVE CUSPS - IMPLICATIONS FOR DEGENERATIVE AORTIC VALVE DISEASE? *Am J Physiol Heart Circ Physiol* 2009 January 16.
- (8) Dasi LP, Sucusky P, de ZD, Sundareswaran K, Jimenez J, Yoganathan AP. Advances in cardiovascular fluid mechanics: bench to bedside. *Ann N Y Acad Sci* 2009 April;1161:1-25.
- (9) Yoganathan AP, He Z, Casey JS. Fluid mechanics of heart valves. *Annu Rev Biomed Eng* 2004;6:331-62.
- (10) Little SH, Chan KL, Burwash IG. Impact of blood pressure on the Doppler echocardiographic assessment of severity of aortic stenosis. *Heart* 2007 July;93(7):848-55.
- (11) Messika-Zeitoun D, Bielak LF, Peyser PA et al. Aortic valve calcification: determinants and progression in the population. *Arterioscler Thromb Vasc Biol* 2007 March;27(3):642-8.
- (12) Rabkin SW. The association of hypertension and aortic valve sclerosis. *Blood Press* 2005;14(5):264-72.

- (13) Hakala SM, Tilvis RS, Strandberg TE. Blood pressure and mortality in an older population: A 5-year follow-up of the Helsinki Ageing Study. *Eur Heart J* 1997 June 2;18(6):1019-23.
- (14) Agmon Y, Khandheria BK, Meissner I et al. Aortic valve sclerosis and aortic atherosclerosis: different manifestations of the same disease? Insights from a population-based study. *J Am Coll Cardiol* 2001 September;38(3):827-34.
- (15) Aksoy Y, Yagmur C, Tekin GO et al. Aortic valve calcification: association with bone mineral density and cardiovascular risk factors. *Coron Artery Dis* 2005 September;16(6):379-83.
- (16) Feuchtner GM, Muller S, Grander W et al. Aortic valve calcification as quantified with multislice computed tomography predicts short-term clinical outcome in patients with asymptomatic aortic stenosis. *J Heart Valve Dis* 2006 July;15(4):494-8.
- (17) Stewart BF, Siscovick D, Lind BK et al. Clinical factors associated with calcific aortic valve disease. Cardiovascular Health Study. *J Am Coll Cardiol* 1997 March 1;29(3):630-4.
- (18) Olsson M, Thyberg J, Nilsson J. Presence of oxidized low density lipoprotein in nonrheumatic stenotic aortic valves. *Arterioscler Thromb Vasc Biol* 1999 May;19(5):1218-22.
- (19) Brown MS, Goldstein JL. Familial hypercholesterolemia: genetic, biochemical and pathophysiologic considerations. *Adv Intern Med* 1975;20:273-96.
- (20) Bermejo J. The effects of hypertension on aortic valve stenosis. *Heart* 2005 March;91(3):280-2.
- (21) Kizer JR, Wiebers DO, Whisnant JP et al. Mitral annular calcification, aortic valve sclerosis, and incident stroke in adults free of clinical cardiovascular disease: the Strong Heart Study. *Stroke* 2005 December;36(12):2533-7.
- (22) Messika-Zeitoun D, Aubry MC, Detaint D et al. Evaluation and clinical implications of aortic valve calcification measured by electron-beam computed tomography. *Circulation* 2004 July 20;110(3):356-62.
- (23) Kizer JR, Wiebers DO, Whisnant JP et al. Mitral annular calcification, aortic valve sclerosis, and incident stroke in adults free of clinical cardiovascular disease: the Strong Heart Study. *Stroke* 2005 December;36(12):2533-7.
- (24) Melina G, Rubens MB, Yacoub MH. Statins, electron-beam CT, and aortic-valve calcification. *Lancet* 2002 July 20;360(9328):258.

- (25) Jian B, Narula N, Li QY, Mohler ER, III, Levy RJ. Progression of aortic valve stenosis: TGF-beta1 is present in calcified aortic valve cusps and promotes aortic valve interstitial cell calcification via apoptosis. *Ann Thorac Surg* 2003 February;75(2):457-65.
- (26) Mohler ER, III, Gannon F, Reynolds C, Zimmerman R, Keane MG, Kaplan FS. Bone formation and inflammation in cardiac valves. *Circulation* 2001 March 20;103(11):1522-8.
- (27) Mohler ER, III. Mechanisms of aortic valve calcification. *Am J Cardiol* 2004 December 1;94(11):1396-402, A6.
- (28) Helske S, Kupari M, Lindstedt KA, Kovanen PT. Aortic valve stenosis: an active atheroinflammatory process. *Curr Opin Lipidol* 2007 October;18(5):483-91.
- (29) Mohler ER, III. Mechanisms of aortic valve calcification. *Am J Cardiol* 2004 December 1;94(11):1396-402, A6.
- (30) Olsson M, Thyberg J, Nilsson J. Presence of oxidized low density lipoprotein in nonrheumatic stenotic aortic valves. *Arterioscler Thromb Vasc Biol* 1999 May;19(5):1218-22.
- (31) Akat K, Borggrefe M, Kaden JJ. Aortic valve calcification: basic science to clinical practice. *Heart* 2009 April;95(8):616-23.
- (32) Durbin AD, Gotlieb AI. Advances towards understanding heart valve response to injury. *Cardiovasc Pathol* 2002 March;11(2):69-77.
- (33) Grossman CM. Human aortic valve calcification. *Circulation* 2003 December 9;108(23):e163.
- (34) Helske S, Oksjoki R, Lindstedt KA et al. Complement system is activated in stenotic aortic valves. *Atherosclerosis* 2008 January;196(1):190-200.
- (35) Satta J, Melkko J, Pollanen R et al. Progression of human aortic valve stenosis is associated with tenascin-C expression. *J Am Coll Cardiol* 2002 January 2;39(1):96-101.
- (36) Dreger SA, Taylor PM, Allen SP, Yacoub MH. Profile and localization of matrix metalloproteinases (MMPs) and their tissue inhibitors (TIMPs) in human heart valves. *J Heart Valve Dis* 2002 November;11(6):875-80.
- (37) Aikawa E, Aikawa M, Libby P et al. Arterial and aortic valve calcification abolished by elastolytic cathepsin S deficiency in chronic renal disease. *Circulation* 2009 April 7;119(13):1785-94.

- (38) Rabkin E, Aikawa M, Stone JR, Fukumoto Y, Libby P, Schoen FJ. Activated interstitial myofibroblasts express catabolic enzymes and mediate matrix remodeling in myxomatous heart valves. *Circulation* 2001 November 20;104(21):2525-32.
- (39) Kaden JJ, Dempfle CE, Grobholz R et al. Inflammatory regulation of extracellular matrix remodeling in calcific aortic valve stenosis. *Cardiovasc Pathol* 2005 March;14(2):80-7.
- (40) Galis ZS, Khatri JJ. Matrix Metalloproteinases in Vascular Remodeling and Atherogenesis: The Good, the Bad, and the Ugly. *Circ Res* 2002 February 22;90(3):251-62.
- (41) Edep ME, Shirani J, Wolf P, Brown DL. Matrix metalloproteinase expression in nonrheumatic aortic stenosis. *Cardiovasc Pathol* 2000 September;9(5):281-6.
- (42) Warren BA, Yong JL. Calcification of the aortic valve: its progression and grading. *Pathology* 1997 November;29(4):360-8.
- (43) Rajamannan NM, Nealis TB, Subramaniam M et al. Calcified rheumatic valve neoangiogenesis is associated with vascular endothelial growth factor expression and osteoblast-like bone formation. *Circulation* 2005 June 21;111(24):3296-301.
- (44) Rajamannan NM, Bonow RO, Rahimtoola SH. Calcific aortic stenosis: an update. *Nat Clin Pract Cardiovasc Med* 2007 May;4(5):254-62.
- (45) Charest A, Pepin A, Shetty R et al. Distribution of SPARC during neovascularisation of degenerative aortic stenosis. *Heart* 2006 December 1;92(12):1844-9.
- (46) Mohler ER, III, Gannon F, Reynolds C, Zimmerman R, Keane MG, Kaplan FS. Bone formation and inflammation in cardiac valves. *Circulation* 2001 March 20;103(11):1522-8.
- (47) Mohler ER, III. Mechanisms of aortic valve calcification. *Am J Cardiol* 2004 December 1;94(11):1396-402, A6.
- (48) Clark-Greuel JN, Connolly JM, Sorichillo E et al. Transforming growth factor-beta1 mechanisms in aortic valve calcification: increased alkaline phosphatase and related events. *Ann Thorac Surg* 2007 March;83(3):946-53.
- (49) Yang X, Meng X, Su X et al. Bone morphogenic protein 2 induces Runx2 and osteopontin expression in human aortic valve interstitial cells: role of Smad1 and extracellular signal-regulated kinase 1/2. *J Thorac Cardiovasc Surg* 2009 October;138(4):1008-15.

- (50) Bella JN. Genomics of Aortic Valve Disease. *Journal of the American College of Cardiology* 2008 August 5;52(6):498.
- (51) Bosse Y, Mathieu P, Pibarot P. Genomics: the next step to elucidate the etiology of calcific aortic valve stenosis. *J Am Coll Cardiol* 2008 April 8;51(14):1327-36.
- (52) Rajamannan NM, Bonow RO, Rahimtoola SH. Calcific aortic stenosis: an update. *Nat Clin Pract Cardiovasc Med* 2007 May;4(5):254-62.
- (53) De Giovanni JV. Aortic stenosis from calcification of congenital bicuspid valve. *Br Med J* 1980 September 6;281(6241):683.
- (54) Garg V. Molecular genetics of aortic valve disease. *Current Opinion in Cardiology* 2006;21(3).
- (55) Song ZZ. Valve calcification and patients with bicuspid aortic valves. *JAMA* 2009 March 4;301(9):935-6.
- (56) Clementi M, Notari L, Borghi A, Tenconi R. Familial congenital bicuspid aortic valve: a disorder of uncertain inheritance. *Am J Med Genet* 1996 April 24;62(4):336-8.
- (57) De Giovanni JV. Aortic stenosis from calcification of congenital bicuspid valve. *Br Med J* 1980 September 6;281(6241):683.
- (58) Cowell SJ, Newby DE, Burton J et al. Aortic valve calcification on computed tomography predicts the severity of aortic stenosis. *Clin Radiol* 2003 September;58(9):712-6.
- (59) Rosenhek R, Rader F, Loho N et al. Statins but not angiotensin-converting enzyme inhibitors delay progression of aortic stenosis. *Circulation* 2004 September 7;110(10):1291-5.
- (60) Koos R, Brandenburg V, Mahnken AH et al. Association of fetuin-A levels with the progression of aortic valve calcification in non-dialyzed patients. *Eur Heart J* 2009 May 8.
- (61) Hakuno D, Kimura N, Yoshioka M, Fukuda K. Molecular mechanisms underlying the onset of degenerative aortic valve disease. *J Mol Med* 2009 January;87(1):17-24.
- (62) Rajamannan NM, Bonow RO, Rahimtoola SH. Calcific aortic stenosis: an update. *Nat Clin Pract Cardiovasc Med* 2007 May;4(5):254-62.
- (63) Dasi LP, Sucusky P, de ZD, Sundareswaran K, Jimenez J, Yoganathan AP. Advances in cardiovascular fluid mechanics: bench to bedside. *Ann N Y Acad Sci* 2009 April;1161:1-25.

- (64) Rajamannan NM, Gersh B, Bonow RO. Calcific aortic stenosis: from bench to the bedside--emerging clinical and cellular concepts. *Heart* 2003 July;89(7):801-5.
- (65) Mehta PK, Griendling KK. Angiotensin II cell signaling: physiological and pathological effects in the cardiovascular system. *Am J Physiol Cell Physiol* 2007 January 1;292(1):C82-C97.
- (66) Jimenez-Candil J, Bermejo J, Yotti R et al. Effects of angiotensin converting enzyme inhibitors in hypertensive patients with aortic valve stenosis: a drug withdrawal study. *Heart* 2005 October;91(10):1311-8.
- (67) Hu WY, Fukuda N, Kanmatsuse K. Growth characteristics, angiotensin II generation, and microarray-determined gene expression in vascular smooth muscle cells from young spontaneously hypertensive rats. *J Hypertens* 2002 July;20(7):1323-33.
- (68) Mohler ER, III, Gannon F, Reynolds C, Zimmerman R, Keane MG, Kaplan FS. Bone formation and inflammation in cardiac valves. *Circulation* 2001 March 20;103(11):1522-8.
- (69) Helske S, Lindstedt KA, Laine M et al. Induction of local angiotensin II-producing systems in stenotic aortic valves. *J Am Coll Cardiol* 2004 November 2;44(9):1859-66.
- (70) Kim JB, Leucht P, Lam K et al. Bone regeneration is regulated by wnt signaling. *J Bone Miner Res* 2007 December;22(12):1913-23.
- (71) Nusse R, Fuerer C, Ching W et al. Wnt signaling and stem cell control. *Cold Spring Harb Symp Quant Biol* 2008;73:59-66.
- (72) Caira FC, Stock SR, Gleason TG et al. Human degenerative valve disease is associated with up-regulation of low-density lipoprotein receptor-related protein 5 receptor-mediated bone formation. *J Am Coll Cardiol* 2006 April 18;47(8):1707-12.
- (73) Rajamannan NM, Subramaniam M, Caira F, Stock SR, Spelsberg TC. Atorvastatin inhibits hypercholesterolemia-induced calcification in the aortic valves via the Lrp5 receptor pathway. *Circulation* 2005 August 30;112(9 Suppl):I229-I234.
- (74) Shao JS, Cheng SL, Pingsterhaus JM, Charlton-Kachigian N, Loewy AP, Towler DA. Msx2 promotes cardiovascular calcification by activating paracrine Wnt signals. *J Clin Invest* 2005 May;115(5):1210-20.
- (75) Massagué J, Chen YG. Controlling TGF- β signaling. *Genes & Development* 2000 March 15;14(6):627-44.

- (76) Chen D, Zhao M, Mundy GR. Bone Morphogenetic Proteins. *Growth Factors* 2004;22(4):233-41.
- (77) Wrana JL. Regulation of Smad activity. *Cell* 2000 January 21;100(2):189-92.
- (78) Clark-Greuel JN, Connolly JM, Sorichillo E et al. Transforming growth factor-beta1 mechanisms in aortic valve calcification: increased alkaline phosphatase and related events. *Ann Thorac Surg* 2007 March;83(3):946-53.
- (79) Yang X, Meng X, Su X et al. Bone morphogenic protein 2 induces Runx2 and osteopontin expression in human aortic valve interstitial cells: role of Smad1 and extracellular signal-regulated kinase 1/2. *J Thorac Cardiovasc Surg* 2009 October;138(4):1008-15.
- (80) Kaden JJ, Bickelhaupt S, Grobholz R et al. Receptor activator of nuclear factor kappaB ligand and osteoprotegerin regulate aortic valve calcification. *J Mol Cell Cardiol* 2004 January;36(1):57-66.
- (81) Wada T, Nakashima T, Hiroshi N, Penninger JM. RANKL-RANK signaling in osteoclastogenesis and bone disease. *Trends Mol Med* 2006 January;12(1):17-25.
- (82) Kaden JJ, Dempfle CE, Kilic R et al. Influence of receptor activator of nuclear factor kappa B on human aortic valve myofibroblasts. *Exp Mol Pathol* 2005 February;78(1):36-40.
- (83) Kaden JJ, Haghi D. Hypertension in aortic valve stenosis--a Trojan horse. *Eur Heart J* 2008 June 26.
- (84) Linhartov+í K, Filipovsk++ J, -îrb+ík R, +át-çrb+íkov+í G, Hani+íov+í I, Ber+ínek V+. Severe aortic stenosis and its association with hypertension: Analysis of clinical and echocardiographic parameters. *Blood Pressure* 2007;16(2):122-8.
- (85) Mehta PK, Griendling KK. Angiotensin II cell signaling: physiological and pathological effects in the cardiovascular system. *Am J Physiol Cell Physiol* 2007 January 1;292(1):C82-C97.
- (86) ntonini-Canterin F, Huang G, Cervesato E et al. Symptomatic Aortic Stenosis: Does Systemic Hypertension Play an Additional Role? *Hypertension* 2003 June 1;41(6):1268-72.
- (87) Briand M, Dumesnil JG, Kadem L et al. Reduced Systemic Arterial Compliance Impacts Significantly on Left Ventricular Afterload and Function in Aortic Stenosis: Implications for Diagnosis and Treatment. *Journal of the American College of Cardiology* 2005 July 19;46(2):291-8.

- (88) Tenenbaum A, Fisman EZ, Schwammenthal E et al. Aortic valve calcification in hypertensive patients: prevalence, risk factors and association with transvalvular flow velocity. *Int J Cardiol* 2004 March;94(1):7-13.
- (89) Hakala SM, Tilvis RS, Strandberg TE. Blood pressure and mortality in an older population: A 5-year follow-up of the Helsinki Ageing Study. *Eur Heart J* 1997 June 2;18(6):1019-23.
- (90) Xing Y, Warnock JN, He Z, Hilbert SL, Yoganathan AP. Cyclic pressure affects the biological properties of porcine aortic valve leaflets in a magnitude and frequency dependent manner. *Ann Biomed Eng* 2004 November;32(11):1461-70.
- (91) Platt MO, Xing Y, Jo H, Yoganathan AP. Cyclic pressure and shear stress regulate matrix metalloproteinases and cathepsin activity in porcine aortic valves. *J Heart Valve Dis* 2006 September;15(5):622-9.
- (92) Mehta PK, Griendling KK. Angiotensin II cell signaling: physiological and pathological effects in the cardiovascular system. *Am J Physiol Cell Physiol* 2007 January 1;292(1):C82-C97.
- (93) Mehta PK, Griendling KK. Angiotensin II cell signaling: physiological and pathological effects in the cardiovascular system. *Am J Physiol Cell Physiol* 2007 January 1;292(1):C82-C97.
- (94) Campos AH, Zhao Y, Pollman MJ, Gibbons GH. DNA microarray profiling to identify angiotensin-responsive genes in vascular smooth muscle cells: potential mediators of vascular disease. *Circ Res* 2003 January 10;92(1):111-8.
- (95) Pendergrass KD, Gwathmey TM, Michalek RD, Grayson JM, Chappell MC. The angiotensin II-AT1 receptor stimulates reactive oxygen species within the cell nucleus. *Biochemical and Biophysical Research Communications* 2009 June 26;384(2):149-54.
- (96) Mehta PK, Griendling KK. Angiotensin II cell signaling: physiological and pathological effects in the cardiovascular system. *Am J Physiol Cell Physiol* 2007 January 1;292(1):C82-C97.

CHAPTER 2

GENERAL METHODOLOGY

2.1 Tissue Extraction and Culture

At least 6 fresh aortic valves were obtained from a local slaughter house within 10 minutes of pig slaughter and rinse twice with ice-cold sterile Phosphate Buffered Saline (PBS, Sigma, St Louis, MO). Valve leaflets did not show any sign of degeneration, tearing or calcification. To ensure that only valve interstitial cells were present in valve tissue, endothelial cell layer was removed from each leaflet surface by immersion of valve tissue in collagenase II 1mg/ml in serum free DMEM (Worthington Biochemical Corp.) for 5 minutes at 37°C and 5% CO₂. To remove excess of collagenase II valve leaflets were rinsed twice with PBS. Following incubation overnight in DMEM supplemented with 10% Fetal Bovine Serum (FBS; Hyclone, Logan UT), and 1% antibiotic/anti-mycotic solution (Sigma) prior to cyclic pressure experiments.

The endothelium significantly modulates the mechanical properties of aortic valve leaflets. These mechanisms could regulate valve and flow dynamics and possibly allow long-term optimal cusp function in its unique mechanical environment¹. In this study, we used whole valve leaflets instead of valvular interstitial cells (VICs) cultures to avoid any changes in VICs phenotype due to isolation and culture procedures. In addition, evidence shows that VICs respond differently to mechanical stimulation when they are isolated than when they are kept in their native valvular tissue. To obtain a pure

population of VICs, the endothelium was removed from leaflets. Endothelial denudation may have multiple effects on the biology of the tissue. It has been proposed that alterations in the mechanical environment of the leaflets could be transduced into a pathobiological response via a two-way communication system between endothelial and interstitial cells. Denudation disrupts this communication and may expose the sub-endothelial interstitial cells to mechanical stimuli that they do not see when the endothelium is intact. This limitation would also be present in cell culture; however, by using an organ culture system VICs were retained in their native three-dimensional ECM. The ECM is important for the transmission of mechanical signals to cells and thus, this system has a distinct advantage over mechanical studies performed with isolated cells. The alternative is *in vivo* studies. Although these have greater physiological relevance, they do not allow for strict mechanical characterization or isolation of the effects of pressure and/or Ang II.

Valve leaflets were placed in 6-well tissue culture plates within a custom designed pressure bioreactor. The pressure magnitude that we have chosen in this study corresponds to the physiological load experienced by the valve under normal and hypertensive conditions. Based on previous studies VICs have genetic response expose to pressure within 2 hour, and thus the gene profile at 24 hours is more likely to represent a more prolonged exposure to pressure The frequency of 1.167Hz corresponds to the physiological heart rate of 70 beats per minute. Each leaflet was randomly assigned to either: (i) normotensive pressure (0-80mm Hg, 1.67 Hz) or (ii) hypertensive pressure (0-120mmHg) a 1.67 Hz (sinusoidal wave; 0.6 sec influx, 0.4 sec outflux). Additionally, temperature and pH were similar in both conditions.

Each experiment was run for 24 hours. Upon completion of experiments, each leaflet was submerged in 1ml of RNA later RNA Stabilization Reagent (Quiagen) to avoid changes in total mRNA expression and stored at 80°C until mRNA isolation.

2.2 RNA Isolation

Each leaflet was transferred directly into 600 µL of a lysis buffer containing RNase inhibitors (Quiagen). Each leaflet was disrupted and homogenized for 30 seconds (2000 rpm) using a rotor stator homogenizer (IKA®). Total RNA from porcine aortic valve interstitial cells (VICs) was extracted using the RNeasy Mini kit (Quiagen, Valencia, CA) following manufacturer's instructions and stored at -80°C. Quality and concentration of total RNA was determined using the Nanodrop ND-1000 spectrophotometer. mRNA samples with 260:280 ratio of 1.9 or higher were used for Real-Time Quantitative PCR.

2.3 Real Time Quantitative –PCR

RT-PCR was carried out using iCycler iQ (Biorad) and iScript one-step RT-PCR kit with SYBR Green (Biorad). A master mix was created using 0.25 µl SYBR® Green One-Step Enzyme Mix, 6.25 µl 2X SYBR® Green Reaction Mix, 0.2 µl of forward and reverse primers and RNase/DNase free distilled water to give a final volume of 11.5 µl per sample. The master mix was pipetted into a 96-well PCR plate and 1 µl of total RNA for each sample (between 250 and 750 ng) was added, giving a final reaction volume of 12.5 µl. cDNA synthesis and PCR amplification was performed using the following steps: 50 oC for 30 minutes then the reaction mixture was heated to 95 oC for 5 min; a 45 cycle two-step PCR was performed consisting of 95 oC for 15 s followed by 1 min at the

annealing temperature. Reactions were carried out using a Thermal Cycler (Bio-Rad Laboratories, Hercules, CA). The specificity of all individual amplification reactions was confirmed by melting curve analysis. Expression values for each gene were calculated relative to 18s mRNA levels using the $\Delta\Delta CT$ method. Each experimental condition was tested in triplicate and the mean and standard deviation were calculated to determine changes in gene expression.

2.4 *In vitro* Pressure Bioreactor

To investigate the effects of mechanical pressure a custom-made, computer-operated dynamic pressure system was designed, fabricated and used in previous studies. The pressure system exposed tissues to mechanical stimulation by increasing the air pressure above the supernatant media. The system consisted of: (1) a pressure chamber, (2) a pneumatic piston, (3) a pressure transducer, (4) an electronic pressure controller (connected to the piston) (5) a load cell conditioner and (6) a computer to control electrical devices. The pressure chambers consist of a half-closed cylindrical stainless steel base covered with a lid at the other end. The two pieces are bolted together to compress a Teflon® gasket, which ensures a hermetic sealing of the chamber. The system is able to house 2 standard 6-well tissue-culture plates.

To produce a change in the pressure within the chamber, a pneumatic piston was integrated to the lid. As the piston moves downward in the chamber space, the Teflon gasket stretched downward as well reducing the volume of the chamber, hence increasing the pressure. The supply of compressed air to the piston is controlled by an electric pressure converter, which converts electrical signal into pressure. For automatic control of pressure, the converter was interfaced to the computer using a load cell conditioner

(Encore Electronics, Inc., Model 4025- 101). The applied pressure was measured using a pressure transducer (Omega Engineering, Inc., PX302-200GV) connected to the lower side of the pressure chamber. The pressure transducer was interfaced to the computer using also the load cell conditioner. The voltage and the pressure signal were acquired with a data acquisition card module (Measurement Devices, PMD1608) and monitored using a in-house developed LabView graphical user program (LABView, National Instruments). LabView was also used to send a pressure waveform to the piston. The applied pressure was sinusoidal 1 Hz for 24h. During experiments, the pressure system (except for the computer and electronic components) was maintained under standard cell culture conditions, that is 37°C, humidified, 5% CO₂ and 95% air environment.

This *in vitro* system allowed us to study VICs behavior within an environment characterized by different levels of extracellular pressure, which is something usual from an *in vivo* environment.

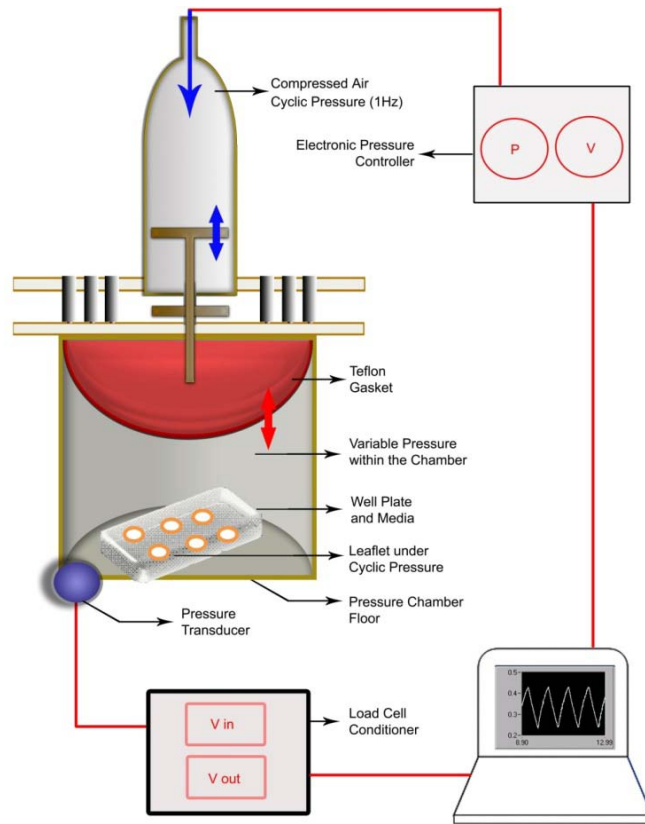


Figure 2.1 Schematic representation of the *in vitro* pressure system. Valve leaflets were placed in 6-well tissue cultures plates within a stainless steel pressure chamber and placed inside an incubator (5% CO₂, 37°C) for 24 hours.

CHAPTER 3

REGULATION OF PORCINE AORTIC VALVE INTERSTITIAL CELL PHENOTYPE BY MECHANICAL AND BIOCHEMICAL STIMULI

3.1 Introduction

Calcific aortic valve disease (CAVD) is the leading cause of aortic valve replacement in the elderly as it affects more than 5% of the population over 65 years old. It accounts for a major fraction of the approximately 300,000 valve replacement surgeries worldwide each year ¹. Calcified valves are characterized by leaflet thickening, expression of specific bone markers and the presence of osteoblast like cells in calcific valve lesions ². Currently, there is no proven pharmacological treatment to stop or reverse the morphological changes seen in calcific valves. One of the key events leading towards the development of calcific aortic valve disease is valvular interstitial cells (VICs) differentiation into osteoblast-like cells. These cells are able to produce bone specific proteins including osteopontin (OPN), alkaline phosphatase (ALP), osteoblast-specific transcription factor RUNX2 and BMPs proteins ³. Multiple studies have shown that mechanical (shear, stretch, pressure) and biochemical (TGF- β , BMP-2, BMP-7) conditions modulate VICs biosynthetic activity and phenotype ⁴⁻⁶. Specifically, BMPs stimulation induces osteogenic differentiation of human VICs *in vitro* ^{7, 8}. These data suggests that while VICs may play a major role in aortic valve calcification, the

calcification process may be developed secondary to a BMP- mediated osteoblast differentiation pathway.

Hypertension is a well known risk factor for CAVD^{9,10}. Epidemiological studies show that hypertension is present in one third of patients with calcific aortic stenosis¹¹, suggesting hypertension as a potential candidate contributing to the development of CAVD. Hypertension can be induced by over expression of Angiotensin II (Ang II), a key member of the renin-angiotensin system (RAS)¹². Interestingly, there is evidence of Angiotensin Converting enzyme and Angiotensin II in human calcified valves, suggesting a role for the renin-angiotensin system in calcific valve stenosis progression¹³. Although clinically relevant, little is known regarding the molecular mechanisms by which hypertension may contribute to the pathogenesis of calcific aortic valve disease.

Since it is likely that conditions that alter the mechanical and biochemical environment of the valve modulate phenotypic conversion of VICs, it therefore became of interest to understand the intracellular signals by which mechanical pressure and Ang II might lead to phenotypic differentiation of VICs. We hypothesized that an environment that resembles hypertensive conditions (i.e elevated pressure, Ang II treatment), induces differentiation of VICs into osteoblast-like cells. We initially evaluated the effects of mechanical pressure on osteogenic markers expression by exposing aortic valve leaflets to two levels of cyclic pressure: normotensive (0-80 mm Hg) and hypertensive (0-120mmHg), and then we tested the combined effects of cyclic pressure and Ang II. We showed that elevated cyclic pressure increased the expression of genes involved in osteoblast differentiation including the non-collagenous bone matrix proteins OPN, ALP, RUNX2, and two essential components of the BMP osteogenic pathway: BMP-7, and

SMAD1. The ability of these genes to promote osteoblast cell differentiation suggests that elevated cyclic pressure may play a key role in promoting VICs differentiation into osteoblast type cells. Additionally, expression of Ang II receptors suggests a role for Ang II in the regulation of osteogenic differentiation of VICs.

3.2 Materials and Methods

3.2.1 Tissue and RNA Harvest

Aortic valve leaflets excised from adult female pigs were obtained at a local slaughterhouse (Sansing Meat Services) and cultured as previously described in Chapter 2. Briefly, leaflets were rinsed in ice-cold sterile PBS (Sigma, St Louis, MO). The endothelium was removed from the leaflet surface using collagenase II solution (2 μ g/ml, Worthington Biochemical Corp.) to simulate the *in vivo* pathogenic milieu. Leaflets (n=6) were incubated overnight in DMEM in 6-well tissue culture plates. For pressure experiments, plates were then placed in a custom pressure chamber shown in Chapter 2 and exposed to normotensive (0-80 mm Hg) or hypertensive cyclic pressure (0-120 mmHg) corresponding to diastolic transvalvular pressure in normotensive and hypertensive conditions, at frequency of 1 Hz for 24 hours. To mimic a biochemical hypertensive environment, culture medium was supplemented with Ang II (300nM, Sigma) at the beginning of pressurization. Thus, four experimental conditions were tested: (1) Valve leaflets exposed to normotensive cyclic pressure (0-80 mmHg); (2) valve leaflets exposed to hypertensive cyclic pressure (0-120 mmHg); (3) valve leaflets exposed to normotensive cyclic pressure with Ang II –conditioned media; and (4) valve leaflets exposed to hypertensive cyclic pressure with Ang II –conditioned media. Upon

completion of experiments, total RNA was extracted as previously described in chapter 2 using the RNeasy Mini kit (Qiagen). RNA quality was confirmed by electrophoresis (2100 Bioanalyzer; Agilent Technologies, Palo Alto, CA). RNA samples with a 260:280 ratio of 1.9 or higher were used for further analysis.

3.2.2 Real Time Quantitative-PCR

Semi-quantitative reverse transcriptase polymerase chain reaction (RT PCR) was done to measure the relative change in mRNA expression of Osteopontin (SSP1), Runt related factor 2 (RUNX2), Alkaline Phosphatase (ALP), bone morphogenetic protein 7 (BMP-7) and Mad related protein 1 (SMAD1). Total RNA isolation, storage and Real-Time RT-PCR were carried out as previously described in chapter 2. Briefly, RNA was obtained from valve samples (n=6) with RNeasy Mini kit (Qiagen). Total RNA (~2 µg) was used for RT-PCR using a Bio-Rad iCycler thermocycler and iScript one-step SYBR Green kit. Primer sequences were designed using Primer 3 software (Table 3.1)¹⁴. Expression values for each gene were calculated relative to 18s mRNA levels using the $\Delta\Delta CT$ method.

Table 3.1 Primers used for RT- PCR analysis

Gene	Accession Number	Primer Sequence 5'-3'		Product Size (bp)
		Sense	Antisense	
RUNX2	NM_001024630	CAGACCAGCAGCACTCC ATA	CAGCGTCAACACCATCATTC	344
SSP1	NM_214023	GGTCTATGGACTGAGGTCAAATC TA	TCCGAGGAAATAGTATTCTGTGGC	397
ALP	AY145130S2	ACCTCGTTGACACCTGGAAG	TCACGTTGTTCTGTTTCAGC	370
BMP-7	NM_001105290	GCTATGCCGCCTACTACTGC	GATGAAGTGGACCAGCGTCT	255
SMAD1	NM_213965	TGCCTCACGTCATCTACTGC	AGAGGCTGTGCTGAGGGTTA	280
18s	NM_001037146	CGGAGAGGGAGCCTGAGAAA	CGGGTCGGGAGTGGGTAAT	233

3.2.3 Immunohistochemistry

Immunohistochemical detection of SSP1, RUNX2-1 and ALP protein expression in aortic valve leaflets was performed. Following exposure to normotensive and hypertensive conditions for 24 hours, leaflet samples were rinsed twice with PBS with 1% BSA, and fixed with 4% PFA (Sigma) in PBS. Additionally samples were fixed in 10% formaldehyde overnight, transferred to 70% ethanol, processed in a tissue processor, embedded in paraffin, and cut in 5 μ m sections. Slides were deparaffinized, then placed in hydrogen peroxide to inhibit endogenous peroxidase activity, and then immersed in blocking agent for 30 minutes. Following slides were incubated overnight at 4 °C with rabbit anti – human SSP1 (Thermo Scientific), anti–human ALP (Zigmed Laboratoties) and anti – human RUNX2-1 (Santa Cruz Biotechnology, CA), slides were washed in buffer and exposed to biotinylated anti-rabbit IgG (Dako) for 30 min (Table 3.2). Cell nuclei were counterstained with hematoxylin. The slides were observed under a photomicroscope (Nikon) equipped with a digital camera. Images were examined with Photoshop (Adobe Photoshop, San Jose, CA). The total amount and distribution of SSP1, RUNX2 and ALP protein expression was compared between different samples.

3.2.4 Western Blot

Valve leaflets was disrupted and homogenized 600 μ L of lysis buffer containing in the presence of protease inhibitors (Quiagen, Valencia, CA) using a rotor stator homogenizer (IKA®). Protein extracts from valve tissue were separated on a 10% SDS–PAGE, and transferred to PVDF membranes (Bio-Rad Laboratories, CA). The blots were probed with goat anti human Angiotensin II Type 1 receptor (AT₁, Santa Cruz Biotechnology,CA) and Angiotensin II Type 1 receptor 2 (AT₂, Santa Cruz

Biotechnology, CA) specific antibodies. Proteins were detected using an HRP conjugated anti-goat IgG secondary antibody (Santa Cruz Biotechnology, CA) and recognized by a peroxidase chemiluminescent detection reagent (Visualizer™ Spray & Glow™, Millipore). GAPDH (Santa Cruz Biotechnology, CA) was used as internal control (Table 3.2).

Table 3.2 Antibodies used for Immunohistochemistry and Western Blot

<i>Target</i>	<i>Primary Antibody</i>	<i>Secondary Antibody</i>
RUNX2	Monoclonal mouse anti-RUNX2 (US Biological, 1:200)	Biotinylated rabbit anti-mouse IgG
ALP	Monoclonal mouse-anti ALP (US Biological, 1:200)	Biotinylated rabbit anti-mouse IgG
SSP1	Monoclonal mouse-anti SSP1 (US Biological, 1:50)	Biotinylated rabbit anti-mouse IgG
AT1	Polyclonal goat anti- AT1 (US Biological, 1:200)	Biotinylated donkey anti- goat IgG
AT2	Polyclonal goat anti- AT2 (US Biological, 1:2000)	Biotinylated donkey anti- goat IgG
GAPDH	Polyclonal goat anti- GAPDH (US Biological, 1:200)	Biotinylated donkey anti- goat IgG

3.2.5 Statistical Analysis

At least six experiments were run for each condition. The level of gene expression was calculated as $2^{-\Delta Ct}$. ΔCt was the difference in cycle threshold between the housekeeping gene, 18s, and the gene of interest. Results for RT PCR are reported as mean \pm 95% confidence interval. One-way analysis of variance (ANOVA) was used to compare differences between groups; all statistical analyses were accomplished using SAS 9.1 analysis software (SAS Institute inc. Carey, NC). A *p* value of 0.05 or less was considered significant.

3.3 Results

3.3.1 Elevated Pressure Induces Osteogenic differentiation of VICs

To determine the effect of elevated cyclic pressure on VICs phenotype, we measured the changes in mRNA expression of three genes that induce osteoblast differentiation: Osteopontin (OSP1), alkaline phosphatase (ALP), Runt-related transcription factor (RUNX2); and two key members of the BMP osteogenic pathway: Bone morphogenic protein (BMP-7) and Mad related factor 1 (SMAD1). The expression levels for OSP1, ALP, RUNX2, BMP-7 and SMAD1 were significantly up regulated in valve leaflets exposed to elevated cyclic pressure (0-120mmHg) after 24 hour treatment ($p < 0.05$). Thus, OSP1 and ALP gene expression levels had a significant increase (18 and 3.8 fold change, respectively) in samples exposed to elevated cyclic pressure compared to control samples (Figures 3.1B, C). RUNX2 levels were strikingly increased by > 2800 fold change (Figure 3.2A). Likewise, gene expression of BMP-7 and SMAD1 was significantly increased by >700 fold ($p < 0.0001$) in valve leaflets exposed to elevated cyclic pressure (Figure 3.2). Given the ability of these genes to drive osteoblastic differentiation, our data demonstrates that elevated cyclic pressure alone is able to induce osteogenic differentiation of VICs and, further, that a BMP osteogenic pathway may be activated.

3.3.2 Exposure to Ang II Decreases Osteogenic Gene Expression of VICs

Ang II is a potent vasoconstrictor hormone that plays a central role in hypertension. To mimic the effects of Ang II- induced hypertension, we next investigated the combined effects of Ang II treatment and cyclic pressure (0-80mm Hg, 0-120 mmHg)

on osteogenic differentiation of VICs. In the presence of Ang II treatment, there was a significant increase in SSP1, RUNX2 and ALP gene levels (2.6, 700, 5.9 fold change, respectively) in valve leaflets exposed to elevated cyclic pressure (0-120mmHg) compared to normotensive conditions (0-80 mm Hg) (Figure 3.1). Conversely, stimulation with Ang II resulted in increased BMP-7 gene levels in normotensive conditions (3.7 fold change) compared to hypertensive conditions (0-120 mm Hg). Stimulation with Ang II significantly reduced SMAD1 gene levels in samples exposed to elevated cyclic pressure. Furthermore, there was no significant difference in SMAD1 gene levels between normotensive and hypertensive conditions (Figure 3.2). Interestingly, Ang II treatment suppressed the expression of SSP1, RUNX2, SMAD1 and BMP-7 by approximately 80%, 26%, 96%, and 92%, respectively, compared with that of the non- Ang treated leaflets exposed to elevated cyclic pressure. In contrast, ALP expression was unchanged with Ang II treatment. This differential response to Ang II treatment suggests a modulating role of Ang II for VICs osteogenic differentiation in hypertensive conditions. Furthermore, there is a synergistic effect of Ang II and hypertensive conditions to negatively regulate gene levels of transcriptional activation of SSP1, RUNX2, SMAD1 and BMP-7 but not of ALP. To our knowledge, there are no previous reports of Ang II-regulated gene expression of SSP1, RUNX2 and SMAD1 in VICs.

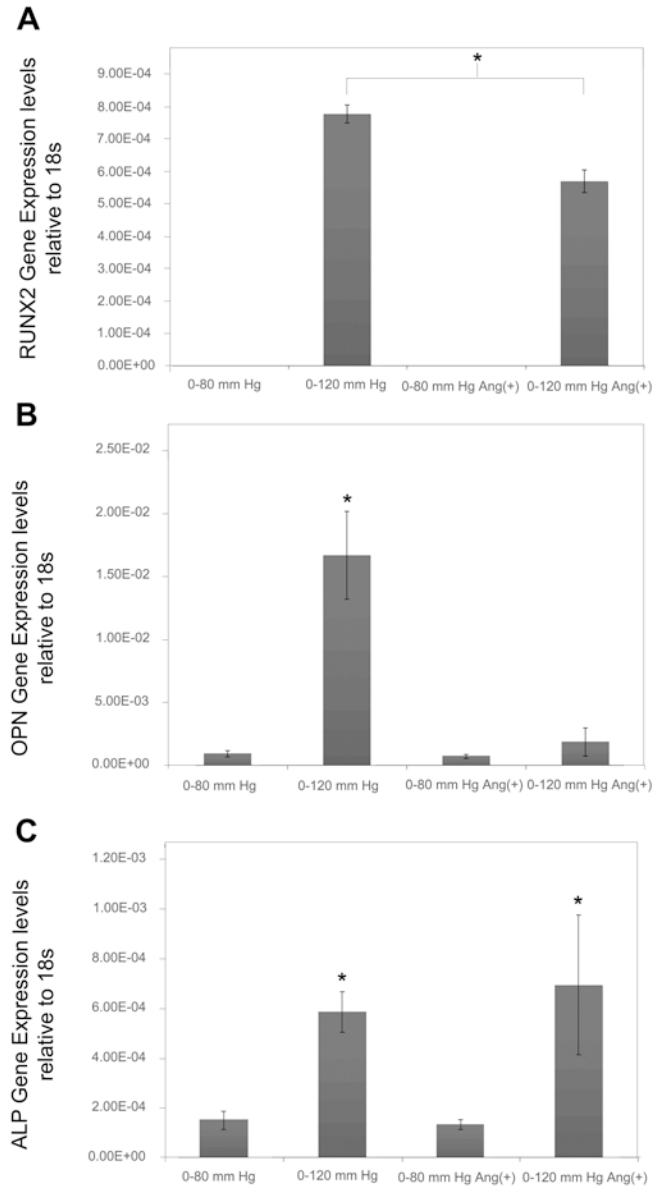


Figure 3.1 mRNA expression levels of osteogenic markers, relative to 18s, in VICs exposed to normotensive (0-80 mmHg) and hypertensive conditions (0-120 mm Hg) for 24 hours. A. RUNX2, B. SSP1 C. ALP. Bars represent mean values + 95% confidence interval: * = $p \leq 0.05$.

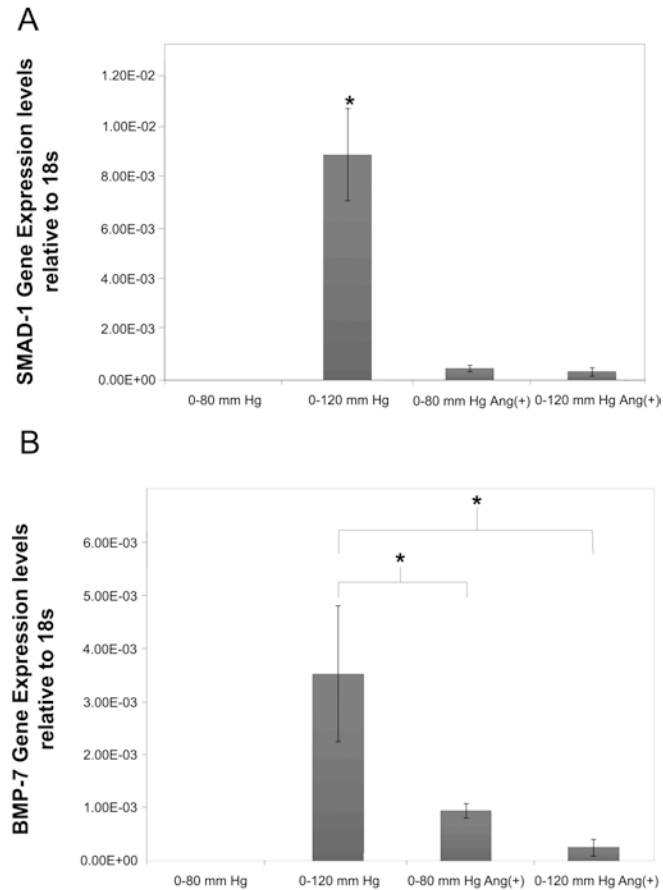


Figure 3.2 mRNA expression levels of osteogenic markers, relative to 18s, in VICs exposed to normotensive (0-80 mmHg) and hypertensive conditions (0-120 mm Hg) for 24 hours. A. SMAD1. B. BMP-7. Bars represent mean values + 95% confidence interval: * = $p < 0.05$.

3.3.3 Exposure to Pressure Increases Osteogenic markers in Valve Leaflets.

Immunochemical staining of porcine aortic leaflets exposed to normotensive and hypertensive conditions in the presence or absence of Ang II showed distinct staining patterns of RUNX2, SSP1 and ALP protein expression. In valve leaflets exposed to hypertensive conditions RUNX2 was detected in abundance through all areas of the leaflet (Figure 3.3 B); and treatment with Ang II markedly attenuated RUNX2 expression (Figure 3.3 J). Complete absence of RUNX2 staining was observed in samples exposed

to normotensive conditions in presence and absence of Ang II (Figure 3.3 A, J). In valve leaflets exposed to normotensive conditions, in presence or absence of Ang II treatment, a slight staining for SSP1 was observed (Figure 3.3B, H). SSP1 expression was markedly increased in samples exposed to hypertensive conditions (0-120 mm Hg). These samples revealed areas of intense staining, demonstrating the enhanced accumulation of SSP1 protein in VICs (Figure 3.3E). SSP1 expression is generally lower and almost completely absent in valve tissue exposed to Ang II under elevated pressure conditions (Figure 3.3K). ALP expression was generally absent in leaflets exposed to normotensive conditions, and treatment with Ang II resulted in a similar pattern of staining (Figure 3.3 C, I). ALP is detected in abundance in leaflets exposed to elevated pressure. The addition of Ang II resulted in stronger staining of ALP. Valve leaflets exposed to normotensive conditions demonstrated low levels of ALP protein expression (Figure 3.3F,L).

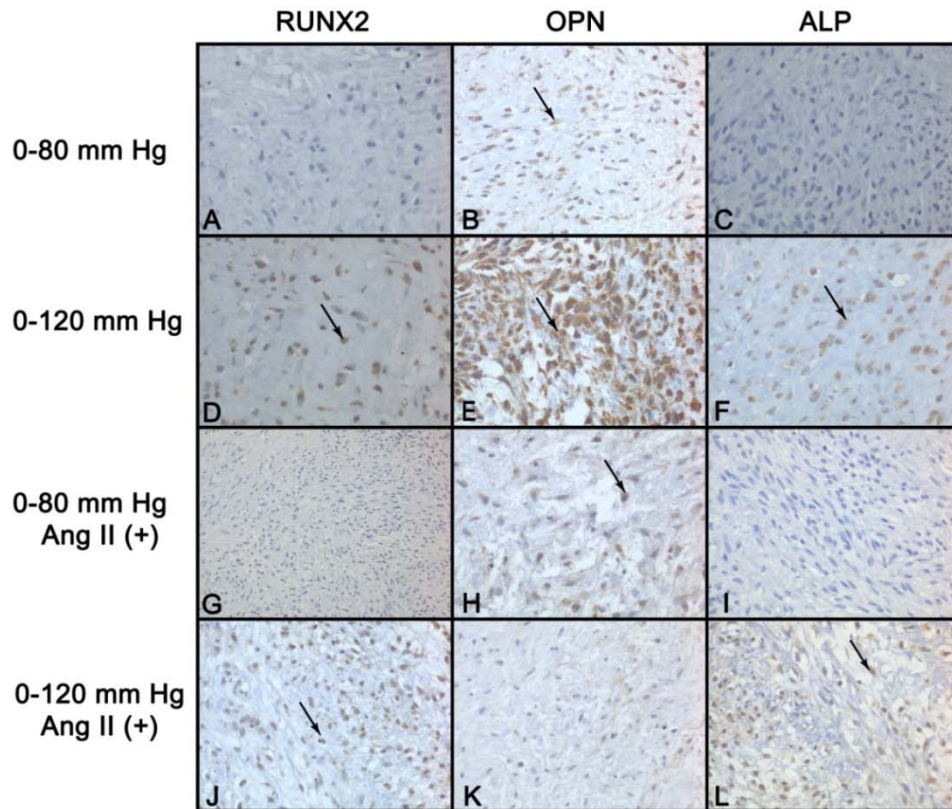


Figure 3.3 Evidence of osteogenic proteins in porcine aortic valve exposed to: normotensive conditions (A - C); hypertensive conditions (D-F), normotensive conditions and Ang II (G-I); hypertensive conditions and Ang II (J-L). Representative immunohistochemical staining (brown, shown by arrows) of RUNX2 (A,D,G,J); SSP1 (B,E,H,K), and ALP (C,F,I,L). Cell nuclei counterstained blue. All frames 40X magnification.

3.3.4 Expression of Ang II Receptors in VICs

From the previous observations, we suggest that SSP1, RUNX2, SMAD1 and BMP-7 gene expression may be negatively regulated by Ang II under hypertensive conditions. Since downstream signaling of Ang II is dependent on specific AT receptor expression, we therefore examined AT1 and AT2 receptor expression in VICs exposed to hypertensive and normotensive conditions by with western blot (Figure 3.4). Western blot analysis showed that VICs exposed to normotensive cyclic pressure (0-80mmHg) or

elevated pressure (0-120mmHg) do not express AT1, but treatment with Ang II increases the levels of AT1 with both levels of pressure. By contrast, AT2 was detected in VICs exposed to both normotensive and elevated cyclic pressure, and valve leaflets treated with Ang II expressed a similar AT2 receptor profile. Because of the effect of Ang II on osteogenic markers expression and the difference in AT1 and AT2 receptor expression in VICs to elevated pressure, we suggest that the changes observed in the expression of osteogenic marker may be potentially mediated through the subsequent activation of the AT1 receptor by Ang II. In addition, it is interesting to find that AT2 receptor was expressed by VICs in normotensive and hypertensive conditions, since previous findings suggest that valve leaflets do not express AT2 receptors under normal or pathological conditions^{15, 16}.

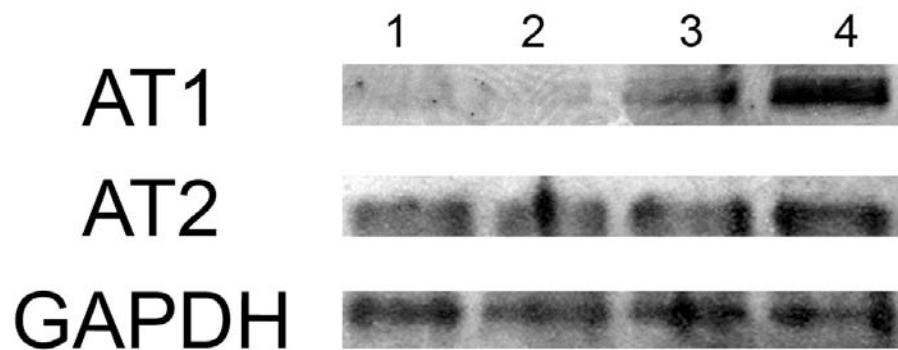


Figure 3.4 Protein expression of Angiotensin type 1 and Angiotensin type 2 receptors from valve leaflets exposed to cyclic pressure and Ang II treatment. Lane 1. normotensive cyclic pressure (0-80 mmHg), Lane 2. hypertensive cyclic pressure (0-120 mmHg); Lane 3. normotensive cyclic pressure Ang II (+), Lane 4. Hypertensive cyclic pressure Ang II (+).

3.4 Discussion

It is widely known that valve calcification is a cell-based process that requires the mediation of an osteoblast phenotype¹⁷. A number of clinical studies suggest a role for hypertension in the development of calcific aortic valve disease^{10, 18}. Clinical and experimental clues of this association include the following: Hypertension is a frequent finding in patients with calcific aortic stenosis, elevated pressure results in alterations in the native hemodynamic environment of the aortic valve (i.e. increased stretch, compression of the ECM, altered flow patterns), and calcified lesions are present on the aortic side of the valve where higher transvalvular pressure gradients occur^{19, 20}. Yet, neither study has been able to establish the precise mechanism by which hypertension might contribute to the development of calcific aortic valve disease.

Close correlations between mechanical loading, biochemical environment and aortic valve biology have been demonstrated by clinical observations and animal studies^{21, 22}. For example, pressure can both positively and negatively regulate systems involved in DNA, collagen, GAGs synthesis, and activation of pro-inflammatory mechanisms²³⁻²⁵. In addition, variation in the biochemical environment (i.e. high levels of TGF- β , BMP-2) promotes phenotypic alterations in VICs and dysregulation of ECM production^{7, 19}. From these observations, it was important to evaluate the potential impact of hypertension on molecular events that lead to calcific aortic valve disease; therefore we examined the effects of elevated pressure and Ang II stimulation, two of the mechanical and biochemical factors observed in hypertension, on osteogenic differentiation of porcine aortic valvular interstitial cells.

The most interesting finding in this study was the intense effect of elevated pressure on VICs phenotype. Elevated pressure was able to modulate VICs osteogenic differentiation by increasing gene expression of specific osteoblast markers SSP1, RUNX2, ALP, SMAD1 and BMP-7. Although some changes in gene expression were observed from biochemical stimuli with Ang II in other treatments, their effects were not as significant as the ones obtained with the elevated pressure alone. Moreover, it was demonstrated that the increased levels of the osteogenic markers were significantly reduced by stimulation with Angiotensin II. To our knowledge, this is the first time that elevated pressure is involved in regulation of VICs osteogenic differentiation via activation of genes participating in osteoblast differentiation and BMP osteogenic pathways. Furthermore, our results suggest possible links between Ang II signaling and activation of osteogenic mechanisms in aortic heart valve.

3.4.1 A Major Role of Elevated Pressure in VICs Osteogenic Differentiation

We showed that elevated cyclic pressure (0-120 mm Hg), with no other mechanical or biochemical interference, directly enhances gene and protein expression of SSP1, ALP and RUNX2 in VICs. These are osteoblast-specific proteins, and their expression is highly regulated in tissues undergoing bone differentiation. RUNX2, SSP1 and ALP expression is essential for maturation of osteoblasts cells and also for an adequate mineralization of bone matrix ^{26, 27}. Genetic deficiency of these proteins is associated with impaired skeletal development ²⁸, highlighting their key role in osteogenic mechanisms. Hence, our results suggest that VICs, stimulated with elevated pressure, undergo a conversion process into osteoblast-like cells. This response is associated with an increased expression of RUNX2, SSP1, and ALP. In addition, our data

demonstrates that physiological levels of pressure are capable to maintain VICs phenotype, as basal gene levels of RUNX2, SSP1, and ALP were detected in VICs exposed to normotensive pressure (0-80 mm Hg). It has been previously reported that treatment with exogenous BMP-2/BMP-7 causes osteogenic differentiation of VICs *in vitro*^{3, 29}. This finding along with evidence that severely calcified aortic valves contain increased levels of RUNX2, OPN, and ALP^{3, 30} confirms the contribution of active osteogenic regulatory pathways in valve calcification.

Further evidences of an osteogenic transformation of VICs exposed to elevated pressure are the increased levels of SMAD1 and BMP-7. SMAD1 is one of the three known receptor-regulated Smads (R-smad); it has been widely studied due to its function as a key transcriptional regulator for multiple genes related to osteogenic mechanisms including OPN and RUNX2³¹. In fact, association of SMAD1 and RUNX2 is required for the progression necessary for the osteoblast differentiation in mesenchymal stem cells *in vitro*²⁷. Studies show that SMAD1 regulation of RUNX2 and OPN is induced by bone morphogenic proteins in human VICs⁷. In addition, SMAD1 expression is an indicator for signaling through BMP pathways. BMP-2 and BMP-7 are well known growth factors, and their effects in osteogenic induction have been thoroughly studied. Consistent with this idea, we found increased expression of BMP-7 gene levels in VICs exposed to elevated pressure. Bone Morphogenetic Protein 7 (BMP-7) belongs to the TGF-beta family; they promote phosphorylation and activation of SMAD proteins through diverse types of BMP receptors. Both BMPs and SMAD proteins are the major mediators of specific osteoblastic differentiation^{28, 32}. The ability of these genes to promote osteoblast differentiation suggests that elevated pressure may have a key role in promoting VICs

differentiation into osteoblast type cells through BMP-mediated signaling. Taken together these findings demonstrate that elevated pressure is able to activate the transcriptional regulation of genes that are essential for osteoblast differentiation pathways in VICs. Hence, elevated pressure through increased expression of BMP-7 and SMAD1 may induce the expression of the osteoblast specific genes RUNX2, SSP1 and ALP and together may function in a positive feedback loop to induce osteoblastic differentiation in VICs (Figure 3.5).

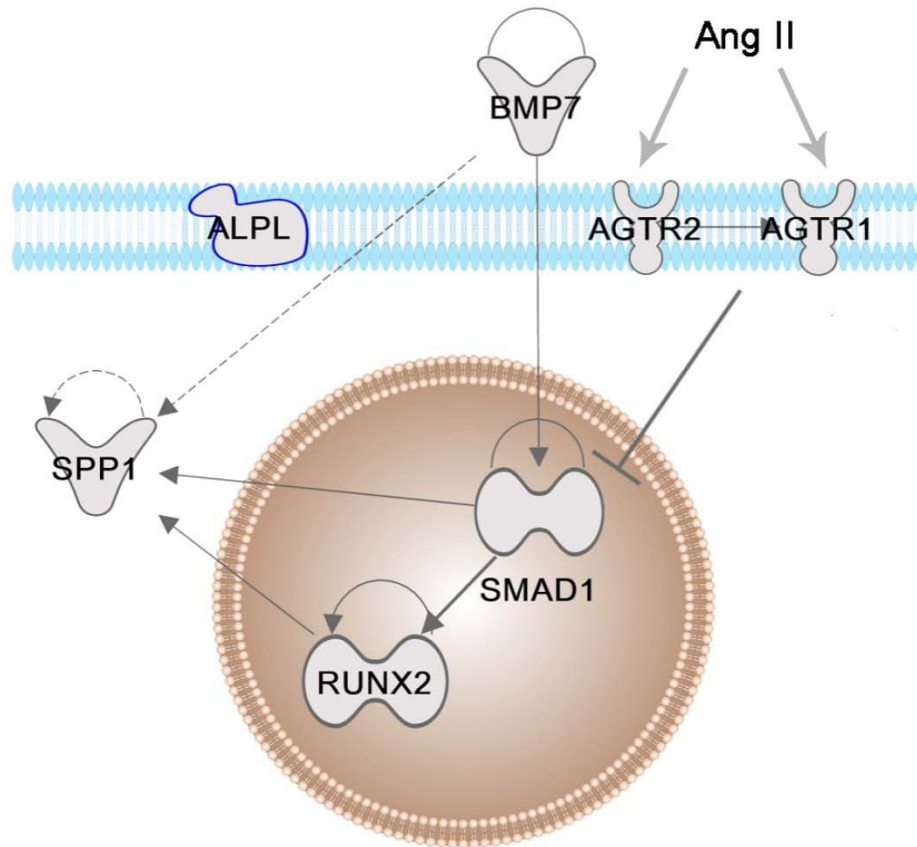


Figure 3.5 Schematic representation of and molecular interactions and cellular location among significantly expressed genes involved in BMP osteogenic signaling pathway. Nodes are displayed using various shapes that represent the functional class of the gene product: Y shaped figures represent transmembrane receptors; down-pointing triangles represent cytokines, horizontal ovals represent transcription regulators. Continuous lines show direct interactions between nodes and dashed lines show indirect interactions. Lines beginning and ending on the same node show self regulation. Arrowheads show directionality of the relationship. SPP1 is the alternative name of SSP1.

3.4.2 Regulatory Role of Ang II in VICs Osteogenic Differentiation

It has been reported that Angiotensin converting enzyme (ACE), Angiotensin II, and the Angiotensin II type 1 receptor (AT1) are up-regulated in human calcified aortic valves, suggesting a role for Ang II in valvular calcification³³. Angiotensin II is a potent

vasoconstrictor hormone that plays a central role in hypertension. The effects of Ang II can be triggered by the binding to two types of receptors: Ang receptor type 1 (AT1) or Ang receptor type 2 (AT2). Both exert opposite effects as AT2 has a pro apoptotic role, which contrasts with the proliferative role of AT1. After binding to receptors, Ang II may stimulate different signaling pathways¹². Based on these observations, it was therefore of interest to define the effects of Ang II in VICs osteogenic differentiation by cyclic pressure. Our data shows that the increase in OPN, RUNX2, SMAD1, and BMP-7 induced by elevated pressure in VICs was markedly attenuated with Ang II treatment. Specifically in VICs exposed to elevated pressure, Ang II suppresses BMP-7, OPN, and SMAD1 gene expression, whereas ALP was not affected. In addition, stimulation with Ang II did not completely inhibited RUNX2 expression. This response may partially result from differential expression of Ang II receptors in VICs. Here, we demonstrated that AT1 was expressed on VICs exposed to elevated cyclic pressure and Ang II. In addition, we showed that VICs expressed AT2 receptors independently of the pressure conditions. These data suggest that factors that modulate osteogenic conversion of VICs are associated with up-regulation of Ang II type 1 receptors. *In vitro* studies have suggested that Angiotensin type 1 and type 2 receptors exhibit opposite functions, thus, AT2 receptors appear to induce pro apoptotic mechanisms that contrast the cell proliferative effects of AT1. It is widely known that AT1 is responsible for most of the effects of Ang II in hypertension. In addition, AT1 receptor and expression of Ang II converting enzyme expression has been proved in VICs from calcified valves³⁴. It has been suggested that the negative effects of AT1 activation might also relate to oxide radical generation, as AT1 receptor activation can lead to up regulation of NADPH

oxidase³⁵, a mechanism for generation of superoxide and elevation of oxidative stress. In conclusion our findings suggest that: (1) elevated pressure may induce VICs osteoblast differentiation by activating other SMAD/BMP independent signaling for RUNX2/ALP expression (i.e. TNF- α / cAMP signaling), (2) Ang II may regulate VICs osteogenic differentiation by negative feedback in SMAD1/BMP-7 signaling, and (3) Ang II type 1 receptor levels may be a determining factor on valve calcification. Our results contrast with previous studies which show that Ang II-stimulation via AT1 significantly increases OPN levels and SMAD1 activation in vascular interstitial cells³⁶; and thus, the differential response to Ang II treatment underlines the phenotypic and functional differences of VICs with their vascular counterparts. We suggest that AT1 II signaling may decrease the levels of osteogenic markers (SMAD1, SSP1) in VICs by two possible mechanisms: (i) through an inhibitory effect on SMAD1 activation or (ii) inducing VICs redox-mediated apoptosis.

Our data regarding AT2 expression are intriguing. Although, it is widely known that AT1 is responsible for most of the effects of Ang II in hypertension, the effects of AT2 are still controversial. Previous data show that AT2 receptor is abundant in atherosclerotic lesions and also AT2 expression increases in hypertensive mice^{37, 38}. However, pharmacological disruption of AT2 leads to accelerated atherosclerosis³. These findings suggest that AT2 expression can itself be a way to moderate the pathophysiological actions of AT1, giving AT2 protective role in hypertension⁴. To our knowledge this is the first study that shows expression of AT2 receptors in VICs. The disparity between our results and those of other reports may be partly explained by the time and conditions in which valve leaflets were exposed to pressure. However,

expression of AT2 receptors in VICs could play a significant role in the pathogenesis of calcific aortic valve disease, and thus, further studies into the effects of AT2 in VICs are needed.

The close association between high levels of osteogenic markers (RUNX2, ALP, SSP1, BMP-7, and SMAD1) and elevated pressure raises the question whether osteogenic differentiation of VICs is the result of direct transmission of mechanical loading by ECM to VICs (i.e. via integrins, membrane receptors) or through activation of secondary processes (i.e. oxidative stress). Although, our study does not address this question, several studies show that oxidative stress promotes a phenotypic shift of vascular smooth muscle cells from contractile to osteogenic phenotype³⁹. In addition, oxidative stress is present in all forms of hypertension and also it is increased in human calcified valves^{40, 41}. Interestingly, it has been shown that BMP expression can be regulated by oxidative stress²⁸. Hence, it is possible that oxidative stress, induced by elevated pressure, might be able to stimulate BMP osteogenic signaling pathways in valve leaflets leading to VICs osteogenic differentiation. Future work will be needed to determine specific links between mechanisms of oxidative stress and activation of osteogenic mechanisms in VICs exposed to elevated cyclic pressure. Although hypertension may not be the only factor leading to the development of aortic valve calcification, our results show that elevated cyclic pressure may promote the development of a calcified lesion by directly influencing VICs osteogenic differentiation. Furthermore, our data demonstrates that hypertensive pressure is a key regulator of VICs phenotype via promoting osteogenic differentiation through a BMP pathway into an osteoblast-like phenotype. In addition, we suggest that Ang II through AT1 receptors play a regulatory role in osteogenic

differentiation mechanisms in VICs. Further studies are required to elucidate the possible links between mechanisms of Ang II receptors and osteogenic differentiation of VICs.

3.5 References

- (1) Akat K, Borggrefe M, Kaden JJ. Aortic valve calcification: basic science to clinical practice. *Heart* 2009 April;95(8):616-23.
- (2) Aksoy Y, Yagmur C, Tekin GO et al. Aortic valve calcification: association with bone mineral density and cardiovascular risk factors. *Coron Artery Dis* 2005 September;16(6):379-83.
- (3) Rajamannan NM, Subramaniam M, Rickard D et al. Human aortic valve calcification is associated with an osteoblast phenotype. *Circulation* 2003 May 6;107(17):2181-4.
- (4) Kaden JJ, Kilic R, Sarikoc A et al. Tumor necrosis factor alpha promotes an osteoblast-like phenotype in human aortic valve myofibroblasts: a potential regulatory mechanism of valvular calcification. *Int J Mol Med* 2005 November;16(5):869-72.
- (5) Smith KE, Metzler SA, Warnock JN. Cyclic strain inhibits acute pro-inflammatory gene expression in aortic valve interstitial cells. *Biomech Model Mechanobiol* 2009 July 28.
- (6) Balachandran K, Sucusky P, Jo H, Yoganathan AP. ELEVATED CYCLIC STRETCH ALTERS MATRIX REMODELING IN AORTIC VALVE CUSPS - IMPLICATIONS FOR DEGENERATIVE AORTIC VALVE DISEASE? *Am J Physiol Heart Circ Physiol* 2009 January 16.
- (7) Yang X, Meng X, Su X et al. Bone morphogenic protein 2 induces Runx2 and osteopontin expression in human aortic valve interstitial cells: role of Smad1 and extracellular signal-regulated kinase 1/2. *J Thorac Cardiovasc Surg* 2009 October;138(4):1008-15.
- (8) Rajamannan NM, Subramaniam M, Stock SR et al. Atorvastatin inhibits calcification and enhances nitric oxide synthase production in the hypercholesterolaemic aortic valve. *Heart* 2005 June;91(6):806-10.
- (9) Stritzke J, Linsel-Nitschke P, Markus MR et al. Association between degenerative aortic valve disease and long-term exposure to cardiovascular risk factors: results of the longitudinal population-based KORA/MONICA survey. *Eur Heart J* 2009 August;30(16):2044-53.
- (10) Lindroos M, Kupari M, Valvanne J, Strandberg T, Heikkila J, Tilvis R. Factors associated with calcific aortic valve degeneration in the elderly. *Eur Heart J* 1994 July;15(7):865-70.
- (11) Bermejo J. The effects of hypertension on aortic valve stenosis. *Heart* 2005 March;91(3):280-2.

- (12) Mehta PK, Griendling KK. Angiotensin II cell signaling: physiological and pathological effects in the cardiovascular system. *Am J Physiol Cell Physiol* 2007 January 1;292(1):C82-C97.
- (13) Ertas FS, Hasan T, Ozdol C et al. Relationship between angiotensin-converting enzyme gene polymorphism and severity of aortic valve calcification. *Mayo Clin Proc* 2007 August;82(8):944-50.
- (14) Rozen S, Skaletsky H. Primer3 on the WWW for general users and for biologist programmers. *Methods Mol Biol* 2000;132:365-86.
- (15) O'Brien KD. Pathogenesis of calcific aortic valve disease: a disease process comes of age (and a good deal more). *Arterioscler Thromb Vasc Biol* 2006 August;26(8):1721-8.
- (16) Helske S, Lindstedt KA, Laine M et al. Induction of local angiotensin II-producing systems in stenotic aortic valves. *J Am Coll Cardiol* 2004 November 2;44(9):1859-66.
- (17) Aksoy Y, Yagmur C, Tekin GO et al. Aortic valve calcification: association with bone mineral density and cardiovascular risk factors. *Coron Artery Dis* 2005 September;16(6):379-83.
- (18) Adler Y, Motro M, Tenenbaum A et al. Aortic valve calcium on spiral computed tomography is associated with calcification of the thoracic aorta in hypertensive patients. *Am J Cardiol* 2002 March 1;89(5):632-5.
- (19) Mohler ER, III. Mechanisms of aortic valve calcification. *Am J Cardiol* 2004 December 1;94(11):1396-402, A6.
- (20) Butcher JT, Simmons CA, Warnock JN. Mechanobiology of the aortic heart valve. *J Heart Valve Dis* 2008 January;17(1):62-73.
- (21) Xing Y, Warnock JN, He Z, Hilbert SL, Yoganathan AP. Cyclic pressure affects the biological properties of porcine aortic valve leaflets in a magnitude and frequency dependent manner. *Ann Biomed Eng* 2004 November;32(11):1461-70.
- (22) Smith KE, Metzler SA, Warnock JN. Cyclic strain inhibits acute pro-inflammatory gene expression in aortic valve interstitial cells. *Biomech Model Mechanobiol* 2009 July 28.
- (23) Warnock JN, Burgess SC, Shack A, Yoganathan AP. Differential immediate-early gene responses to elevated pressure in porcine aortic valve interstitial cells. *J Heart Valve Dis* 2006 January;15(1):34-41.

- (24) Xing Y, He Z, Warnock JN, Hilbert SL, Yoganathan AP. Effects of constant static pressure on the biological properties of porcine aortic valve leaflets. *Ann Biomed Eng* 2004 April;32(4):555-62.
- (25) Xing Y, Warnock JN, He Z, Hilbert SL, Yoganathan AP. Cyclic pressure affects the biological properties of porcine aortic valve leaflets in a magnitude and frequency dependent manner. *Ann Biomed Eng* 2004 November;32(11):1461-70.
- (26) Drissi MH, Li X, Sheu TJ et al. Runx2/Cbfa1 stimulation by retinoic acid is potentiated by BMP2 signaling through interaction with Smad1 on the collagen X promoter in chondrocytes. *J Cell Biochem* 2003 December 15;90(6):1287-98.
- (27) Lee KS, Kim HJ, Li QL et al. Runx2 is a common target of transforming growth factor beta1 and bone morphogenetic protein 2, and cooperation between Runx2 and Smad5 induces osteoblast-specific gene expression in the pluripotent mesenchymal precursor cell line C2C12. *Mol Cell Biol* 2000 December;20(23):8783-92.
- (28) Chen D, Zhao M, Mundy GR. Bone Morphogenetic Proteins. *Growth Factors* 2004;22(4):233-41.
- (29) Rajamannan NM, Subramaniam M, Stock SR et al. Atorvastatin inhibits calcification and enhances nitric oxide synthase production in the hypercholesterolaemic aortic valve. *Heart* 2005 June;91(6):806-10.
- (30) Kim KM. Calcification of matrix vesicles in human aortic valve and aortic media. *Fed Proc* 1976 February;35(2):156-62.
- (31) Wrana JL. Regulation of Smad activity. *Cell* 2000 January 21;100(2):189-92.
- (32) ten DP, Goumans MJ, Itoh F, Itoh S. Regulation of cell proliferation by Smad proteins. *J Cell Physiol* 2002 April;191(1):1-16.
- (33) Jimenez-Candil J, Bermejo J, Yotti R et al. Effects of angiotensin converting enzyme inhibitors in hypertensive patients with aortic valve stenosis: a drug withdrawal study. *Heart* 2005 October;91(10):1311-8.
- (34) Helske S, Lindstedt KA, Laine M et al. Induction of local angiotensin II-producing systems in stenotic aortic valves. *J Am Coll Cardiol* 2004 November 2;44(9):1859-66.
- (35) Pendergrass KD, Gwathmey TM, Michalek RD, Grayson JM, Chappell MC. The angiotensin II-AT1 receptor stimulates reactive oxygen species within the cell nucleus. *Biochemical and Biophysical Research Communications* 2009 June 26;384(2):149-54.

- (36) Rodriguez-Vita J, Sanchez-Lopez E, Esteban V, Ruperez M, Egado J, Ruiz-Ortega M. Angiotensin II Activates the Smad Pathway in Vascular Smooth Muscle Cells by a Transforming Growth Factor- β -Independent Mechanism. *Circulation* 2005 May 17;111(19):2509-17.
- (37) Johansson ME, Wickman A, Fitzgerald SM, Gan LM, Bergstrom G. Angiotensin II, type 2 receptor is not involved in the angiotensin II-mediated pro-atherogenic process in ApoE^{-/-} mice. *J Hypertens* 2005 August;23(8):1541-9.
- (38) Johansson ME, Fagerberg B, Bergstrom G. Angiotensin type 2 receptor is expressed in human atherosclerotic lesions. *J Renin Angiotensin Aldosterone Syst* 2008 March;9(1):17-21.
- (39) Huaizhou Y, Haichun Y, Qiuyu Z et al. Advanced Oxidation Protein Products Induce Vascular Calcification by Promoting Osteoblastic Trans-Differentiation of Smooth Muscle Cells via Oxidative Stress and ERK Pathway. *Renal Failure* 2009 May;31(4):313-9.
- (40) Wang D, Strandgaard S, Iversen J, Wilcox CS. Asymmetric dimethylarginine, oxidative stress, and vascular nitric oxide synthase in essential hypertension. *Am J Physiol Regul Integr Comp Physiol* 2009 February;296(2):R195-R200.
- (41) Liberman M, Bassi E, Martinatti MK et al. Oxidant generation predominates around calcifying foci and enhances progression of aortic valve calcification. *Arterioscler Thromb Vasc Biol* 2008 March;28(3):463-70.

CHAPTER 4
FUNCTIONAL MODELING OF PRESSURE INDUCED GENE EXPRESSION
REVEALS MECHANOSENSITIVE SIGNALING PATHWAYS
IN THE AORTIC VALVE

4.1 Introduction

Non-rheumatic aortic valve disease is characterized by chronic inflammation, increased extracellular matrix (ECM) remodeling, proliferation and differentiation of valvular interstitial cells (VICs) and the development of calcific lesions on the valve^{1, 2}. Evidence shows that pathological changes in valve tissue can be triggered by an altered hemodynamic environment, underlining the importance of mechanical loading in valve structure and function^{3, 4}. Numerous epidemiological and histological studies have suggested hypertension as a contributing factor for the development of aortic valve disease^{5, 6}. The potential mechanisms connecting hypertension with initiation and progression of aortic valve disease include: (1) hypertensive pressure raises the diastolic transvalvular pressure across the valve, increasing the mechanical strain experienced by the valve; (2) hypertension may disturb the hemodynamic environment, thus influencing valve cell behavior; and (3) hypertension may play a key role in the activation of several biological processes that induce aortic valve remodeling and disease⁷. Furthermore, a number of *in vitro* models have shown that cyclic pressure plays an important role in valve ECM synthesis, pro-inflammatory and capthesin gene expression⁸⁻¹¹. In addition, it

has been reported that transvalvular pressure has a direct effect on VICs stiffness and collagen synthesis¹². These findings suggest that a causal relationship exists between increased cyclic pressure and the pathogenesis of aortic valve disease. However, the mechanisms by which mechanical pressure acting on VICs leads to signaling regulation, gene expression, and ECM modulation remain unclear. Our hypothesis is that elevated pressure plays a key role in the development of aortic valve disease by activating inflammatory and valve remodeling mechanosensitive pathways. To identify transcription factors, regulatory genes and molecular mechanisms underlying valve response to elevated pressure, we used Affymetrix porcine microarrays and compared global gene expression profiles of porcine aortic valve leaflets exposed to cyclic pressures of 0-80 or 0-120 mmHg for 24 hours, representing physiological normotensive and hypertensive diastolic transvalvular pressure, respectively. Here, we showed that elevated pressure plays a critical role in the transcriptional regulation of pro-apoptotic and ECM remodeling mechanisms in aortic valve tissue, which are important factors in the development of aortic valve disease. These processes are associated with the expression of several pro-inflammatory genes, matrix metalloproteases (MMPs) and pro-apoptotic genes. Taken together, our data provides valuable evidence of the relevant molecular mechanisms activated by elevated cyclic pressure that have been previously observed in aortic valve disease.

4.2 Materials and Methods

4.2.1 Tissue Culture and RNA Harvest

Aortic valve leaflets excised from adult female pigs were obtained at a local slaughterhouse (Sansing Meat Services) and cultured as previously described in Chapter 2. Briefly, leaflets were rinsed in ice-cold sterile PBS (Sigma, St Louis, MO). The endothelium was removed from the leaflet surface using collagenase II solution (2 µg/ml, Worthington Biochemical Corp.) to simulate the *in vivo* pathogenic milieu. Leaflets were incubated overnight in DMEM in 6-well tissue culture plates (n=3). For pressure experiments, plates were then placed in a custom pressure chamber shown in Chapter 2 and exposed to normotensive (0-80 mm Hg) or hypertensive cyclic pressure (0-120 mmHg) at frequency of 1 Hz for 24 hours. Upon completion of experiments, total RNA was extracted as previously described in Chapter 2 using the RNeasy Mini kit (Qiagen). RNA quality was confirmed by electrophoresis (2100 Bioanalyzer; Agilent Technologies, Palo Alto, CA).

4.2.2 cDNA Microarrays

All protocols for RNA target preparation and hybridization were as described in the Affymetrix GeneChip Expression Analysis Technical Manual (Affymetrix, Santa Clara, CA). Briefly, total RNA (~70 ng of mRNA) was used for linear, two-cycle amplification by *in vitro* transcription and a total of 10 µg of single stranded cRNA was hybridized to GeneChip® Porcine Genome Array following the manufacturer's set protocol (Affymetrix). The array data and images were collected with the Affymetrix GeneChip Scanner 3300.

4.2.3 Microarray Data Analysis

mRNA expression levels were evaluated using the microarray software (Microarray Suite ver. 5.0; Affymetrix), which calculated three detection levels (present, marginal, absent) and the size of the messages, by considering both the intensities of the signals which were emitted from the probe sets and the number of probe pairs in which the perfect match was specific. The signal intensities for all probes in of each microarray were normalized and log transformed. The t test with the option of unequal variance was used to calculate P values for each gene. The fold change and Q values for each gene were calculated with SAM program with permutation of 500¹³. A p value < 0.05 was considered statistically significant.

4.2.4 Gene Ontology Analysis and Data Modeling

Porcine genes with no existing Gene Ontology (GO) annotation were manually GO annotated based on sequence similarity to human proteins using GOanna¹⁴ to search against the UniProtKB database¹⁵. To model the dataset, GO terms for differentially expressed (DE) genes were grouped based on the three organizing principles of GO: Cellular Component (CC), Molecular Function (MF) and Biological Process (BP). Each category was subjected to high-level analysis using the GOA whole protein SlimViewer. In addition, a specific set of GO Biological Process terms were selected based on their relevance to aortic valve disease (Table 4.1). Gene products within each GO term were scored to have a quantitative value of their changes in valve tissue that was exposed to elevated pressure. Ingenuity Pathways analysis (IPA; www.ingenuity.com) was used to identify statistically overrepresented interactions and pathways for our DE dataset. Since

IPA database does not include porcine genes, human orthologs of porcine genes were manually searched for in UniprotKB database and used as input gene identifiers in IPA.

Table 4.1 Selected GO Biological Processes with differentially expressed genes associated with aortic valve disease.

GO ID	GO Term Description
GO:0048771	tissue remodeling
GO:0034103	regulation of tissue remodeling
GO:0030198	extracellular matrix organization
GO:0043085	positive regulation of catalytic activity
GO:0043086	negative regulation of catalytic activity
GO:0008284	positive regulation of cell proliferation
GO:0008285	negative regulation of cell proliferation
GO:0030154	cell differentiation
GO:0045595	regulation of cell differentiation
GO:0045597	positive regulation of cell differentiation
GO:0045669	positive regulation of osteoblast differentiation
GO:0050729	positive regulation of inflammatory response
GO:0002376	immune system process
GO:0002526	acute inflammatory response
GO:0002684	positive regulation of immune system process
GO:0001818	negative regulation of cytokine production
GO:0001819	positive regulation of cytokine production
GO:0006915	Apoptosis
GO:0043065	positive regulation of apoptosis
GO:0043069	negative regulation of programmed cell death
GO:0043068	positive regulation of programmed cell death
GO:0043066	negative regulation of apoptosis
GO:0006916	anti-apoptosis
GO:0006917	induction of apoptosis
GO:0045768	positive regulation of anti-apoptosis
GO:0019987	negative regulation of anti-apoptosis

4.2.5 Real Time Quantitative-PCR

Microarray-based differential mRNA expression of MMP-3, MMP-1 and IL-6 was validated using semi-quantitative real-time RT-PCR. Total RNA isolation, storage

and Real-Time RT-PCR were carried out as previously described in chapter 2. Briefly, RNA was obtained with RNeasy Mini kit (Qiagen). Total RNA ($\approx 2 \mu\text{g}$) was used for RT-PCR using a Bio-Rad iCycler thermocycler and iScript one-step SYBR Green kit. Primer sequences were designed (Table 4.2) using Primer 3 software ¹⁶. Expression values for each gene were calculated relative to 18s mRNA levels using the $\Delta\Delta\text{CT}$ method.

Table 4.2 Primers used for RT- PCR validation

Gene	Accession Number	Primer Sequence 5'-3'		Fragment Size (bp)
		Sense	Antisense	
MMP3	NM_001166308	TGTGGAGTTCCTGATGTTGG	GGCTGAAGTCTCCGTGTTCT	240
MMP1	NM_001166229	TTTCCTGGGATTGGCAAC	TCCTGCAGTTGAACCAGCTA	233
IL6	NM_214399	CACCAGGAACGAAAGAGAGC	GTTTTGTCCGGAGAGGTGAA	204

4.2.6 Microarray Quality Check

Metrics like noise, background, Scale factor, and the ratio of intensities' of 3 probes to 5' probes for Actin and GAPDH genes were analyzed for chip quality control. Spiked in controls (*B. subtilis* genes lys, phe, thr, and dap) were added to the total RNA at known concentrations at the beginning of the experiment. Their intensity values were used to monitor the linear amplification and labeling process. The performance of the hybridization control genes (*E. coli* genes BioB, BioC and BioD and P1 Bacteriophage cre) was also used for determining the quality of each chip.

4.3 Results

4.3.1 mRNA Isolation

The amount of total mRNA isolated from aortic valve leaflets (n= 6) was between 50-70 ng per sample. RNA integrity number (RIN) ranged from 1.8 to 2.0, based on the ratio between the 28S and 18S ribosomal RNA bands from the Bioanalyzer gel-like image (Figure 4.1).

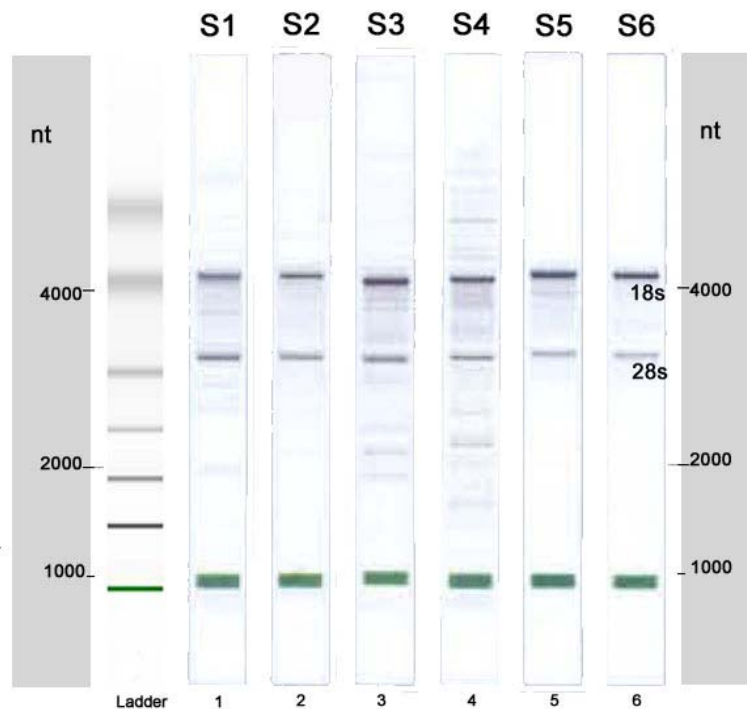


Figure 4.1 The image shows a total mRNA gel like-image produced by the Bioanalyzer. (Six samples used in the microarray experiment are shown). Lane L: Size markers. Lanes 1-3: total mRNA from valve leaflets exposed to normotensive cyclic pressure (0-80 mmHg), Lanes 4-6: total mRNA from valve leaflets exposed to hypertensive cyclic pressure (0-120 mmHg). The 28S and 18S distinctive ribosomal RNA bands are observed for all samples.

4.3.2 Differential Gene Expression in Elevated Pressure Conditions

Transcriptome analysis of porcine aortic valve tissue was performed to determine the distinct genetic profile of valve tissue exposed to 0-80 mmHg (normotensive/control) and 0-120 mmHg (hypertensive) cyclic pressure. Microarray experiments were performed in three biological replicates for both experimental conditions. A set of 1441 genes was identified as differentially expressed (DE) in hypertensive conditions compared to controls. Of these, 735 transcripts ($\approx 51\%$) were significantly increased ($p < 0.05$) in valve tissue exposed to elevated pressure compared to valve tissue exposed to control pressure. In addition, valve tissue exposed to elevated pressure had 706 transcripts ($\approx 49\%$) whose levels were significantly decreased compared to controls. Because our hypothesis states that elevated pressure activates inflammatory and valve remodeling mechanisms in valve tissue, we confirmed our microarray results by verifying the expression of three genes associated with ECM remodeling and inflammation: Matrix metalloproteinase-3 (MMP-3; 134 fold change), Matrix metalloproteinase-1 (MMP-1; 7.99 fold change) and Interleukin-6 (IL6; 10 fold change) using quantitative RT-PCR. MMP-3 and MMP-1 expression levels were consistent with our microarray results ($p < 0.05$); however, IL6 levels were increased by a much greater degree than in the microarray data (Figure 4.2).

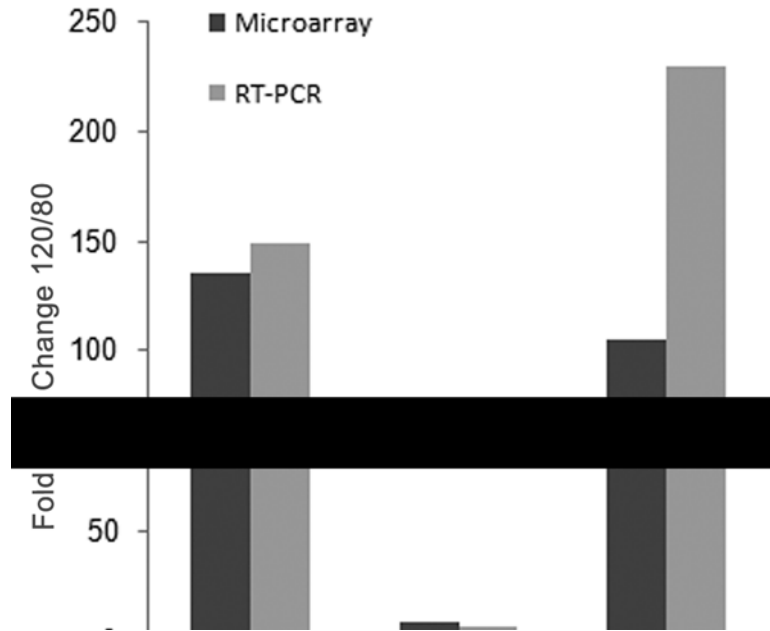


Figure 4.2 Real-time PCR validation of microarray data. Gene expression patterns from microarray analysis (dark bars) and semi-quantification through RT-PCR (clear bars). Values represent fold change in gene expression of samples in hypertensive conditions relative to normotensive conditions.

4.3.3 Improved Annotation of the Pig Genome

Interpretation of functional genomics data (including array datasets) relies on both structural and functional annotation of gene and gene products. Structural annotation is the demarcation of functional elements within genomic sequence while GO functional annotation attributes known processes, functions and cellular locations to those same structural elements. Only 12% of the DE porcine transcripts had GO-annotation based on pig genes. However, of the transcripts with no GO, 27% had similarity to genes from other species based on probe classification from NetAffx analysis center (Affymetrix). Sequence homology was used to add GO annotation for 545 transcripts with incomplete GO functional annotation, bringing the total number of GO annotated transcripts to 37%.

The remaining 718 DE transcripts did not meet our homology cut off criteria (See Materials and Methods). A set of 723 DE transcripts was used for further GO and IPA analysis. The complete list of DE transcripts can be accessed in the GEO database (<http://www.ncbi.nlm.gov/geo/GSE15211>) and functional annotation has been submitted to the AgBase database where they will be made publicly available.

4.3.4 Functional Modeling

Analysis of DE genes through GO was conducted to allow detection of biological processes affected during exposure of valve tissue to hypertensive pressure. Therefore, GO Cellular Component (CC) shows that a large number of increased DE transcripts are located in the extracellular region (61%) and membrane (56%), compared to normal samples (Figure 4.3). These results suggest that high pressure induces changes in valve architecture through increased expression of ECM structural components. Analysis of GO Molecular Function (MF) indicates that under high pressure, there is an increase in the number of genes involved in protein binding activity, catalytic activity, nucleic acid binding activity and signal transducer activity (Figure 4.4). Up-regulated genes in the hypertensive samples were predominantly genes involved in catabolic and proteolytic activity, with specific roles in ECM remodeling¹⁷. In addition, changes in nucleic acid binding and signal transducer activity suggest activation of transcriptional mechanisms and activation of VICs. Notably, antioxidant activity and translation regulator activity were only found in hypertensive samples. Furthermore, oxidoreductase activity was decreased, suggesting valve tissue vulnerability to reactive oxygen species and activation of pro-inflammatory mechanisms.

Analysis of GO Biological Process (BP) showed several processes that were consistent with our hypothesis of alteration in inflammatory and valve remodeling mechanisms, but also distinct biological processes such as transport, secretion, cell motion, cell communication, cell differentiation and cell death were affected by elevated pressure (Figure 4.5).

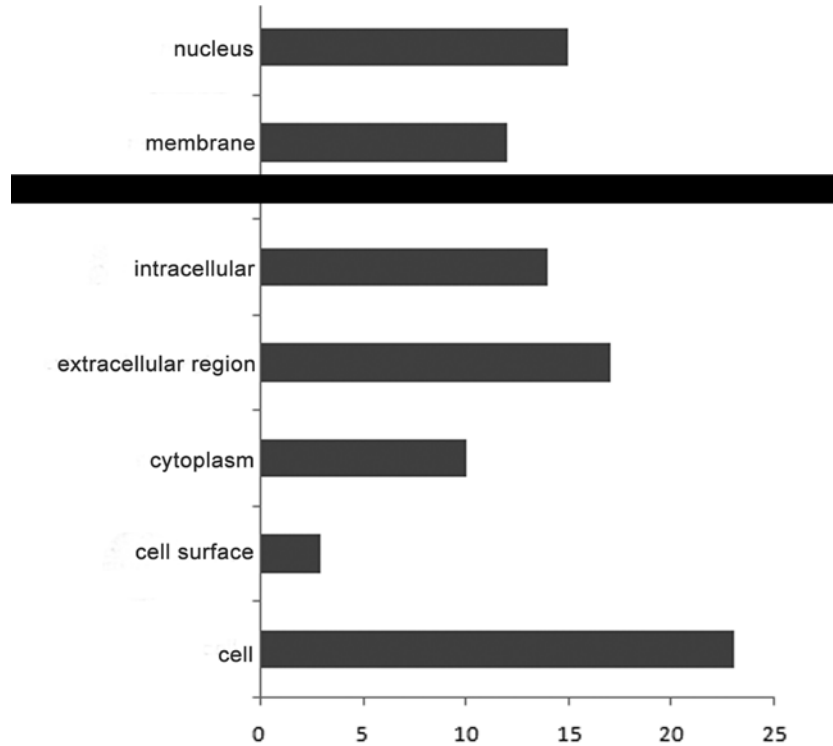


Figure 4.3 Cellular localization of differentially expressed transcripts from hypertensive tissue. GO Cellular Component annotations were summarized to broad level terms using the GOA whole proteome GO Slim set. The net regulatory effect was determined by subtracting the number of decreased proteins from the number of increased proteins in each GOSlim category.

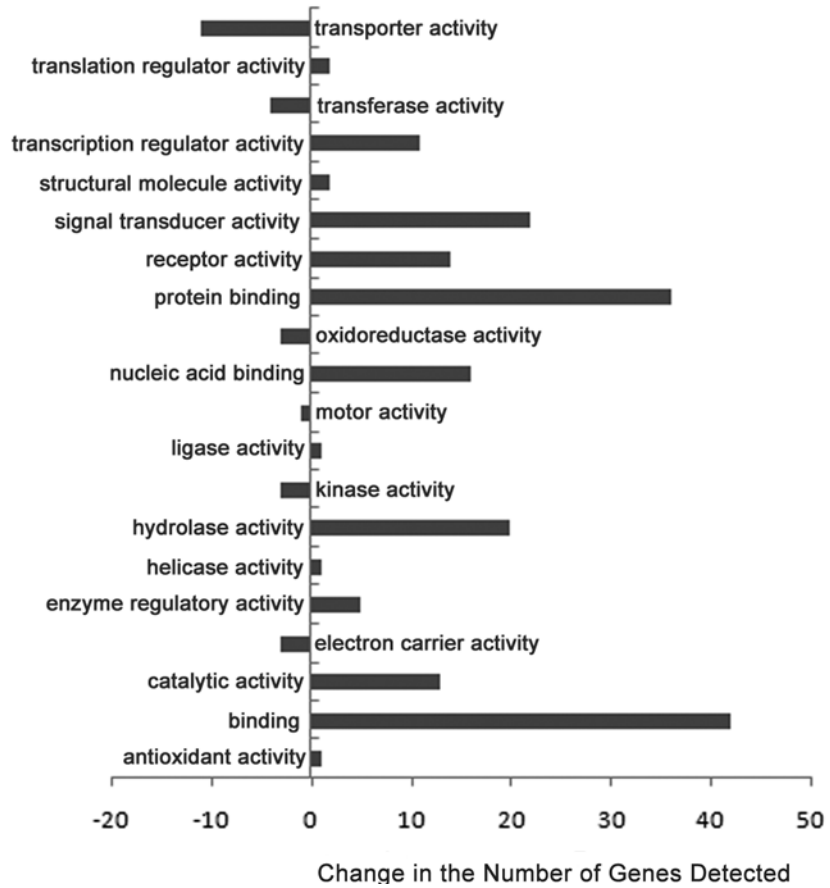


Figure 4.4 Molecular Functions of differentially expressed transcripts from hypertensive tissue. GO Molecular function annotation were summarized to broad level terms using the GOA whole proteome GO Slim set. The net regulatory effect was determined by subtracting the number of decreased proteins from the number of increased proteins in each GOSlim category.

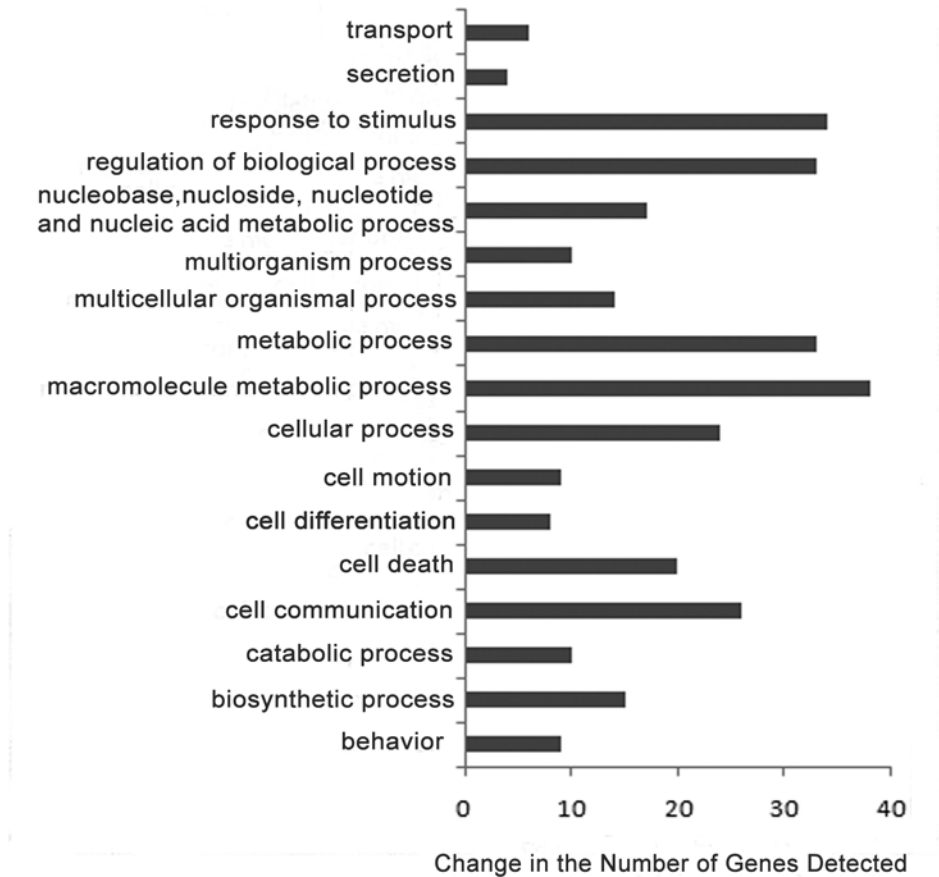


Figure 4.5 Biological Process of differentially expressed transcripts from hypertensive tissue. GO Biological Process were summarized to broad level terms using the GOA whole proteome GO Slim set. The net regulatory effect was determined by subtracting the number of decreased proteins from the number of increased proteins in each GOSlim category.

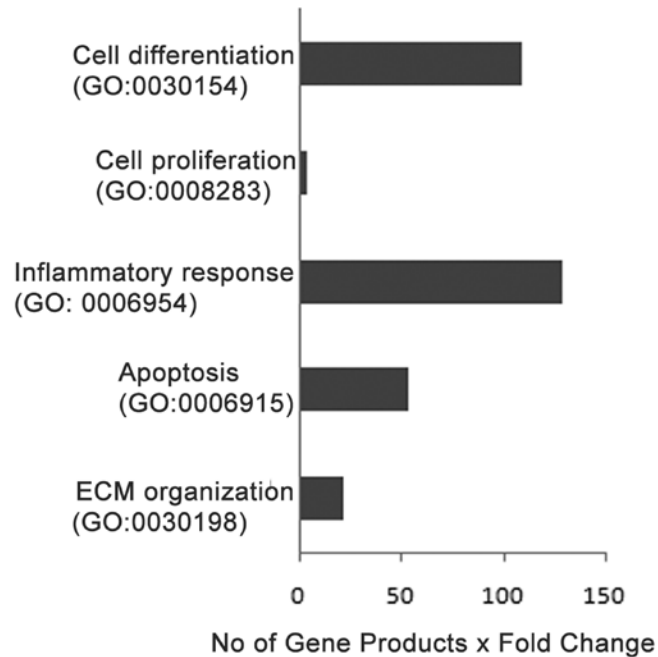


Figure 4.6 Potential biological processes involved in valve remodeling. Comparison of gene expression levels of four potential valve remodeling mechanisms suggested by hypothesis-driven GO modeling.

We used hypothesis-driven GO analysis (see Materials and Methods) to specifically examine the role of four biological processes associated with aortic valve disease: ECM remodeling, inflammation, cell differentiation and/or proliferation and cell death (Table 4.1)18. GO-modeling showed an overall increase in ECM remodeling, inflammation, cell differentiation and pro-apoptotic activity in VICs exposed to hypertensive pressure (Figure 4.6). Consistent with our hypothesis, all the differentially expressed genes from our data set within the GO BP categories of ECM organization, inflammatory response, cell death, cell differentiation were mapped into signaling networks with IPA on networks. Therefore, two major networks were chosen (i) TP53 network and (ii) Cell death network. The TP53 network (Figure 4.7) shows the

interaction of a number of genes implicated in a broad range of biological processes, including ECM remodeling (MMP-1, MMP-3, TIMP-1, TIMP3), pro-inflammatory mechanisms (IL-8, IL-6, IL-1 β , IL-1A), immune-related genes (MCP-1, ICAM-1, SELP, SELL,) and antioxidant mechanisms (SOD2, GPX7), but that are transcriptionally regulated by Tumor suppression factor TP53. Importantly, some of these genes are associated with the development of aortic valve disease¹⁹. In addition, TP53 represses the expression of genes that promote cell cycle progression. The cell death network (Figure 4.8) consists of a set of interconnected genes involved in pro apoptotic mechanisms. In particular, the association of pro-apoptotic genes (CYCS, FAS, CASP3, CASP7, CASP8) with genes that have a predominantly negative effect in the occurrence of apoptosis (BIRC3, BIRC2, BIRC5) was observed. These genes are involved in specific pro-apoptotic pathways and are of particular interest given that apoptosis is a rare process in normal aortic heart valves; in contrast, in aortic valve disease the occurrence of apoptosis increases²⁰. Interestingly, the tumor suppressor gene TP53 also positively regulated genes involved in the initiation of apoptosis.

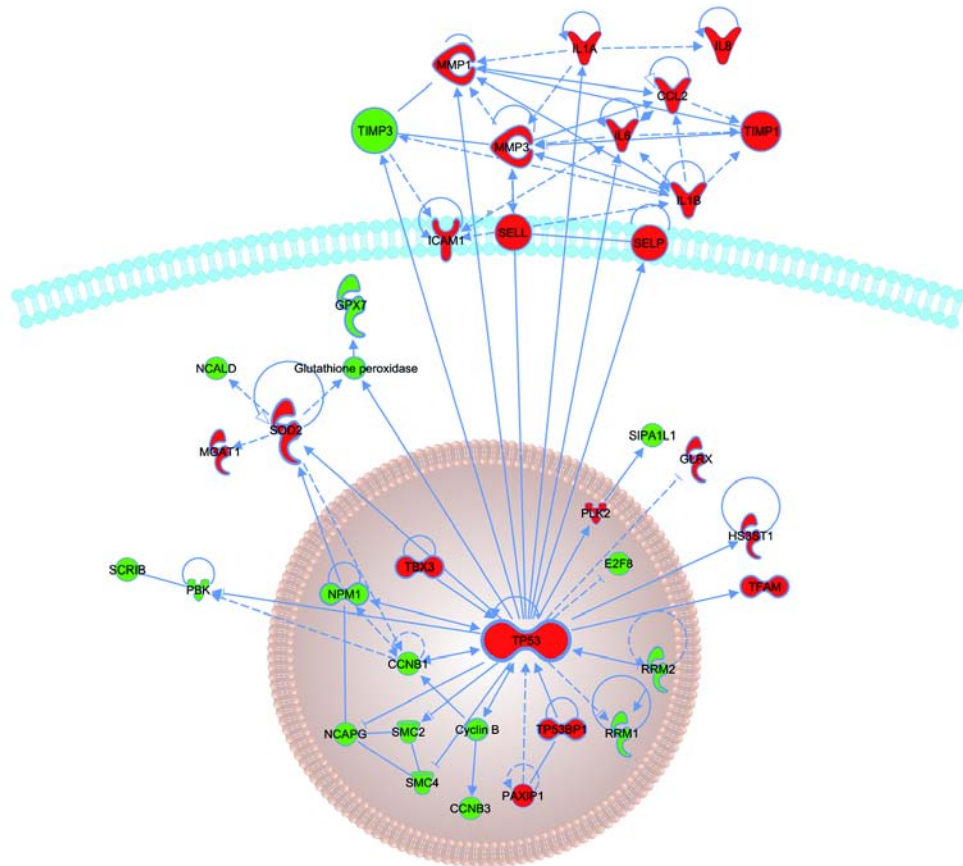


Figure 4.7 TP53 network. The network shows molecular interactions among significantly expressed genes involved in cell inflammatory response, ECM remodeling, oxidative stress and the transcription factor TP53 under elevated pressure conditions. Green color represents a decrease and red represents an increase in gene expression. Nodes displayed represent the functional class of the gene product: down-pointing triangles represent kinases; diamonds represents enzymes, horizontal ovals represent transcription regulators; and circles represent other types of molecules. Continuous lines show direct interactions between nodes and dashed lines show indirect interactions. Lines beginning and ending on the same node show self regulation. Arrowheads show directionality of the relationship.

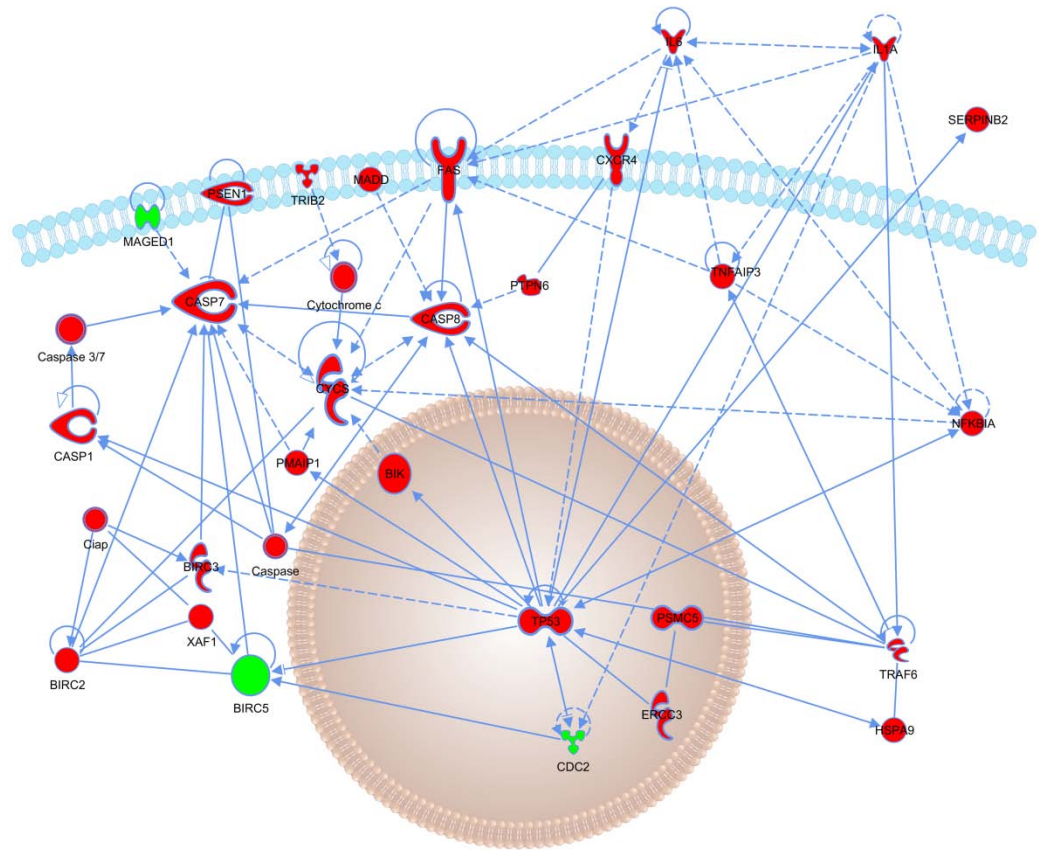


Figure 4.8 Cell Death network. The network shows the molecular interactions among significantly expressed genes involved in pro apoptotic mechanisms in which gene expression was altered by elevated pressure. Symbols are as described in the legend for figure 4.7.

4.4 Discussion

Multiple molecular and cellular mechanisms are associated with the initiation and progression of aortic valve disease. Well-documented manifestations of aortic valve disease associated with alterations in valve architecture include increased ECM remodeling, expression of pro-inflammatory cytokines, calcification, lipid deposition and changes in valve cell phenotype²¹. *In vitro* models are used to demonstrate the regulatory role of mechanical stimuli in valve structure and cellular function. Specifically, it has been shown that mechanical loading (e.g. shear, tension etc) promotes changes in

expression levels of a set of genes involved in ECM synthesis, cell differentiation and DNA synthesis in valve cells^{9, 21-23}. These changes may be caused by the activation and inactivation of specific regulatory mechanisms related to ECM remodeling and cell activation. However, none of the current models evaluates the molecular mechanisms leading to these changes and whether or not elevated pressure plays a critical role.

In the present study, we used a combination of GO-based and pathway-based analyses to identify novel genes and molecular mechanisms that are activated in valve tissue during exposure to elevated pressure conditions. Our results show that elevated pressure induces a gene expression pattern in valve tissue that is considerably similar to that seen in aortic valve disease, underlining the key role of hypertension as an initiating factor in the onset of pathogenesis. In addition, our analysis revealed a set of genes that were not previously known to be regulated in valve tissue in a pressure dependent manner. In particular, this set of genes is associated with two highly connected networks; the TP53 network, and the cell death network. These networks are associated with an increase in ECM remodeling, inflammation and apoptotic mechanisms. Modeling these networks has facilitated the discovery of some very specific genes that could potentially be targeted for the treatment of aortic heart valve disease.

4.4.1 TP53 Network

TP53 is a tumor suppressor gene that controls cell cycle progression, cell growth and apoptosis through transcriptional activation of matrix metalloproteinases (MMPs), cytokines, proteases, growth factors, etc. TP53 can be activated by several signals, including oxidative stress²⁴. Our findings show that exposure of valve tissue to elevated pressure induces TP53 over expression and the expression of a number of TP53 target

genes. These genes include, among others, ECM remodeling enzymes, pro-inflammatory cytokines and oxidative stress enzymes. TP53 induction by elevated pressure increases valve ECM degradation by stimulating promoter activity of MMPs and decreasing the expression TIMPs²⁵. These findings indicate that TP53 is an important mediator of valve remodeling mechanisms. Specifically, it suggests that TP53 may contribute to valve dysfunction by altering the expression of genes that participate in ECM turnover. To our knowledge this is the first study to show TP53 gene expression is activated by pressure in aortic valve tissue.

The role of TP53 in the transcription of a number of genes predicted to generate or respond to oxidative stress has been revealed in multiple studies²⁶. It has been proposed that these genes can induce oxidative stress leading to TP53-dependent apoptosis. Our findings show that elevated pressure induced the expression of two of ROS associated genes: superoxide dismutase 2 (SOD2) and Glutathione peroxidase 7 (GPX7). The SOD2 gene has a specific role in ROS production, whereas the GPX7 gene is associated with ROS degradation. Both genes have been shown to be actively regulated by TP53²⁷. Elevated pressure induces an increase in SOD2 gene levels, which contrast with decreased levels of GPX7 gene expression in valve tissue. Our results strongly suggest that there is an imbalance in the antioxidant enzyme system of VICs. Furthermore, it may contribute to an oxidative stress response followed by an increase in apoptosis in the valve after exposure to elevated pressure. Of particular interest in this network is the increase of the SOD2 and TP53 genes. Studies have shown SOD2 expression to be increased following death receptor activation that is activated by TP53²⁸. Thus, it is unclear if the antioxidant mechanism and ROS production are a cause or a

consequence of TP53 pro-apoptotic mechanism. It will be necessary to determine the potential involvement of elevated pressure in the production of reactive oxygen in a time dependent manner to fully understand the relationship between SOD2 and TP53 gene expression in heart valves. These data show conclusively that TP53 is the key effector in the transcriptional cascade regulating valve tissue pro-apoptotic and ECM remodeling mechanisms in response to elevated pressure.

4.4.2 Cell Death Network

Apoptosis plays an important role in normal tissue homeostasis. Specifically, normal valve tissue homeostasis is dependent on the balance between cell proliferation and death of VICs^{22, 29}. However, any imbalance can result in undesirable apoptosis or cell growth of VICs. If activated VICs do not undergo apoptosis, excessive ECM deposition may occur leading to valve dysfunction. Therefore it is of interest to attempt to understand the intracellular signals by which elevated pressure might stimulate pro-apoptotic mechanisms in valve tissue. The molecular mechanisms underlying apoptosis in cells are complex and only partially understood. Two main mechanisms have been identified: (i) the extrinsic or death receptor pathway, which requires stimulation of membrane receptors (eg. FAS, TGF- β , etc) by their ligands and (ii) the intrinsic mitochondrial pathway, which requires binding of the Bcl-2 family members to the mitochondrial membrane. Both mechanisms converge in the activation of several members of the caspase family, release of cytochrome c, and the initiation of pro-apoptotic mechanisms. Furthermore, both mechanisms can be activated by diverse stimuli (e.g. oxidative stress, TP53 activation, growth factors). Cross talk between the

mitochondrial and extrinsic pathway is possible through activation of the pro-apoptotic proteins BID or BAX via TP53.

Our results show that elevated pressure triggered the expression of several genes that are involved in different steps of the death receptor pathway including FAS receptor, three members of the caspase family (CASP1, CASP7, CASP8) and cytochrome C. These genes are transcriptionally regulated by TP53, thus the death receptor pathway is a TP53-dependent apoptosis pathway. Considering the fact that oxidative stress has been shown to modulate TP53 activity, and that TP53 regulates FAS receptor-mediated apoptosis, the increased FAS gene expression may be expected to be associated with the increased expression of TP53 and the induction of ROS by elevated pressure. In addition to the death receptor signaling triggered by elevated pressure, increased expression of BID, a pro-apoptotic Bcl-2 family member, suggest that there might be cross-talk between the two pathways and that they are activated by elevated pressure. Furthermore, our data suggests that an anti-apoptotic mechanism was altered. We observed decreased expression of genes involved in negative regulation of apoptosis, such as BIRC5. This transcription factor belongs to the IAP family, which is a potent caspase inhibitor and is required to maintain a balance between cell proliferation and apoptosis. Thus, elevated pressure was able to activate pro-apoptotic and anti-apoptotic mechanisms simultaneously in aortic valve tissue. The enhanced expression of pro-apoptotic genes in VICs indicates that cell turnover is another important mechanism influenced by elevated pressure. Furthermore, it suggests dysregulation of mediators of apoptosis in valve tissue that favors apoptosis.

Although pressure is one of the main components of the valvular environment, the effect of elevated pressure on VICs has not previously been thoroughly examined. Our results show that pressure plays a critical role in the regulation of valve tissue homeostasis. Together, the microarray analyses with IPA suggest strongly that TP53 plays an essential role in regulating genes that promote ECM synthesis and apoptosis in valve tissue in a pressure dependent manner. Furthermore, the genetic profiles of valve tissue exposed to elevated pressure share common abnormal genetic features observed in aortic valve disease, providing validation to our experimental model. Changes in gene expression levels related to the inflammatory response, ECM remodeling and cell death occurring in elevated pressure conditions were attributed to the activation of VICs as a response to increased mechanical loading. Our results suggest that the valve remodeling mechanisms activated by elevated pressure could lead to the development of aortic valve disease.

4.5 References

- 1) Bosse Y, Mathieu P, Pibarot P. Genomics: the next step to elucidate the etiology of calcific aortic valve stenosis. *J Am Coll Cardiol* 2008 April 8;51(14):1327-36.
- (2) Butcher JT, Simmons CA, Warnock JN. Mechanobiology of the aortic heart valve. *J Heart Valve Dis* 2008 January;17(1):62-73.
- (3) Thubrikar MJ, Aouad J, Nolan SP. Comparison of the *in vivo* and *in vitro* mechanical properties of aortic valve leaflets. *J Thorac Cardiovasc Surg* 1986 July;92(1):29-36.
- (4) Willems IE, Havenith MG, Smits JF, Daemen MJ. Structural alterations in heart valves during left ventricular pressure overload in the rat. *Lab Invest* 1994 July;71(1):127-33.
- (5) Rabkin SW. The association of hypertension and aortic valve sclerosis. *Blood Press* 2005;14(5):264-72.
- (6) Little SH, Chan KL, Burwash IG. Impact of blood pressure on the Doppler echocardiographic assessment of severity of aortic stenosis. *Heart* 2007 July;93(7):848-55.
- (7) Rajamannan NM, Bonow RO, Rahimtoola SH. Calcific aortic stenosis: an update. *Nat Clin Pract Cardiovasc Med* 2007 May;4(5):254-62.
- (8) Platt MO, Xing Y, Jo H, Yoganathan AP. Cyclic pressure and shear stress regulate matrix metalloproteinases and cathepsin activity in porcine aortic valves. *J Heart Valve Dis* 2006 September;15(5):622-9.
- (9) Warnock JN, Burgess SC, Shack A, Yoganathan AP. Differential immediate-early gene responses to elevated pressure in porcine aortic valve interstitial cells. *J Heart Valve Dis* 2006 January;15(1):34-41.
- (10) Xing Y, He Z, Warnock JN, Hilbert SL, Yoganathan AP. Effects of constant static pressure on the biological properties of porcine aortic valve leaflets. *Ann Biomed Eng* 2004 April;32(4):555-62.
- (11) Xing Y, Warnock JN, He Z, Hilbert SL, Yoganathan AP. Cyclic pressure affects the biological properties of porcine aortic valve leaflets in a magnitude and frequency dependent manner. *Ann Biomed Eng* 2004 November;32(11):1461-70.
- (12) Merryman WD, Youn I, Lukoff HD et al. Correlation between heart valve interstitial cell stiffness and transvalvular pressure: implications for collagen biosynthesis. *Am J Physiol Heart Circ Physiol* 2006 January;290(1):H224-H231.

- (13) Tusher VG, Tibshirani R, Chu G. Significance analysis of microarrays applied to the ionizing radiation response. *Proc Natl Acad Sci U S A* 2001 April 24;98(9):5116-21.
- (14) The universal protein resource (UniProt). *Nucleic Acids Res* 2008 January;36(Database issue):D190-D195.
- (15) Boutet E, Lieberherr D, Tognolli M, Schneider M, Bairoch A. UniProtKB/Swiss-Prot. *Methods Mol Biol* 2007;406:89-112.
- (16) Rozen S, Skaletsky H. Primer3 on the WWW for general users and for biologist programmers. *Methods Mol Biol* 2000;132:365-86.
- (17) Galis ZS, Khatri JJ. Matrix metalloproteinases in vascular remodeling and atherogenesis: the good, the bad, and the ugly. *Circ Res* 2002 February 22;90(3):251-62.
- (18) Hakuno D, Kimura N, Yoshioka M, Fukuda K. Molecular mechanisms underlying the onset of degenerative aortic valve disease. *J Mol Med* 2009 January;87(1):17-24.
- (19) Akat K, Borggreffe M, Kaden JJ. Aortic valve calcification - basic science to clinical practice. *Heart* 2008 July 16.
- (20) Vermeulen K, Berneman ZN, Van Bockstaele DR. Cell cycle and apoptosis. *Cell Prolif* 2003 June;36(3):165-75.
- (21) Smith KE, Metzler SA, Warnock JN. Cyclic strain inhibits acute pro-inflammatory gene expression in aortic valve interstitial cells. *Biomech Model Mechanobiol* 2009 July 28.
- (22) Balachandran K, Sucusky P, Jo H, Yoganathan AP. ELEVATED CYCLIC STRETCH ALTERS MATRIX REMODELING IN AORTIC VALVE CUSPS - IMPLICATIONS FOR DEGENERATIVE AORTIC VALVE DISEASE? *Am J Physiol Heart Circ Physiol* 2009 January 16.
- (23) Sucusky P, Balachandran K, Elhammali A, Jo H, Yoganathan AP. Altered shear stress stimulates upregulation of endothelial VCAM-1 and ICAM-1 in a BMP-4- and TGF-beta1-dependent pathway. *Arterioscler Thromb Vasc Biol* 2009 February;29(2):254-60.
- (24) Birukov KG. Cyclic stretch, reactive oxygen species and vascular remodeling. *Antioxid Redox Signal* 2009 February 2.
- (25) Kaden JJ, Dempfle CE, Grobholz R et al. Interleukin-1 beta promotes matrix metalloproteinase expression and cell proliferation in calcific aortic valve stenosis. *Atherosclerosis* 2003 October;170(2):205-11.

- (26) Taylor RC, Cullen SP, Martin SJ. Apoptosis: controlled demolition at the cellular level. *Nat Rev Mol Cell Biol* 2008 March;9(3):231-41.
- (27) Paravicini TM, Touyz RM. Redox signaling in hypertension. *Cardiovasc Res* 2006 July 15;71(2):247-58.
- (28) Hussain SP, Amstad P, He P et al. p53-induced up-regulation of MnSOD and GPx but not catalase increases oxidative stress and apoptosis. *Cancer Res* 2004 April 1;64(7):2350-6.
- (29) Jian B, Narula N, Li QY, Mohler ER, III, Levy RJ. Progression of aortic valve stenosis: TGF-beta1 is present in calcified aortic valve cusps and promotes aortic valve interstitial cell calcification via apoptosis. *Ann Thorac Surg* 2003 February;75(2):457-65.

CHAPTER 5

SUMMARY AND CONCLUSIONS

Calcific aortic valve disease is one of the most complex cases of cardiac diseases. If untreated, progression of the disease leads to 50-60% mortality rate following year onset of symptoms. Despite the high prevalence and the increasing morbidity and mortality of this condition, the exact molecular mechanisms that are involved in the development and progression of the disease are still unclear. Evidence of this fact is that valve replacement, with either mechanical prosthetic or bioprosthetic valves, is the only viable treatment for the disease. On average, 50,000 aortic valve replacements every year occur both in Europe and in the United States. However, this involves open heart surgery with its attendant risks and high costs for health organizations that are estimated to be around 1 billion US dollars per year in the United States alone. Currently there is not proven pharmacological treatment that will stop or reverse the morphological changes seen in calcific aortic disease.

In vivo, the aortic valve is constantly exposed to a variety of humeral and hemodynamic factors, and thus, a major limiting factor in the understanding of the disease is the lack of well defined experimental models that resemble native valve environment *in vitro*. It is well established that one of the major causes of this pathological condition is the exposure of valve tissue to non-physiological hemodynamic

stresses. The focus of this study was on the quantification of the effects of elevated pressure on valve calcification. At this point, it must be noted that other sources of mechanical load (stretch, shear) are present in the native environment of the valve. However, elucidation of the effects of elevated pressure does serve as an important clue that hypertension might both mediate molecular alterations and promote a calcifying cell phenotype in aortic valve.

Correlation studies between aortic valve calcification and hypertension suggest that the calcification process may occur as a result to the abnormal environment generated by elevated pressure. While development of calcific aortic valve disease requires the coordination of many factors that include pro inflammatory stimuli, valvular ECM remodeling, and pro-apoptotic mechanisms, a critical step in the calcification process is the osteoblast transformation of valvular interstitial cells (VICs). The question of the potential interrelation of hypertension with valve calcification and its functional role concerning regulation osteogenic differentiation of valvular interstitial cells has not been established.

To elucidate the potential regulatory functions of hypertension in valve calcification, we evaluated the effects of elevated pressure on osteogenic differentiation of valve interstitial cells *in vitro*. In addition, we investigated the potential molecular mechanisms mediating the differentiation process. In the first part of this work (Chapter 3), we characterized the phenotypic changes of valve interstitial exposed to physiological and pathological levels of cyclic pressure. Our results indicate the potential capacity of elevated pressure to induce valve calcification by regulation of osteogenesis-associated genes in valvular interstitial cells.

Based on the observations presented in Chapter 2, where pressure induced new gene expression of three typical osteoblast specific genes, we identified in the following section of the study, the global gene expression patterns and signaling pathways activated in aortic heart valve exposed to hypertensive pressure. We showed that elevated cyclic pressure is a potent regulator of gene expression levels in valve tissue, thus elevated cyclic pressure was able to activate several molecular mechanisms that relate to ECM tissue remodeling: inflammation, cell death, and osteogenic differentiation. Changes in gene expression levels related to the inflammatory response, ECM remodeling and cell proliferation occurring in elevated pressure conditions are expected to result from the activation of VICs as a response to increased mechanical loading. Our results suggest that the valve remodeling mechanisms activated by elevated pressure lead to the development of calcific aortic valve disease.

We concluded that hypertensive pressure plays an important role in transcriptional activation of several mechanisms, including local production of proteins, such as osteopontin, runt related factor 2, alkaline phosphatase, which mediate tissue calcification; expression pro inflammatory cytokines, activation of oxidative stress, and apoptosis signaling pathways; along with changes in tissue matrix, including the up regulation of matrix metalloproteinases and TP53 activity. In addition, valve interstitial cells undergo phenotypic transformation into osteoblasts that may be regulated by the BMP-7 signaling pathway.

Together, our data identifies new considerable factors that relate elevated pressure to the initiation of calcific aortic valve disease, but further work is required to identify additional target genes in the calcification process that may be inhibited to form the basis

of new effective pharmacological treatments. A further approach might be to target intermediate effectors of the Ang II signaling pathway to understand the roles of this system in aortic heart valve.

APPENDIX A
PORCINE GENECHIP SPECIFICATIONS

Porcine GeneChip Genome Array Specifications	
Number of probe sets	23,937
Number of transcripts,	23,256
Total # of probe sets including species specific controls	23,973
Number of arrays in set One	One
Array format	100
Feature size	11 μ m
Oligonucleotide probe length	25-mer
Probe pairs/sequence	11
Hybridization controls:	bioB, bioC, bioD from <i>E. coli</i> and cre from P1 Bacteriophage
Poly-A controls:	<i>dap, lys, phe, thr, trp</i> from <i>B. subtilis</i>
Housekeeping/Control genes:	Porcine genes from Test3 Array: Alpha Actin, Angiotensinbinding protein, CTLA4, Erythropoietin receptor, GAPDH, inflammatory response protein 6, and Leptin. Additionally, there are newly selected control probe sets for Beta Actin (ACTB), Glyceraldehyde-3-phosphate dehydrogenase (GAPD, G3PD, GAPDH), Eukaryotic elongation factor1 alpha1 (EEF1A1).
Detection sensitivity	1:100,000*

* As measured by detection in comparative analysis between a complex target containing spiked control transcriptions and a complex target with no spikes.

The sequence information for this array was selected from public data sources including Porcine UniGene Build 28, and GenBank® mRNAs (August 2004)

APPENDIX B
MICROARRAY INTERNAL CONTROLS

Origin of Control	Control Gene Name	Type of Controls
<i>b.subtilis</i>	<i>lis</i> <i>Phe</i> <i>thr</i> <i>dap</i>	Poly-A-tailed sense RNAs used as controls for the labeling and hybridization process. Used to estimate assay sensitivity
<i>E.coli</i>	<i>bioB</i>	Antisense biotinylated cRNAs used as hybridization controls
	<i>bioC</i>	
	<i>bioD</i>	
P1 Bacteriophage	<i>Cre</i>	
<i>Synthetic</i>	<i>B2 Oligo</i>	Grid alignment

APPENDIX C
HYBRIDIZATION PERFORMANCE OF MICROARRAYS

	Samples					
	80 S1		80 S1		80 S3	
	Sig 3'	3/5' ratio	Sig 3'	3/5' ratio	Sig 3'	3/5' ratio
Spike Controls						
AFFI - R2-EC bioB	490.4	1.03	234.9	0.98	347.7	1.06
AFFI - R2-EC bioC	1214.3	0.98	600.8	0.99	940.1	1
AFFI - R2-EC bioD	5188.7	0.96	2798.1	0.94	3988.6	0.93
AFFI - R2-EC CRE	18727	1.33	14499.9	1.76	15851.4	1.5
AFFI - R2-EC DAP	2911.3	15.88	2777.2	17.29	1953.4	11.53
AFFI - R2-EC LYS	251.8	6.84	210.6	6.99	123.7	6.62
AFFI - R2-EC PHE	558.8	3.64	470.3	4.93	323.2	5.54
AFFI - R2-EC THR	951.1	17.96	985.3	17.51	683.2	10.84
Background (Avg)	56.42		71.64		74.69	
Scaling Factor	1.722		1.642		1.341	
NOISE (RawQ)	2.09		2.49		2.69	
Present	57.80%		57.90%		59.50%	
Average Signal (P)	1192.8		1196.3		1150.6	
Average Signal (A)	27.5		27.7		26.3	
	120 S1		120 S2		120 S3	
	Sig 3'	3/5' ratio	Sig 3'	3/5' ratio	Sig 3'	3/5' ratio
Spike Controls						
AFFI - R2-EC bioB	360.5	0.85	506.1	0.94	563.8	0.87
AFFI - R2-EC bioC	1151	1.01	1415.3	1.02	1605.4	0.98
AFFI - R2-EC bioD	4633	0.92	6130.7	0.98	6597.3	0.9
AFFI - R2-EC CRE	17061	1.34	21651.1	1.34	21912.6	1.27
AFFI - R2-EC DAP	2775.8	14.31	1862.7	11.5	1138.3	12.49
AFFI - R2-EC LYS	192.2	7.47	142.8	4.93	82	3.44
AFFI - R2-EC PHE	406.1	4.07	328.6	3.18	257	4
AFFI - R2-EC THR	893.6	11.75	831.4	12.19	539.2	17.12
Background (Avg)	62.17		65.72		81.63	
Scaling Factor	1.404		1.883		1.91	
NOISE (RawQ)	2.22		2.37		2.99	
Present	58.80%		54.60%		58.40%	
Average Signal (P)	1161.2		1338.8		1231.6	
Average Signal (A)	25		32.4		29.1	

APPENDIX D
GENES DIFFERENTIALLY EXPRESSED IN PORCINE VALVE TISSUE IN
RESPONSE TO ELEVATED CYCLIC PRESSURE

Affymetrix ID	Gene	Description	Effect	P value	Affymetrix ID	Gene	Description	Effect	P value
Ssc.5955.1.A1_at	IL10RB	interleukin 10 receptor, beta	+	0.049	Ssc.4949.2.S1_a_at	TBP	TATA box binding protein	+	0.0409
Ssc.8833.1.S1_at	IL15	interleukin 15	+	0.04	Ssc.4466.1.S1_at	TEC	tec protein tyrosine kinase	+	0.015
Ssc.113.1.S1_at	IL1A	interleukin 1, alpha	+	0.011	Ssc.23477.1.S1_at	TFIP11	tuftsin interacting protein 11	+	0.0102
Ssc.17573.1.S1_at	IL1B	interleukin 1, beta	+	0.015	Ssc.11784.1.S1_at	TIMP1	metallopeptidase inhibitor 1	+	0.0102
Ssc.62.2.S1_a_at	IL6	interleukin 6 (interferon, beta 2)	+	0.011	Ssc.19638.1.S1_at	TNXB	tenascin XB	+	0.0401
Ssc.658.1.S1_at	IL8	interleukin 8	+	0.016	Ssc.16010.1.S1_at	TP53	tumor protein p53	+	0.0477
Ssc.15769.1.A1_at	KCNE4	potassium voltage-gated channel	+	0.046	Ssc.5030.1.A1_at	TPSAB1	tryptase alpha/beta 1	+	0.0371
Ssc.3968.1.S1_at	WFDC2	WAP four-disulfide core	+	0.0093	Ssc.16217.1.S1_at	TTL	tubulin tyrosine ligase	+	0.0049
Ssc.12803.1.S1_at	ACOX1	acyl-Coenzyme A oxidase 1, palmitoyl	-	0.01	Ssc.1320.1.A1_at	LGALS1	lectin, galactoside-binding, soluble1	-	0.017
Ssc.11051.1.S1_at	ADSSL1	adenylosuccinate synthase like 1	-	0.03	Ssc.15397.1.S1_at	LMCD1	LIM and cysteine-rich domains 1	-	0.032
Ssc.5822.1.S1_at	ALOX5AP	arachidonate 5-lipoxygenase-activate	-	0.04	Ssc.24153.1.S1_at	LPAR1	lysophosphatidic acid receptor 1	-	0.003
Ssc.12241.1.A1_at	ANXA2	annexin A2	-	0.02	Ssc.22086.1.A1_at	MAGED1	melanoma antigen family D1	-	0.006
Ssc.16545.1.S1_at	AP1S1	adaptor-related protein complex 1	-	0.048	Ssc.16336.1.S1_at	MET1	malic enzyme	-	0.028
Ssc.22406.1.A1_at	AQP1	aquaporin 1	-	0.031	Ssc.19462.1.S1_at	MEF2C	myocyte enhancer factor 2C	-	0.003
Ssc.15238.1.S1_at	AURKB	aurora kinase B	-	0.045	Ssc.13047.1.A1_at	MLPH	melanophilin	-	0.047
Ssc.432.1.S1_at	BIRC5	baculoviral IAP repeat-containing 5	-	0.005	Ssc.7315.1.S1_at	NDUFA4L2	NADH dehydrogenase	-	0.016
Ssc.17287.1.A1_at	C5ORF13	chromosome 5 ORF13	-	0.015	Ssc.3869.1.A1_at	NDUFC1	NADH dehydrogenase	-	0.014
Ssc.4633.1.A1_at	C7	complement component 7	-	0.005	Ssc.19546.1.S1_at	NME4	non-metastatic cells 4	-	0.018
Ssc.381.1.S1_at	CCL27	Chemokine ligand 27	-	0.039	Ssc.15963.1.S1_at	NPY2R	neuropeptide Y receptor Y2	-	0.029
Ssc.14182.1.A1_at	CCNB1	cyclin B1	-	0.04	Ssc.15842.1.S1_at	NR12	nuclear receptor1	-	0.041
Ssc.873.1.S1_at	CDC2	cell cycle 2	-	0.011	Ssc.16635.1.S1_at	NUDT14	nudix 14	-	0.013
Ssc.2895.1.S1_at	CDK4	cyclin-dependent kinase 4	-	0.007	Ssc.3386.1.A1_at	PBK	PDZ binding kinase	-	0.041
Ssc.7286.1.S1_at	CDKN3	cyclin-dependent kinase inhibitor 3	-	0.026	Ssc.27608.2.S1_a_at	PCDH11X	protocadherin 11 X-linked	-	0.032
Ssc.864.1.S1_at	CFH	complement factor H	-	0.017	Ssc.18677.1.S1_at	PLUNC	palate	-	0.04
Ssc.19688.1.S1_at	CHRNA1	cholinergic receptor, nicotinic, alpha1	-	0.002	Ssc.21810.1.S1_at	PON3	paraoxonase 3	-	0.024
Ssc.9013.1.S1_at	CNN1	calponin 1	-	0.023	Ssc.8046.1.A1_at	PP1A	peptidylprolyl isomerase A	-	0.041
Ssc.16327.1.A1_at	COL5A3	collagen, type V, alpha 3	-	0.034	Ssc.6764.2.S1_at	PPP3CA	protein phosphatase 3	-	0.036
Ssc.16184.1.S1_s_at	CYP19A1	cytochrome P450, family 19	-	0.027	Ssc.26124.1.S1_at	PRKACB	protein kinase, cAMP-dependent beta	-	0.036
Ssc.28474.1.S1_at	DDX4	DEAD box	-	0.001	Ssc.11942.1.S1_at	PTGFRN	prostaglandin F2 receptor negative reg.	-	0.001
Ssc.18981.1.A1_at	DGAT1	diacylglycerol O-acyltransferase	-	0.031	Ssc.17250.1.S1_a_at	QDPR	quinoid reductase	-	0.012
Ssc.2155.1.S1_at	DIRAS3	DIRAS family 3	-	0.011	Ssc.11024.1.S1_at	RAB1B	RAB1B, member RAS	-	0.004
Ssc.14.1.S1_at	DLAT	dihydropyrimidine S-acetyltransferase	-	0.023	Ssc.3102.1.S1_at	RAD54L	RAD54-like	-	0.022
Ssc.87.1.S1_at	EGF	epidermal growth factor	-	0.005	Ssc.5563.2.S1_a_at	RBP1	retinol binding protein 1, cellular	-	0.004
Ssc.2258.1.S1_at	EGFL8	EGF-like-domain, multiple 8	-	0.028	Ssc.7096.1.S1_at	RHOA	ras homolog gene family, member A	-	0.046
Ssc.7362.2.S1_at	EPRS	glutaryl-prolyl-HRNA synthetase	-	0.048	Ssc.10226.1.A3_at	RHOB	ras homolog, member B	-	0.014
Ssc.2698.1.S1_at	FAAH	fatty acid amide hydrolase	-	0.012	Ssc.1598.1.S1_at	RXRBB	retinoid X receptor, beta	-	0.012
Ssc.231.1.S2_at	FOX1	ferredoxin 1	-	0.004	Ssc.6742.1.A1_at	SCP2	sterol carrier protein 2	-	0.046
Ssc.11858.1.S1_at	FMOD	fibromodulin	-	0.026	Ssc.3934.1.S1_at	15-Sep	Selenoprotein 15	-	0.02
Ssc.2405.1.A1_at	GATA6	GATA binding protein 6	-	0.03	Ssc.15405.1.S1_at	SLC22A2	solute carrier 22 member 2	-	0.032

*(+), increased expression. (-), decreased expression.

Affymetrix ID	Gene	Description	Effect	P value	Affymetrix ID	Gene	Description	Effect	P value
Ssc.5955.1.A1_at	IL10RB	interleukin 10 receptor, beta	+	0.049	Ssc.4949.2.S1_a_at	TBP	TATA box binding protein	+	0.0409
Ssc.8833.1.S1_at	IL15	interleukin 15	+	0.04	Ssc.4466.1.S1_at	TEC	tec protein tyrosine kinase	+	0.015
Ssc.113.1.S1_at	IL1A	interleukin 1, alpha	+	0.011	Ssc.23477.1.S1_at	TFIP11	tuftsin interacting protein 11	+	0.0102
Ssc.117573.1.S1_at	IL1B	interleukin 1, beta	+	0.015	Ssc.11784.1.S1_at	TIMP1	metallopeptidase inhibitor 1	+	0.0102
Ssc.62.2.S1_a_at	IL6	interleukin 6 (interferon, beta 2)	+	0.011	Ssc.19638.1.S1_at	TNXB	tenascin XB	+	0.0401
Ssc.658.1.S1_at	IL8	interleukin 8	+	0.016	Ssc.16010.1.S1_at	TP53	tumor protein p53	+	0.0477
Ssc.3968.1.S1_at	KCNE4	potassium voltage-gated channel	+	0.046	Ssc.5030.1.A1_at	TPSAB1	tryptase alpha/beta 1	+	0.0371
Ssc.15769.1.A1_at	WFDC2	WAP four-disulfide core	+	0.0093	Ssc.16217.1.S1_at	TTL	tubulin tyrosine ligase	+	0.0049
Ssc.12803.1.S1_at	ACOX1	acyl-Coenzyme A oxidase 1, palmitoyl	-	0.01	Ssc.1320.1.A1_at	LGALS1	lectin, galactoside-binding, soluble1	-	0.017
Ssc.11051.1.S1_at	ADSSL1	adenylosuccinate synthase like 1	-	0.03	Ssc.15397.1.S1_at	LMCD1	LIM and cysteine-rich domains 1	-	0.032
Ssc.5822.1.S1_at	ALOX5AP	arachidonate 5-lipoxygenase-activate	-	0.04	Ssc.24153.1.S1_at	LPAR1	lysophosphatidic acid receptor 1	-	0.003
Ssc.12241.1.A1_at	ANXA2	annexin A2	-	0.02	Ssc.22086.1.A1_at	MAGED1	melanoma antigen family D1	-	0.006
Ssc.16545.1.S1_at	AP1S1	adaptor-related protein complex 1	-	0.048	Ssc.16336.1.S1_at	ME1	malic enzyme	-	0.028
Ssc.22406.1.A1_at	AQP1	aquaporin 1	-	0.031	Ssc.19462.1.S1_at	MEF2C	myocyte enhancer factor 2C	-	0.003
Ssc.15238.1.S1_at	AURKB	aurora kinase B	-	0.045	Ssc.13047.1.A1_at	MLPH	melanophilin	-	0.047
Ssc.432.1.S1_at	BIRC5	baculoviral IAP repeat-containing 5	-	0.005	Ssc.7315.1.S1_at	NDUFA4L2	NADH dehydrogenase	-	0.016
Ssc.17287.1.A1_at	C5ORF13	chromosome 5 ORF13	-	0.015	Ssc.3869.1.A1_at	NDUFC1	NADH dehydrogenase	-	0.014
Ssc.4633.1.A1_at	C7	complement component 7	-	0.005	Ssc.19546.1.S1_at	NME4	non-metastatic cells 4	-	0.018
Ssc.381.1.S1_at	CCL27	Chemokine ligand 27	-	0.039	Ssc.15963.1.S1_at	NPY2R	neuropeptide Y receptor Y2	-	0.029
Ssc.14182.1.A1_at	CCNB1	cyclin B1	-	0.04	Ssc.15842.1.S1_at	NR112	nuclear receptor1	-	0.041
Ssc.873.1.S1_at	CDC2	cell cycle 2	-	0.011	Ssc.16635.1.S1_at	NUDT14	nudix 14	-	0.013
Ssc.2895.1.S1_at	CDK4	cyclin-dependent kinase 4	-	0.007	Ssc.3386.1.A1_at	PBK	PDZ binding kinase	-	0.041
Ssc.7286.1.S1_at	CDKN3	cyclin-dependent kinase inhibitor 3	-	0.026	Ssc.27608.2.S1_a_at	PCDH11X	protocadherin 11 X-linked	-	0.032
Ssc.864.1.S1_at	CFH	complement factor H	-	0.017	Ssc.18677.1.S1_at	PLUNC	palate	-	0.04
Ssc.19688.1.S1_at	CHRNA1	cholinergic receptor, nicotinic, alpha1	-	0.002	Ssc.21810.1.S1_at	PON3	paraoxonase 3	-	0.024
Ssc.9013.1.S1_at	CNN1	calponin 1	-	0.023	Ssc.8046.1.A1_at	PPIA	peptidylprolyl isomerase A	-	0.041
Ssc.16327.1.A1_at	COL5A3	collagen, type V, alpha 3	-	0.034	Ssc.6764.2.S1_at	PPP3CA	protein phosphatase 3	-	0.036
Ssc.16184.1.S1_s_at	CYP19A1	cytochrome P450, family 19	-	0.027	Ssc.26124.1.S1_at	PRKACB	protein kinase, cAMP-dependent beta	-	0.036
Ssc.28474.1.S1_at	DDX4	DEAD box	-	0.001	Ssc.11942.1.S1_at	PTGFRN	prostaglandin F2 receptor negative reg.	-	0.001
Ssc.18981.1.A1_at	DGAT1	diacylglycerol O-acyltransferase	-	0.031	Ssc.17250.1.S1_a_at	QDPR	quinoid reductase	-	0.012
Ssc.2155.1.S1_at	DIRA3	DIRAS family 3	-	0.011	Ssc.11024.1.S1_at	RAB1B	RAB1B, member RAS	-	0.004
Ssc.14.1.S1_at	DLAT	dihydrolipamide S-acetyltransferase	-	0.023	Ssc.3102.1.S1_at	RAD54L	RAD54-like	-	0.022
Ssc.87.1.S1_at	EGF	epidermal growth factor	-	0.005	Ssc.5563.2.S1_a_at	RBP1	retinol binding protein 1, cellular	-	0.004
Ssc.2258.1.S1_at	EGLF8	EGF-like-domain, multiple 8	-	0.028	Ssc.7096.1.S1_at	RHOA	ras homolog gene family, member A	-	0.046
Ssc.7362.2.S1_at	EPRS	glutamyl-prolyl-tRNA synthetase	-	0.048	Ssc.10226.1.A3_at	RHOB	ras homolog, member B	-	0.014
Ssc.2698.1.S1_at	FAAH	fatty acid amide hydrolase	-	0.012	Ssc.1598.1.S1_at	RXRB	retinoid X receptor, beta	-	0.012
Ssc.231.1.S2_at	FDX1	ferredoxin 1	-	0.004	Ssc.6742.1.A1_at	SCP2	sterol carrier protein 2	-	0.046
Ssc.11858.1.S1_at	FMOD	fibromodulin	-	0.026	Ssc.3934.1.S1_at	15-Sep	Selenoprotein 15	-	0.02
Ssc.2405.1.A1_at	GATA6	GATA binding protein 6	-	0.03	Ssc.15405.1.S1_at	SLC22A2	solute carrier 22 member 2	-	0.032

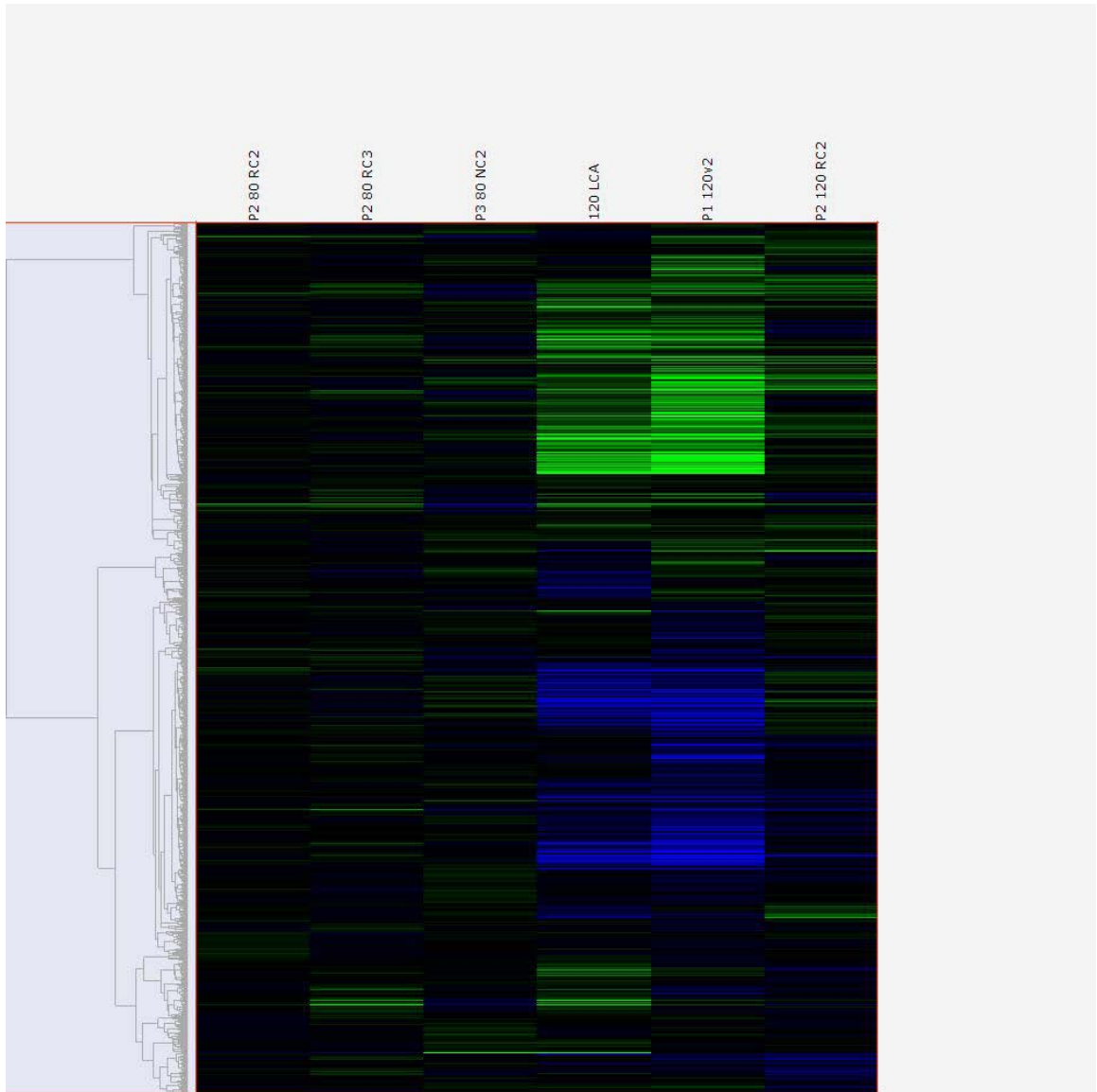
*(+), increased expression. (-), decreased expression.

Affymetrix ID	Gene	Description	Effect	P value	Affymetrix ID	Gene	Description	Effect	P value
Ssc.24144.1.S1_at	ACVR1B	activin receptor, type IB	+	0.012	Ssc.15827.1.S1_at	KPNA1	karyopherin alpha 1	+	0.038
Ssc.15924.1.S1_at	ACVR2A	activin A receptor, type IIA	+	0.021	Ssc.15980.1.S1_at	LBP	lipopolysaccharide binding	+	0.038
Ssc.4679.1.S1_at	ANG	angiogenin	+	0.002	Ssc.4729.1.S1_at	LEAP2	lived antimicrobial peptide 2	+	0.018
Ssc.170.1.S1_at	ARG1	arginase, liver	+	0.033	Ssc.13769.1.S1_at	LTF	lactotransferrin	+	0.023
Ssc.16110.1.A1_at	BIRC3	baculoviral repeat-containing3	+	0.018	Ssc.17343.1.A1_at	LYVE1	hyaluronan receptor 1	+	0.013
Ssc.21774.1.S1_at	BMP7	bone morphogenetic protein 7	+	0.033	Ssc.14512.1.S1_at	MAN1A1	mammosidase, alpha1	+	0.0154
Ssc.4680.1.S1_at	BOP1	block of proliferation 1	+	0.03	Ssc.20755.1.S1_at	MGAT1	glycoprotein beta-1.2-	+	0.037
Ssc.10460.1.S1_at	C2	complement component 2	+	0.046	Ssc.28326.1.S1_at	MGAT4C	glycoprotein beta-1.4	+	0.001
Ssc.7543.1.A1_at	CASP3	caspase 7	+	0.049	Ssc.16013.1.S1_at	MMP1	matrix metalloproteinase 1	+	0.038
Ssc.31212.1.S1_at	CASP8	caspase 8	+	0.018	Ssc.15927.2.S1_at	MMP3	matrix metalloproteinase 3	+	0.027
Ssc.657.1.A1_at	CCL2	chemokine ligand 2	+	0.028	Ssc.15640.1.S1_at	MT3	metallothionein 3	+	0.019
Ssc.23797.1.S1_at	CCL4	chemokine ligand 4	+	0.022	Ssc.2014.1.S1_at	MYLPF	fast skeletal myosin light	+	0.038
Ssc.30833.1.S1_at	CCL4L1	chemokine ligand 4	+	0.018	Ssc.16122.1.S1_at	NFATC2	nuclear factor activate T-cells	+	0.038
Ssc.9738.1.A1_at	CEBPB	enhancer binding protein	+	0.017	Ssc.4759.1.S1_at	NFKBIA	nuclear factor of kappa light	+	0.017
Ssc.11074.1.S1_at	CFD	complement factor D	+	0.04	Ssc.16226.1.S1_at	ODF1	outer dense fiber	+	0.032
Ssc.10998.1.A1_at	CLK1	GDC-like kinase 1	+	0.037	Ssc.108.1.S1_at	OXR	oxytocin receptor	+	0.045
Ssc.645.1.S1_at	CSTA	cystatin A	+	0.047	Ssc.27893.2.S1_at	PHF20	PHD finger protein 20	+	0.006
Ssc.4989.1.A1_at	CTH	cystathionase	+	0.098	Ssc.15899.1.S1_at	PLK2	polo-like kinase 2	+	0.048
Ssc.19692.1.S1_at	CXCL2	chemokine ligand 2	+	0.119	Ssc.23774.3.S1_at	PLS1	plasmin 1	+	0.041
Ssc.719.1.S1_a_at	CXCL5	chemokine ligand 5	+	0.009	Ssc.15919.1.A1_at	PMAIP1	phorbol-12-myristate Protein	+	0.033
Ssc.7176.1.A1_at	CXCR4	chemokine receptor 4	+	0.011	Ssc.11661.2.S1_at	PPP1CC	protein phosphatase 1,	+	0.055
Ssc.16261.1.S1_at	CYP2C18	cytochrome P450, family 2,	+	0.044	Ssc.202.1.S1_at	PRSS34	protease, serine, 34	+	0.007
Ssc.26326.1.S1_at	CYP3A43	cytochrome P450, family 3	+	0.049	Ssc.24672.1.A1_at	PSEN1	presenilin 1	+	0.0333
Ssc.15273.1.S1_at	DHX16	DEAH box	+	0.034	Ssc.16187.1.S1_at	PTGDS	prostaglandin D2 synthase	+	0.0428
Ssc.10199.2.S1_a_at	DTNBP1	dystrobrevin binding protein 1	+	0.027	Ssc.23801.1.S1_at	RETN	resistin	+	0.0426
Ssc.14497.1.S1_at	FAS	Fas TNF receptor	+	0.01	Ssc.27728.1.S1_at	RNF114	ring finger protein 114	+	0.033
Ssc.11155.2.S1_at	FOXO1	forkhead box O1	+	0.021	Ssc.9334.1.S1_at	RPIA	ribose 5-phosphate A	+	0.0027
Ssc.29003.1.S1_at	GDF11	growth differentiation factor 11	+	0.047	Ssc.18347.1.A1_s_at	SIPR5	sphingosine-1-P receptor 5	+	0.041
Ssc.1206.1.A1_at	GLRX	glutaredoxin	+	0.043	Ssc.12776.1.A1_at	SELL	selectin L	+	0.043
Ssc.16056.1.S1_at	GPD2	glycerol-3-phosphate	+	0.041	Ssc.290.1.S1_at	SELP	selectin P	+	0.043
Ssc.16049.1.A1_at	GSC	goosecoid homeobox	+	0.011	Ssc.30700.1.S1_at	SIC25A36	solute carrier family 25,	+	0.027
Ssc.15862.1.S1_at	HHEX	hematopoietically homeobox	+	0.032	Ssc.11757.1.S1_at	SMAD1	SMAD family member 1	+	0.0318
Ssc.210.6.S1_x_at	HLA-DQB2	MHC class II, DQ beta 2	+	0.009	Ssc.3706.1.S1_at	SOD2	superoxide dismutase 2,	+	0.0034
Ssc.222.1.S1_at	HLA-DRA	MHC class II, DR alpha	+	0.038	Ssc.3706.1.S2_at	SOD2	superoxide dismutase 2,	+	0.0091
Ssc.777.1.S1_at	HSD11B1	hydroxysteroid	+	0.004	Ssc.279.1.S1_at	STAR	steroidogenic acute protein	+	0.0027
Ssc.6728.1.S1_at	HSP90AA1	heat shock protein 90kDa	+	0.021	Ssc.3409.1.A1_at	STAT3	signal active transcription 3	+	0.0173
Ssc.11187.1.S1_at	ICAM1	intercellular adhesion molecule 1	+	0.028	Ssc.16351.1.S2_at	STAT5A	signal active transcription 5A	+	0.03
Ssc.17033.1.S1_at	HIGD2A	HIG1 domain family, member 2A	-	0.024	Ssc.9661.1.S1_at	TIMP3	metalloproteinase inhibitor 3	-	0.028
Ssc.12457.1.S1_at	HN1	hematological and neurological expressed 1	-	0.007	Ssc.24358.1.S1_at	TK1	thymidine kinase 1, soluble	-	0.006

*(+), increased expression. (-), decreased expression

APPENDIX E

HIERARCHICAL CLUSTERING OF MICROARRAY HYBRIDIZATIONS



*Cluster analysis of hybridizations and genes performed using GeneTraffic UNO (Iobion Informatics LLC).